University of Kentucky
UKnowledge

Theses and Dissertations--Pharmacy | College of Pharmacy

2017

# EFFECTS OF CORE AND SHELL MODIFICATION TO TETHERED NANOASSEMBLIES ON SIRNA THERAPY

Steven Rheiner
*University of Kentucky*, Steven.rheiner@uky.edu
Digital Object Identifier: https://doi.org/10.13023/ETD.2017.272

Right click to open a feedback form in a new tab to let us know how this document benefits you.

## Recommended Citation

Rheiner, Steven, "EFFECTS OF CORE AND SHELL MODIFICATION TO TETHERED NANOASSEMBLIES ON SIRNA THERAPY" (2017). *Theses and Dissertations--Pharmacy*. 73.
https://uknowledge.uky.edu/pharmacy_etds/73

This Doctoral Dissertation is brought to you for free and open access by the College of Pharmacy at UKnowledge. It has been accepted for inclusion in Theses and Dissertations--Pharmacy by an authorized administrator of UKnowledge. For more information, please contact UKnowledge@lsv.uky.edu.

STUDENT AGREEMENT:

I represent that my thesis or dissertation and abstract are my original work. Proper attribution has been given to all outside sources. I understand that I am solely responsible for obtaining any needed copyright permissions. I have obtained needed written permission statement(s) from the owner(s) of each third-party copyrighted matter to be included in my work, allowing electronic distribution (if such use is not permitted by the fair use doctrine) which will be submitted to UKnowledge as Additional File.

I hereby grant to The University of Kentucky and its agents the irrevocable, non-exclusive, and royalty-free license to archive and make accessible my work in whole or in part in all forms of media, now or hereafter known. I agree that the document mentioned above may be made available immediately for worldwide access unless an embargo applies.

I retain all other ownership rights to the copyright of my work. I also retain the right to use in future works (such as articles or books) all or part of my work. I understand that I am free to register the copyright to my work.

REVIEW, APPROVAL AND ACCEPTANCE

The document mentioned above has been reviewed and accepted by the student's advisor, on behalf of the advisory committee, and by the Director of Graduate Studies (DGS), on behalf of the program; we verify that this is the final, approved version of the student's thesis including all changes required by the advisory committee. The undersigned agree to abide by the statements above.

Steven Rheiner, Student

Dr. Younsoo Bae, Major Professor

Dr. David Feola, Director of Graduate Studies

# EFFECTS OF CORE AND SHELL MODIFICATION TO TETHERED NANOASSEMBLIES ON SIRNA THERAPY

---

DISSERTATION

---

A dissertation submitted in partial fulfillment of the
requirements for the degree of Doctor of Philosophy in the
College of Pharmacy
at the University of Kentucky

By
Steven Neil Rheiner
Lexington, Kentucky
Director: Dr. Younsoo Bae, Associate Professor of Pharmaceutical Sciences

Lexington, Kentucky

Copyright © Steven Rheiner 2017

ABSTRACT OF DISSERTATION

# EFFECTS OF CORE AND SHELL MODIFICATION TO TETHERED NANOASSEMBLIES ON SIRNA THERAPY

siRNA therapy is an emerging technique that reduces protein expression in cells by degrading their mRNAs via the RNA interference pathway (RNAi). Diseases such as cancer often proliferate due to increased protein expression and siRNA therapy offers a new method of treatment for those diseases. Although siRNA therapy has shown success *in vitro*, it often fails *in vivo* due to instability in the blood stream. To overcome this limitation, delivery vehicles are necessary for successful transfection of siRNA into target cells and cationic polymers have been widely studied for this purpose. However, complexes between siRNA and delivery vehicles made from cationic polymers exhibit stability issues in the blood stream which results in toxicity and low transfection. This work hypothesizes that improvement of vehicle/siRNA complex stability will improve siRNA transfection efficiency. To test this, the contributions and outcomes of poly(ethylene glycol) [PEG] shell and hydrophobic core modification to a polyethylenimine (PEI) based tethered nanoassemblies (TNAs) were examined. Initially, hydrophobic modification of palmitate (PAL) to the core of the TNA yielded improved transfection efficiency due to an enhanced endosomal escape capability. However, this modification also reduced the TNA/siRNA complex stability. This indicated that the core hydrophobicity must be balanced in order increase stability while increasing transfection efficiency. Additionally, TNAs made from PEG and PEI did not cause transfection in our initial study. The PEG shell density was found to be too great and thereby reduced transfection efficiency. Reducing the PEG density by lowering PEG molecular weight, reducing attachment percentage, and removing small PEI impurities from the synthesis stock increased overall transfection efficiency and unimolecularity of the TNA complexes. This indicated that the shell composition of the TNA must be tuned in order to improve particle design. Further study of the hydrophobically modification to TNAs yielded unintended effects on the transfection efficiency evaluation assay. These particles exhibited an siRNA independent reduction in the reporter protein used to observe transfection, or a false positive effect, that was not previously observed. It was found that this false positive was influence mainly by the hydrophobic group rather than the cationic polymer backbone. Cellular stress was observed in cells dosed with the hydrophobically

modified TNAs which lead to over ubiquitination and rapid degradation of the luciferase protein. This demonstrated that core components of TNAs could cause cellular stress and influence interaction outside of the TNA. Overall, this work demonstrates that hydrophobic core and PEG shell modification require balancing and consideration to improve properties of future cationic polymer based siRNA delivery vehicle design.

Keywords: Tethered nanoassemblies, siRNA therapy, gene delivery, cationic polymer, chemical modification, transfection

Steven Rheiner

7/13/17

Date

EFFECTS OF CORE AND SHELL MODIFICATION TO TETHERED NANOASSEMBLIES ON SIRNA THERAPY

By

Steven Neil Rheiner

Dr. Younsoo Bae
Director of Dissertation

Dr. David Feola
Director of Graduate Studies

7/13/17
Date

To my wife and family, without your love and support I would not have been able to accomplish this.

ACKNOWLEDGMENTS

Firstly, I would to thank my thesis advisor, Dr. Younsoo Bae, whose support and guidance has been instrumental to my success in my PhD training. I would like to thank Dr. Bae for the opportunity to learn from him and his lab in order to forge a path of my own in such an interesting research field. I sincerely appreciate Dr. Bae's mentoring and invaluable advice throughout my research.

Secondly, I would also like to thank my committee members, Dr. Patrick McNamara, Dr. Daniel Pack, and Dr. Edith Glazer, for their guidance through my research, qualifying exam, and defense. Their advice and help throughout my graduate studies has been invaluable to my development as a scientist and furthering my research.

Further, I would like to thank the Cancer Nanotechnology Training Center (CNTC) of the University of Kentucky for the opportunity to participate in such a wonderful program. The CNTC granted me the opportunity to gain insight into my research project from a diverse group in a collaborative setting. This knowledge and opportunity was valuable to my research and scientific career. Special thanks to Dr. Piotr Rychahou, Dr. Brad Anderson, and Dr. Robert Yokel for their insight into my research project and Tonya Vance for her help throughout the traineeship.

I would also like to thank all current and past lab members of the Bae laboratory that have shared their experience and knowledge to assist with research and growth as a scientist. Their advice has proven invaluable to my scientific development. I would like to extend special thanks to Derek Reichel whose critical analysis of my writing and

experimentation has been a valuable source of improvement. Additionally, I would like to thank all past lab members, Dr. Andrei Ponta, Dr. Pengxiu Cao, Dr. Geunwoo Jin, Dr. Matthew Dickerson, and Amber Jerke, for their assistance and support.

I would like to acknowledge and give thanks to all other faculty and staff members throughout my graduate career, especially graduate coordinator Catina Rossoll and director of graduate studies Dr. Jim Pauly at the College of Pharmacy at University of Kentucky. They have given me guidance and advice throughout my graduate career that has helped keep me on track even in difficult times.

I would like to thank and show appreciation to my family. My wife, Faith Rheiner, has always been by myside to help me through all the ups and downs my graduate career has brought about. Her love and support has been crucial to my success. I would like to thank my parents Richard and Cathryn Rheiner, sister Rebecca Rheiner, aunt and uncle Dr. Mike Cotta and Patti Cotta, and all my other family members that have shown me love and support my entire life. They have provided a strong support system that I needed in order to be successful. I would also like to thank my friends, Greg Laver, Liam Flavin, Danny Jasinski, Dan Binzel, Rob Wensing, Kevin Chen, Matt McErlean, and Ryan Hughes, as well as many others who have also provided an invaluable support system and advice throughout the years.

Finally, I would also like to give special thanks to Richard Rheiner, Dr. Mike Cotta, and Dr. Matthew Wheeler. They have helped to foster and guide my interest in science as well as provide wisdom in difficult times during my education. Their advice has guided many of my decisions and helped me to realize my dreams.

## Table of Contents

## List of Figures

## List of Tables

# Chapter 1: Tethered Nanoassemblies for siRNA Therapy

## 1.1. Genetic Disease Treatment and siRNA Therapy

Genetic diseases, such as cancer, are caused by damaged cells with abnormal protein expressions that allows these cells to grow rapidly and without checks[1-2]. Current small molecule therapies to target these diseases only target a small subset of proteins involved in their proliferation. Currently, small molecule drugs cannot target many of these abnormally expressed proteins. Instead, the drugs target proteins and pathways that are not necessarily specific to the proteins involved in the disease which can kill both healthy and diseased cells[3-4]. A more specific and tailored therapy would involve targeting the specific proteins known to cause the disease. Nucleic acids that alter the expression of specific proteins, known as gene therapy, has been widely studied since its discovery nearly 40 years ago[5].

Gene therapy has the potential to upregulate or downregulate protein expression in diseased cells. Gene therapy can upregulate specific protein expression in diseased cells by introducing exogenous DNA containing the code for the targeted protein[6-7]. This DNA will be translated and replicated in the nucleus just as other genes providing multiple copies of the targeted protein[8]. Though many genetic diseases can benefit from an increase in protein expression, it is often a long-term or permanent solution that may not be desirable. To achieve the desired effect in cells, DNA is either delivered via plasmid or injected in to the genome. Though plasmid activity can be long term but not permanent, gene insertion is permanent and if not inserted correctly will cause genetic damage leading to more cell issues[9]. Conversely, Gene therapy achieves protein downregulation using a less permanent method which is inherently safer[10-11]. Introducing

a short length of RNA complimentary to an endogenous mRNA or DNA that is complimentary to an endogenous DNA gene sequence, referred to as “antisense” nucleotides, will form pairs with the endogenous genetic material to prevent their transcription or translation. This is a reversible process that will inhibit specific protein production, called antisense therapy[12]. Currently, antisense therapy is widely studied due to its increased safety compared to protein upregulation methods.

Antisense therapy uses two mechanisms to reduce protein expression: physically blocking translation and transcription or inducing degradation of complimentary mRNA. Initially, it was discovered that complimentary RNA and DNA could physically block translation and transcription by tightly binding to regions that produce the targeted protein[13]. Complimentary DNA was found to prevent translation but it was a reversible process which shortened the time of the antisense effect. Further investigation in to complimentary RNA discovered that it could promote cleavage of the mRNA by RNases in the cell[14]. This improved upon physically blocking mRNA translation by degrading the mRNA and improving the therapy. In 1994, an endogenous pathway was discovered that could promote mRNA degradation using specific lengths of double stranded RNA, called the RNA interference pathway (RNAi)[15-16] (**Figure 1.1**).

RNAi is an endogenous pathway that uses 21-25 base pairs of small interfering RNA (siRNA) complimentary to a portion of the mRNA of a targeted protein[17]. Once siRNA enters the cytoplasm of the cell, a dicer complex takes up the siRNA to load it in to the RNA induced silencing complex (RISC). RISC then unwinds and removes one strand of the siRNA while keeping the other as a guide strand. The siRNA loaded RISC screens mRNA present in the cytoplasm until it reaches a region complimentary to the siRNA

guide strand. RISC's RNase activity then cleaves the mRNA. RISC may then release the siRNA guide strand to pick up another piece of siRNA or reclaim the previous guide strand to seek out more mRNA. This effect is continuous until the siRNA is degraded within the cell[18].

The concept of RNAi has been proven *in vitro* using multiple diseased cell lines and many different protein targets[19-22] but very little siRNA has succeeded in *in vivo* testing. At the *in vivo* level, siRNA is introduced to clearance mechanisms, blood proteins, and immune responses that quickly degrade and remove naked siRNA from the blood stream. RNases present in blood serum will rapidly degrade siRNA generating a short half-life ranging from 5 minutes to 1 hour[23-24]. Additionally, siRNA is cleared due to its small size overcome these issues, further reducing its half-life in the blood stream. This short half-life is a large problem for siRNA circulation which prevents it from reaching its active site and hinders its clinical potential[25]. To improve the efficacy of siRNA, current studies are focused on increasing stability of siRNA in the bloodstream by different means.

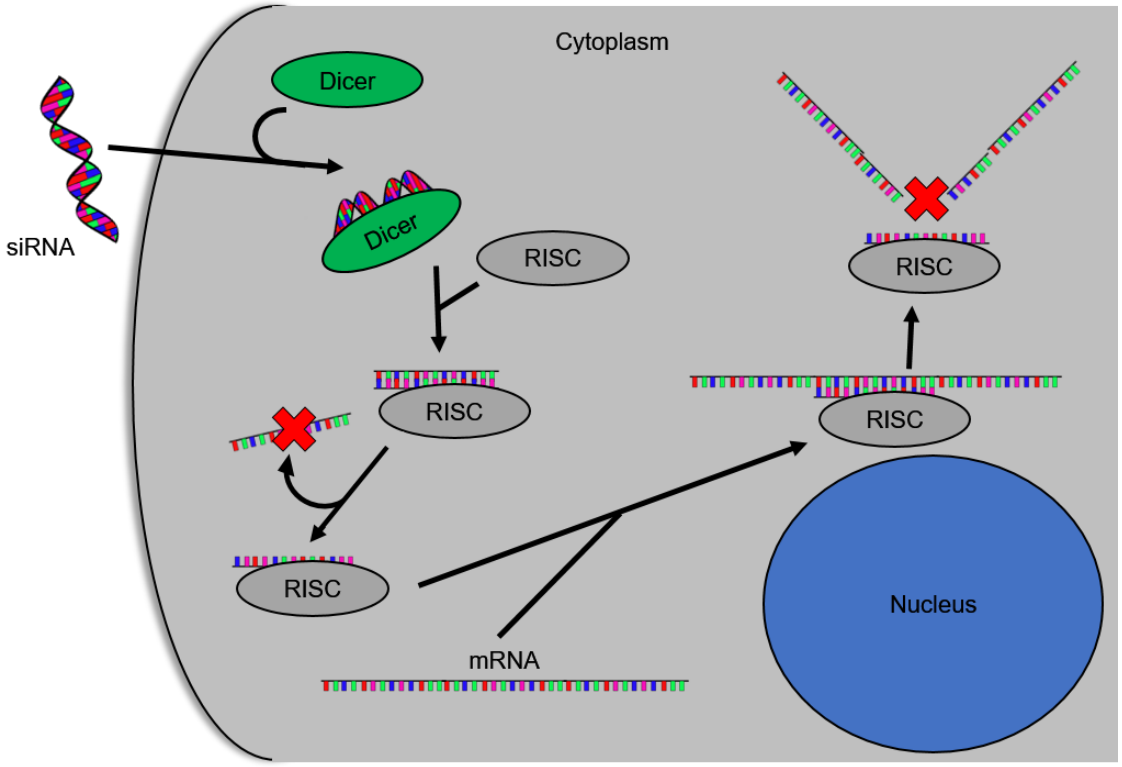


**Figure 1.1: RNA Interference Pathway**

mRNA degradation pathway induced by small interfering RNA (siRNA) in the cell involving the RNA induced silencing complex (RISC)

## 1.2. Tethered Nanoassembly (TNA) as siRNA Delivery Vehicles

As mentioned in the previous section, siRNA is in need of a means to improve its stability in the blood stream. Many methods have been investigated to increase siRNAs stability, including chemical modification of siRNA[26-28], but research in to siRNA delivery vehicles has been at the forefront of this field. siRNA delivery vehicles are designed to protect siRNA by encapsulating them which prevents RNase degradation. Further, these vehicles should also help usher the siRNA to the location of the targeted cells and in to their cytoplasm, either through endosomal escape or another uptake method[29]. These factors will allow delivery vehicles to enhance siRNA therapy.

Initially viral delivery systems were developed as gene therapy delivery vehicles for both DNA and siRNA[30-31]. Viral delivery vehicles are viruses, such as retroviruses or adeno-associated viruses, that have part of their genetic code altered to prevent replication and include a copy of the targeted gene[32]. The viral vectors will inject genetic material in to the cell using the viral mechanism. These can be used in siRNA therapy by employing small hairpin RNA (shRNA) which will be replicated inside the cell to consistently produce the desired siRNAs[33]. However, viral delivery presents safety issues including risk of the virus replicating or random insertion of genetic material into the cellular genome which can interfere with normal cellular processes[34-35]. These safety issues have led to increased research in to non-viral delivery systems.

Non-viral delivery systems include a wide range of vectors including polymer and lipid based systems[36-38]. Lipid based systems, such as liposomes[39-40] and lipid nanoparticles[41-42], have been investigated for siRNA delivery as they were already a well-studied system for drug delivery. These lipid based vehicles usually include lipids

modified with cationic head groups in order to form an ionic complex with the siRNA[43]. The cationic charge density of the lipid vehicle can be tuned by including non-cationic lipids along with the cationic lipids[44]. However, these vehicles often have lower efficiency when forming complexes compared to cationic polymers. Cationic polymers are synthetic and natural based polymers, such as poly-l-lysine (PLL)[45] and polyethylenimine (PEI)[46-47], that have a high cationic charge density[48]. Again, these polymers form ionic complexes with siRNA and offer base for modification to tune the vehicle for desired delivery characteristics.

Although both lipid and polymer based systems have value to deliver siRNA, this work focuses on cationic polymer based delivery vehicles because of their intrinsic properties which offer advantages to siRNA delivery. These properties include: high cationic charge density[49], endosomal escape capability[50], ease of modification[51], and control of particle size[52]. Cationic polymers include repeating units containing primary, secondary, and sometimes tertiary amines. The pKas of these amines determine that they are usually protonated at physiological pH which increases binding of siRNA to the polymer. Some polyamine compounds, including PEI[53], have multiple pKas for their amines due to their close proximity to other amines leading to a unique endosomal escape ability called the proton sponge effect[54-55]. The proton sponge effect occurs when the polymer/siRNA complex enters the endosome. As the endosome decreases its pH to become a lysosome, the polymer increases the protonation of its amines. This removes hydrogens from the inside of the endosome, forcing the endosome pump in more ions and swell in order to lower its pH. Eventually, the endosome will burst and release the vehicle to the cytoplasm of the cell. This creates one mechanism of endosomal escape for these

polymers. Additionally, the cationic groups can interact with membranes which causes disruption and frees the polymer/siRNA complex[56-57]. These cationic groups also offer sites for modification of the polymer by relatively simple chemistry, such as n-hydoxysuccinimide (NHS) coupling[58-59]. This can tune the vehicle for its intended purpose. Further tuning can be done by altering the chain length of the polymer to change the size of the polymer/siRNA complexes. Size of the complex is important to avoid immune response (diameter > 100 nm)[60] and renal clearance (diameter < 15 nm)[61].

Based on these advantages, this work uses a model cationic polymer based delivery system called a tethered nanoassembly (TNA). TNAs are a delivery vehicle consisting of the cationic backbone, such as PEI or PLL, which poly(ethylene glycol) [PEG] and other chemical modifications which are chemically linked, or "tethered". TNAs were designed to help elucidate the contribution of polymer/siRNA complex stability to transfection efficiency and overall efficacy of siRNA delivery. While increased stability can be achieved through modification, discussed further in section 1.3, the inherent design of the vehicle also contributes to complex stability. A long chain cationic polymer was used as a backbone so that a single polymer can form complexes with siRNA rather than multiple polymers, which is common for these delivery vehicles. The resulting unimolecular system can increase the uniformity of the vehicles and siRNA entrapment, thereby increasing complex stability.

### 1.3. Chemical Modifications to Improve siRNA Therapy Efficacy

Cationic polymer based delivery vehicles are widely studied because of their advantageous properties for delivering siRNA but these vehicles have difficulty achieving success in *in vivo* models. This is often due to a lack of siRNA/vehicle

complex stability that can result in increased toxicity, low siRNA uptake in to the cell, and increased siRNA clearance[62-63]. Poor complex stability results in polymers breaking free from the complex which will increase non-specific interaction and toxicity, both in the blood stream[64] and inside the cell[65]. As more polymers break free, the siRNA is less protected from degradation and doesn't reach its target site. This indicates that complex stability is crucial to delivery vehicle efficacy. In order to overcome these issues, research has been focused on modification of the polymers making up the delivery vehicle to improve complex stability and efficacy.

Chemical modification to siRNA delivery vehicles can alter physical and chemical properties of the complex in order to improve its stability and efficacy[66-67]. When considering chemical modifications, two properties play a key role: cationic surface charge[68] and secondary structure formation[69]. Increased cationic surface charge can cause both toxicity and accelerated blood clearance due to non-specific interactions with cellular membranes and blood proteins[70-72], respectively. Therefore, reducing the surface charge will benefit the overall efficacy of the complex. Surface charge reduction is often done by covalent modification of PEG to the vehicle, or pegylation. Additionally, increasing the types of forces, i.e. ionic interaction or hydrophobic interaction, used by a vehicle to form its secondary structure can increase stability of the siRNA/vehicle complex and reduce the amount of free polymer in formulation[73-74]. This reduces toxicity and improves delivery of siRNA to its target site[75-77]. There are multiple ways to increase secondary structure formation[78-79], however inclusion of hydrophobic moieties[80-81] on cationic polymers is common. Based on this, this work focuses on pegylation and hydrophobic modification of cationic polymer delivery vehicles.

Pegylation siRNA/vehicle complexes can enhance complex stability by reducing surface charge and preventing off-target effects. Modification of vehicles with PEG produces a field of PEG around the outside of the vehicle, also known as a PEG shell[82]. This PEG shell has been shown to reduce surface charge by hiding the charged moieties toward the center of the vehicle, or core[83]. This gives the vehicle what has been referred to as "stealth" properties including reduced ionic interaction with blood proteins and cellular membranes, reduced opsinization of the vehicle and removal by the immune system, and avoiding renal clearance by increasing vehicle diameter[84]. It should be noted that reduced cellular membrane interaction reduces toxicity caused by membrane disruption, the main mechanism of toxicity for cationic polymers, but it is also required to activate endocytosis[85-87], which is a main mechanism of cellular uptake for cationic polymer delivery vehicles. Additionally, pegylation can also benefit secondary structure formation by pushing the polymer towards a core/shell structure[73]. These actions of pegylation have proven to benefit vehicles by increasing circulation time and vehicle stability which increases the efficacy of the vehicle[88-89].

Hydrophobic modification to cationic polymers can improve complex stability and enhance intracellular uptake by increasing the secondary structure formation[80]. Hydrophobic modification is the introduction of a hydrophobic group to the cationic polymer. These groups give the polymer a mechanism other than ionic forces to form a secondary structure with itself or other polymers[90]. This prevents unwanted release of polymer and siRNA from the complex. It has also been shown that genetic materials may use the hydrophobic groups in complex formation[91-92], therefore increasing the binding efficiency of the polymer to siRNA and further stabilizing the siRNA/vehicle complex.

Hydrophobic modification also provides additional benefits such as increasing cellular membrane interactions[93-94]. Increasing membrane interactions can increase endocytosis by increasing activation of this pathway as well as increasing endosomal escape through interaction and disruption of the endosomal membrane.

Understanding the effects of chemical modification on cationic polymers can often be difficult due to variance in properties of different cationic polymers. Modifications, such as with PEG and hydrophobic groups, can often have similar effects across polymers but it becomes difficult to attribute specifics effects to modifications. The TNA model system used in this work offers a uniform system to pinpoint effects from modifications. TNAs offer a backbone to which many different modifications can be tethered. The design of these particles allows for sequential modification and analysis where differences between TNAs can be attributed to specific modifications. These findings can likely translate to other cationic polymers. This system will bring more focus on the effects of chemical modification to cationic polymer delivery vehicles.

Based on this background, this work hypothesizes that increasing the stability of the delivery vehicle through chemical modification will increase its siRNA transfection efficiency. In the subsequent studies, the contributions of hydrophobic core modification and pegylation of the shell on transfection efficiency and complex stability are elucidated using a model colon cancer cell line (HT29). This work will modify TNAs with hydrophobic moieties and PEG as a model system for these modifications in order to gather information that is relevant to both PEI based siRNA delivery vehicles as well as other cationic polymer based vehicles. This will increase our understanding of these

modifications in order to improve future particle design of both TNAs and other cationic polymer delivery vehicles.

# Chapter 2: Effects of Hydrophobic Core Modification on TNA stability and siRNA transfection

This section was adapted with permission from work published by the author in AIMS Biophysics on July 30th, 2015[95]. I would like to extend a special acknowledgment to Dr. Piotr Rychahou who assisted with the cell line and transfection methods.

## 2.1. Introduction

As mentioned in the previous chapter, gene therapy using siRNA, siRNA therapy, has been investigated to treat different genetic diseases, including cancer[96-97]. Currently, siRNA therapy has shown great promise in treating undruggable proteins and pathways in an *in vitro* setting. However, siRNA's shows poor stability, rapid degradation, and low circulation time in the bloodstream[98-99]. This makes progression from *in vitro* to *in vivo* evaluation difficult. In order for siRNA therapy to be viable in a clinical setting, the siRNA must be protected during delivery to its target site. Therefore, there has been a push to develop siRNA delivery carriers that overcome these hurdles.

Though multiple types of carriers have been studied for delivery of siRNA[98, 100], this work focuses on cationic polymer based delivery vehicles. Delivery vehicles typically form ionic complexes between the cationic portions of the vehicle and the anionic phosphate backbone of siRNA. In this regard, the poly-amine nature of cationic polymers enhances their abilities as delivery vehicles because of their high cationic charge density which improves ionic complexation with siRNA[101-103]. One such example of a cationic polymer is branched poly(ethylene imine) (bPEI)[64]. bPEI contains primary, secondary, and tertiary amines, which are protonated at physiological pH, that may be used in combination to complex with siRNA in a high efficiency[104], resulting in bPEI offering a highly charged, nanosized delivery carrier for siRNA. Although PEI can be toxic to cells, bPEI is considered a safer alternative to linear PEI because it often shows comparatively

lower cytotoxicity[105]. However, issues of stability and off-target effects in the presence of negatively charged serum proteins and other anions in the bloodstream prevent bPEI/siRNA polyplexes from success in vivo[74].

Typically to increase the stability of the polyplexes, the ratio of polymer to siRNA is increased which introduces excess polymer in to the formulation. However, the polymers that fail to interact with the siRNA, or free polymers, are left separate from other polyplexes which often cause various adverse effects due to the increased availability of their cationic groups[106]. Polymers that weakly interact with the complexed siRNA can dissociate from the polyplex in the presence of the competing anion. This can further reduce the stability of the polyplex and further dissociation until the siRNA is no longer protected[107]. Additionally, cationic polymers used in excess can also create a large positive surface charge detrimental to the polyplexes safety and stability[108-109]. High surface charge and free polymers are known to reduce the particle circulation time in vivo, cause cytotoxicity, decrease stability of the formulation, and fail to protect siRNA before delivery to target sites[73, 110]. These all culminate in a lack of transfection efficiency and stability of the siRNA formulation but modifications to the existing polymers could help to return the lost efficacy.

Modification to both the core and shell of cationic polymer based delivery vehicles can address these unwanted aspects of formulation[111]. Excess cationic surface charge can be attenuated through pegylation, or covalent modification of the polymer with [poly(ethylene glycol): PEG][112]. Pegylation creates a hydrophilic shell around the particle that shields and increases the circulation time of the polyplexes by reducing interactions with its environment and neutralizing its surface charge[113]. Free polymer in the

formulation can be decreased by increasing the attractive forces between the polymers in the polyplex core. Hydrophobic interaction has been shown to enhance particle stability by allowing the polymer chain to interact with itself as well as the siRNA[114-116]. Nucleic acid strands have shown to interact with hydrophobic groups once their anionic charge has been neutralized which would further stabilize the complex[117]. Additionally, if siRNA dissociates from the complex, the particle can stay together based on the hydrophobic interactions and prevent free polymer generation[118]. Alternatively, linking all free cationic polymer together, effectively forming a unimolecular system, will reduce free polymer in formulation because it would remove free polymer from the system all together. By modifying a single cationic polymer to covalently link with multiple other moieties including PEG and hydrophobic groups, a single polymer could form a complex with siRNA creating a unimolecular particle with no ability to dissociate its components from itself yet siRNA would be free to associate and disassociate. By reducing the free polymer and surface charge of the cationic polymer delivery vehicle, efficacy and stability should increase resulting in increased transfection efficiency.

Based on this background, we hypothesized that siRNA transfection efficiency will improve by protecting siRNA in the core of a unimolecular cationic nanoassembly with improved complex stability. To test this, the work in this chapter set out to create polymer nanoassemblies stabilized with a lipophilic core and examine the effects of complex stability on transfection efficiency, toxicity, and intracellular siRNA delivery. Polymer nanoassemblies were synthesized by tethering hydrophilic polymer chains, PEG, onto a single polymer backbone (branched PEI: PEI) while modifying the core of the nanoassemblies with lipophilic pendant groups (palmitate: PAL). **Figure 2.1** illustrates

two types of polymer tethered nanoassemblies (TNAs) used in this chapter, PEG-PEI (2P) and PEG-PEI-PAL (3P). 2P has cationic moieties in the core and thus attract siRNA to prepare polyionic complexes while 3P has a hydrophobic core modified with PAL to increase stability of the complexes through ionic and hydrophobic interactions between the core and siRNA payload. The PAL content in 3P was also modulated at varying ratios to prepare TNAs that behave between 2P and 3P. For this chapter, the siRNA-loaded TNAs were designed to reduce luciferase, an exogenous bioluminescent protein, expression level within a cell so that its efficacy in vitro could be examined through a facile method.

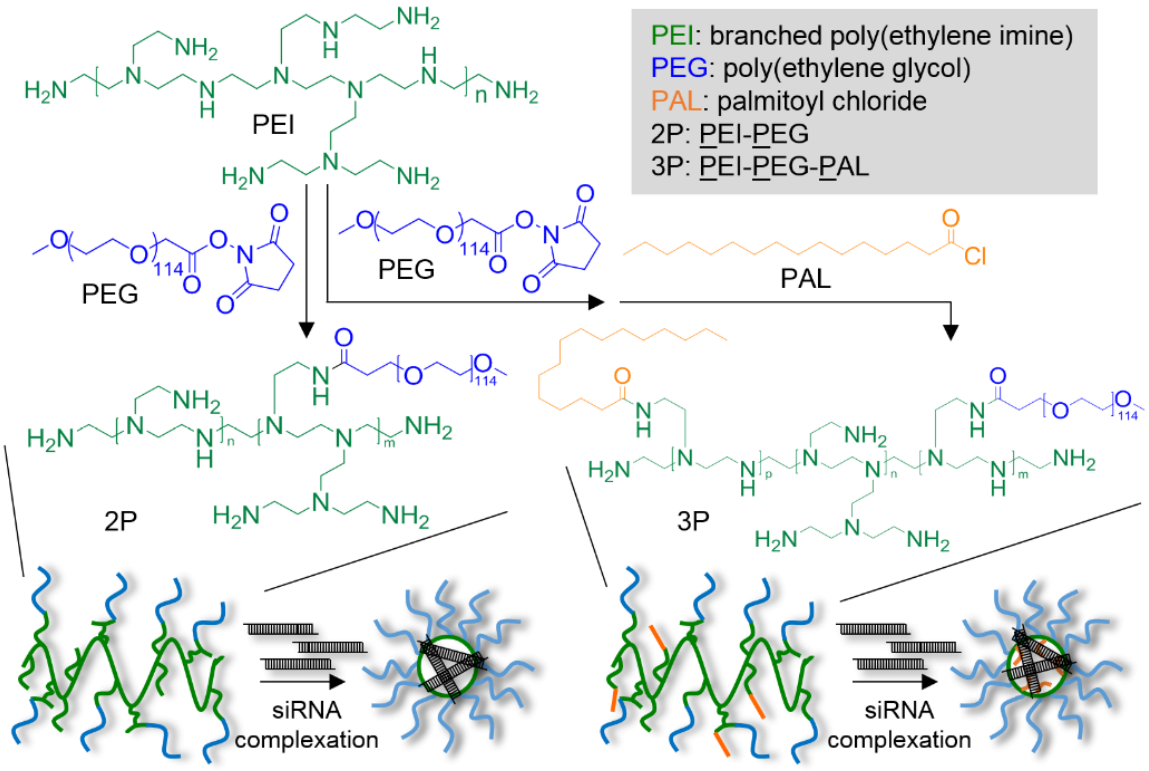


**Figure 2.1. Synthesis of tethered nanoassemblies (TNAs) for siRNA delivery.**

TNAs were designed to form a unimolecular assembly entrapping siRNA in the core. The amount of PAL was controlled to modify lipophilicity of the core of TNAs.

## 2.2. Materials and Methods

### 2.2.1. Materials and Cells

PEG (5 kDa, α-methoxy-ω-NHS activated) was purchased from NanoCS (New York, NY). Branched PEI (bPEI) and palmitoyl chloride were purchased from Sigma Aldrich (St. Louis, MO). HEPES buffer (pH 8.0, 1 M), pyridine, NuSieve agarose gtg, dialysis membrane with molecular cut-off (MWCO) of 8 and 100 kDa, dylight-547, Lysotracker, and other organic solvents were purchased from Fisher Scientific (Waltham, MA). siRNA was synthesized with a sequence of 5'-GUUGGCACCAGCAGCGCACUU-3', and a siGLO RISC-free control siRNA was purchased from GE Dharmacon (Lafayette, CO). A human colon cancer HT-29 cell line was purchased from American Type Culture Collection (ATCC, Manassas, VA). McCoy's 5A, 0.05% trypsin/EDTA, and phosphate buffered saline (PBS) were from GE Healthcare (Logan, UT). Fetal bovine serum (FBS) was purchased from Atlanta Biologicals (Flowery Branch, GA). HT-29 cells were cultured in McCoy's 5A media supplemented with 10% FBS according to all ATCC recommendations. Cells were maintained at logarithmic growth in a humidified environment with 5% $CO_2$ at 37 °C.

### 2.2.2. Synthesis of stabilized TNAs

TNAs were synthesized from 25 kDa bPEI, 5 kDa NHS-PEG, and Palmitoyl chloride. Before use, bPEI was dialyzed using 100 kDa MWCO membrane against water for 1 day to remove small impurities. bPEI was reacted with 5 kDa PEG NHS ester, at a 1:100 molar ratio, in a mixed solution of DMSO and HEPES (1:1) at room temperature. The reaction produced PEG-PEI (2P), which was purified by dialysis using a 100 kDa

MWCO membrane for 5 days in water, and collected by freeze drying. PEG-PEI was further reacted with palmitoyl chloride at 1:100, 1:50, and 1:30 molar ratios in THF at 40 °C for 2 hours in the presence of pyridine as a scavenger of a hydrochloric acid byproduct to create PEG-PEI-PAL (3P), 3P mid, and 3P low respectively. The reaction solutions were precipitated in diethyl ether and subsequently dialyzed in water prior to freeze drying.

### 2.2.3. Characterization of stabilized TNAs

The purity and uniformity of TNAs were determined by gel permeation chromatography (GPC) (Asahipak GF-7M column, 2 mg/mL, PBS, 0.5 mL/min, 40 °C) Molecular weights were determined by comparing peak retention time to PEG standards. The diameter and surface charge of TNAs were determined by dynamic light scattering and zeta potential measurements (Zetasizer Nano, Malvern, UK). Particle solutions of 2 mg/ml were loaded into disposable zeta cuvettes and read for particle size and then zeta potential in the usage.

Extent of palmitoylation was examined by fluorescamine assay. Fluorescamine powder was dissolved in DMSO to 10 mg/ml. Particles were dissolved in a 50/50 mixture of DMSO/water to a concentration of 1 mg/ml. 100 μL of each particle solution and blank DMSO/water was added to a clear 96 well plate and then 10 μL of the fluorescamine solution was added immediately before reading on a fluorescent plate reader at 390/460 excitation/emission (SpectraMax M5, Molecular Devices). The fluorescence intensity of the blank was subtracted from the experimental wells and then experimental wells compared with each other.

### 2.2.4. Analysis of TNAs and siRNA Interactions

To determine siRNA/TNA complex formation ratios, TNA complexes were formed by mixing solutions of particles at several concentrations from 0.1 and 100 mg/ml in Optimem with 720 nM siRNA in Optimem. Solutions were mixed at a 1:1 ratio and allowed to equilibrate for 30 minutes at room temperature. 20 μL of each solution and 5 μL of low range DNA ladder were loaded to 4% agarose gel and run at 100 volts for 80 minutes at room temperature. The gel was stained in 200 ml of 100 ng/ml ethidium bromide in TAE (Tris-Acetate 0.04 M, EDTA 0.001 M) buffer, rinsed 3 times in TAE buffer, and imaged via Typhoon GLA 9500 (GE Healthcare, Logan, UT) fluorescent imager under the ethidium bromide filter set.

siRNA release from TNAs was determined using a competing anion assay. Complexes were formed by mixing solutions of particles, concentrated in optimem media at 10 mg/ml, with 720 nM fluorescently-labeled siRNA optimem solution at a 1:1 ratio to a final concentration of 5 mg/ml of particle and 360 nM of siRNA for 30 minutes at room temperature. 20 μL of the complex solutions were added to 10 μL solutions of varying heparin concentration. 0, 10, 100, 1000, and 5000 μg/ml concentrations were used to create weight ratios of siRNA/heparin between 0 and 500. 10 minutes later, 20 μL of each solution was loaded onto an agarose gel and run at 100 V for 80 minutes. The gel was imaged using Typhoon equipped with a cy3 filter set (dylight-547 compatible).

siRNA protection by TNAs was determined by TNA/siRNA complex incubation in media containing RNases. Complexes were prepared for particle-siRNA release study above were also used for siRNA protection study. Complex solutions (20 μL) were incubated with 20 μL of active FBS or heat-inactivated FBS. A control was created by

adding complex solution to RNase free water (20 μL, respectively) and then frozen. 20 μL of sample solution was loaded and run on 4% agarose gel in TAE buffer at 100 V for 80 minutes. After the gel was run, the gel was imaged with Typhoon through the cy3 filter set.

### 2.2.5. *In vitro* transfection efficiency of TNAs

Cells were seeded at 5,000 cells per well into a white opaque 96 well plate for 24 hours. After 24 hours, Complex solutions were created by mixing 100 μL of 10 mg/ml particle solutions with 100 μL of 720 nM anti-luciferase siRNA, all solution in optimem. These were incubated at room temp for 30 minutes. Control Solutions were created by setting aside 200 μL of optimem for a blank control and mixing 100 μL of 720 nM anti-luciferase siRNA solution with 100 μL optimem or 100 μL of optimem containing 5 μL of RNAiMAX agent to create a naked siRNA control and RNAiMAX control, respectively. These were incubated at room temp for 30 minutes except the RNAiMAX control which was incubated for 20 minutes, per manufacturer's instructions.180 μL of each solution was added to 720 μL of McCoy's 5A supplemented with 10% FBS creating a final concentration of 1 mg/ml particle concentration, 72 nM siRNA, and 0.5 μL well of RNAiMAX concentration. Media was removed from each well and 100 μL of complex solutions and controls were to the wells, n=8. The plates were incubated until their endpoints (24, 48, or 72 hours) and then assayed for bioluminescence. Cells were injected with 100 μL of 0.1 mg/ml luciferin solution in PBS via a GloMax luminometer (Promega). Bioluminescence intensity was integrated over a 10 second period and recorded by the luminometer. Blank control wells were used to compare normal bioluminescence intensity to the experimental wells and data is reported as percentage

luciferase activity. This data was then normalized based on a viability assay described later to account for cell death in the reduction of luciferase signal. For the 2P/3P combination experiments after 24 hours incubation, 20 μL of media was removed from each well. 20 μL of 10 mg/ml 3P optimem solution was added to wells containing 2P and 20 μL of optimem was added to all other wells. Cells were then incubated for a further 48 hours, and subjected to viability and bioluminescence assays as described previously.

### 2.2.6. Toxicity of TNAs *in vitro*

After the transfection assay was completed, each plate underwent a resazurin assay. 10 μL of a 100 mM solution of resazurin in PBS was added to each well of the 96 well plate. The plate was returned to the incubator for 3 hours and then read on a SpectraMax M5 (Molecular Devices) fluorescent plate reader at an excitation/emission of 560/590. A control of blank media with resazurin was used to subtract out background fluorescence and then fluorescence intensity was compared between each experimental well and the blank control wells to give a percentage of viable cells.

### 2.2.7. *In vitro* intracellular uptake and trafficking of fluorescent siRNA in TNAs

8 well glass slides were plated with 10,000 cells per well in McCoy's 5A media supplemented with 10% FBS. 24 hours later, complex solutions were created based on the endpoint of the imaging study. To image siRNA within the cell, 30 μL of 10 mg/ml unlabeled particle solutions and 30 μL of 720 nM dylight-547 labeled siRNA were mixed. To image siRNA/particle colocalization, 30 μL of 10 mg/ml fluorescein labeled particle solutions and 30 μL of 720 nM dylight-547 labeled siRNA were mixed. To image particle/lysosome colocalization, 30 μL of 10 mg/ml fluorescein labeled particle

solutions with 30 μL of 720 nM unlabeled siRNA were mixed. To image combination of 2P/3P, 30 μL of 10 mg/ml fluorescein labeled 2P solutions with 30 μL of 720 nM unlabeled siRNA were mixed. Controls of naked siRNA and blanks were created by mixing 30 μL of 720 nM dylight-547 labeled siRNA with 30 μL of optimem and 30 μL of optimem with 30 μL of optimem, respectively. All solutions were incubated at room temp for 30 minutes. Afterwards, 60 μL of each solution was added to 240 μL of McCoy's 5A supplemented with 10% FBS creating a final concentration of 1 mg/ml particle concentration and 72 nM siRNA. Media was then removed from each well and 200 μL of complex solutions were added to the wells and incubated for 48 hours. Additionally, for the 2P/3P combination study, 24 hours after dosage 30 μL of media was removed from the well and 30 μL of 10 mg/ml fluorescein labeled 3P was added. 48 hours after dosage, cells were rinsed with PBS 3 times, fixed with formalin for 20 minutes, stained with Hoechst 33342 and Lysotracker red (if applicable), and rinsed another 3 times. Cells were imaged at 100X on a Zeiss axiovert 200M fluorescent microscope using dapi, texas red, and fluorescein filter sets. Images were captured for the fluorescein and Texas red filter for fluorescein particles and siRNA, respectively, while using the same exposure between images to compare fluorescent intensity between them.

Cells (5,000 cells/well) were seeded into a white 96 well plate. After 24 hours, Complex solutions and controls were created by mixing 100 μL of 720 nM dylight-547 labeled siRNA optimem solution with 100 μL of 10 mg/ml 3P optimem solution or 100 μL of optimem, respectively. These were incubated at room temp for 30 minutes. One plate was stored in 4C for 30 minutes along with particle and control solutions to be used with the plate. Media was removed from the wells and 100 μL of control and complex

solutions were added to the plate (n=4). The plated was returned to 4 ºC. Another plate was treated identically but kept at 37 ºC. After 4 hours, the plates were rinsed with cold PBS three times and read on a fluorescent plate reader at excitation/emission of 557/570. The fluorescence intensity was compared with an untreated control well at each temperature.

## 2.3. Results

### 2.3.1. The hydrophobicity of the TNA core reduces interactions between siRNA and TNA

TNAs were synthesized as shown in **Figure 2.1**. All TNAs were uniform and contained no impurities as confirmed by a single peak shown on GPC (**Figure 2.2**). DLS and zeta-potential measurements confirmed that 2P and 3P were less than 40 nm in diameter and had a neutral surface charge regardless of PAL modification (**Table 2.1**). These results indicate that PAL is mostly present in the core of TNAs and the PEG shell efficiently shields the charge and hydrophobic groups. However, there is a discrepancy between the DLS measured polydispersity index (PDI) and the sharpness of the GPC peak from 3P.

Modification of the core with PAL groups did not seem to affect the surface properties of TNAs although it altered lipophilicity and molecular conformation of the core. GPC revealed that the molecular weights of 2P and 3P were 128 and 158 kDa, respectively. Although the exact number of primary amines on bPEI is unknown, our estimation based on the molecular weights of bPEI (25 kDa) and TNAs suggests that approximately 10% and 55% of binding sites on bPEI were conjugated with PEG and

PAL, respectively. To further confirm the reaction, a fluorescamine assay was used to compare the amounts of remaining primary amines between 2P and 3P. 3P contained fewer primary amines per particle than 2P, corresponding with the GPC estimation.

Interactions between siRNA and TNAs were characterized in 3 different ways: siRNA uptake by TNAs, binding strength of TNA to siRNA, and protection of siRNA from degradation. To confirm siRNA entrapment, **Figure 2.3** shows various concentrations of particle complexed with a fixed concentration, 5 μg/ml for effective visualization, of siRNA. 2P showed partial siRNA entrapment at particle concentrations between 0.05 and 0.5 mg/ml, and full complexation at 5 mg/mL and above. This gives the weight ratio between particle and siRNA necessary for complete entrapment of siRNA within the particle. 3P showed partial entrapment only at 50 mg/ml yet required a concentration for complexation too high for in vitro experiments.

**Figure 2.3** also shows how strongly siRNA was bound to the particles by measuring its release from siRNA TNA complexes after incubation with increasing siRNA/anion weight ratios of a competing anion heparin, a glycosaminoglycan found in extracellular matrices of many tissues. This was used to mimic conditions the TNA complex would encounter once inside the cell as ionic binding competition is the most common mechanism of siRNA release. 2P appeared to require a large ratio of heparin to release siRNA, indicating a large binding affinity, while 3P showed no heparin necessary for release as it failed to form stable complexes with siRNA.

In order to examine the potential of TNAs to protect siRNA from degradation, TNA complexes were incubated with a high level (50%) of FBS. Both naked siRNA and 3P complexes were unstable in the presence of both active and heat-treated FBS due to

nuclease degradation, whereas 2P protected siRNA for the duration. This was expected as 3P had not previously shown complexation with siRNA but 2P had shown tight binding to the siRNA. These results would give 2P greater potential as an in vivo formulation compared with 3P because of 2Ps ability to form complexes and protect the siRNA.

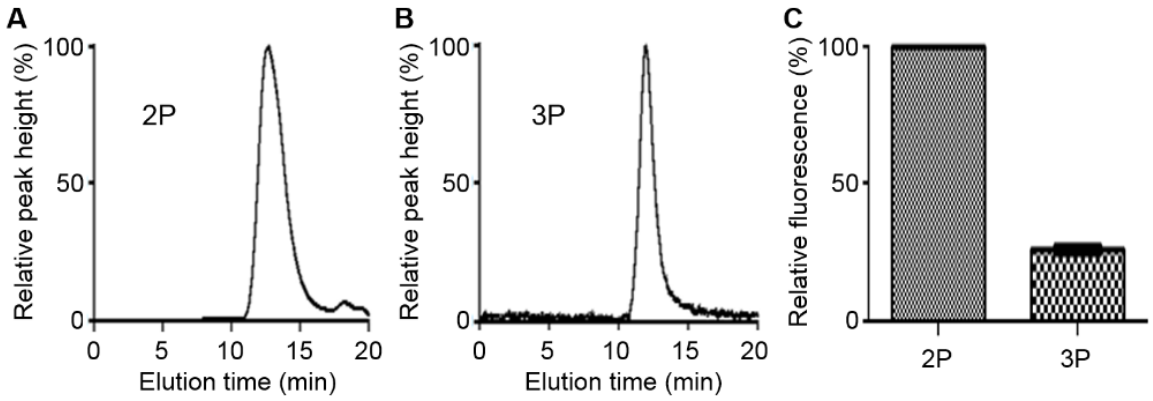


**Figure 2.2. Characterization of TNAs.**

GPC spectra showing uniform size distribution and purity of 2P (A) and 3P (B). Primary amine assay using fluorescamine to determine relative primary amine content of 3P compared to 2P (C), approximately 35% primary amines remain on 3P compared to 2P.

**Table 2.1. Particle diameter, polydispersity index (PDI), and zeta potential of 2P and 3P particles**

| | 2P | 3P |
|---|---|---|
| Size (nm) | 23.19 ± 1.05 | 34.33 ± 3.95 |
| PDI | 0.18 | 0.559 |
| Zeta Potential (mV) | 2.66 ± 0.32 | -1.99 ± 0.23 |

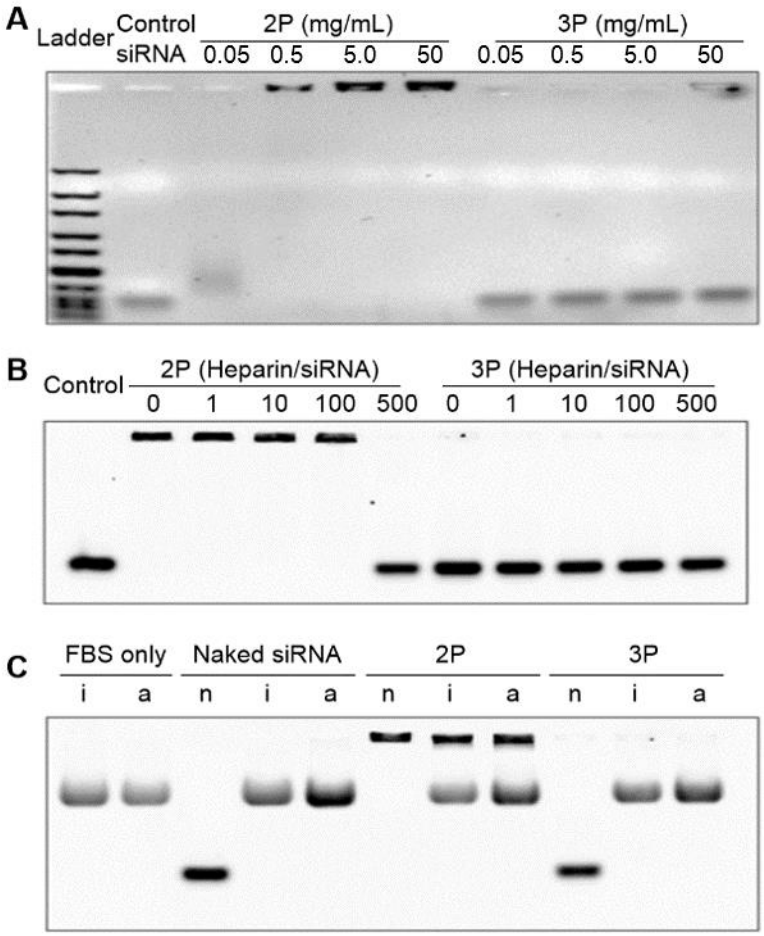


**Figure 2.3. Complex formation and stability of TNAs.**

TNAs were mixed with siRNA (360 nM) at varying ratios to determine a particle concentration required for forming neutral siRNA complexes (A). siRNA-loaded TNAs (5 mg/mL) were incubated with heparin to determine complex stability in the presence of anionic counterparts other than siRNA in a solution (B). siRNA-loaded TNAs were also incubated with nuclease free water (n), heat-inactivated FBS (i), and active FBS (a) to determine protective effects of TNAs in cell culture media with digestive enzymes (C). Naked siRNA at 360 nM and FBS alone used as controls.

### 2.3.2. Increased hydrophobicity of the TNA core increases TNA transfection efficiency

In order to assess the delivery efficacy of the TNA complexes, bioluminescence was used as a facile method of protein reduction quantification. Luciferase protein was introduced to HT-29 colorectal adenocarcinoma cells so that it was stably expressed at all times (HT-29-LUC). Anti-luciferase siRNA uses the RNAi pathway to degrade luciferase mRNA, attenuating protein production. This allows for easy detection of remaining protein by addition of luciferin substrate. The amount of protein remaining correlates to siRNA delivery efficacy[18].

HT-29-LUC cells were incubated with siRNA-TNA complexes and 72 hours later the cells were examined for luminescence and cell viability (**Figure 2.4**). Particle concentrations used were 1 mg/ml or 20% that of what was found to be full complexation in previous experiments (5 mg/ml) due to 20% the amount of siRNA (1 μg/ml) to be used in vitro. Initially, 2P showed no transfection but 3P showed approximately 70% reduction of the luciferase activity, attributed to siRNA delivery. The transfection efficiency of 3P was comparable to that of Lipofectamine RNAiMax, a commercially available transfection reagent. To further examine the transfection efficiency of both particles, transfection was monitored daily for total 4 days past dosage. 3P and RNAiMax showed a similar transfection profile, reducing luciferase expression continuously for 4 days, but 2P induced no transfection in the same period of time. Additionally, neither 2P nor 3P exhibited any noticeable toxicity under our experimental condition while RNAiMAX showed mild toxicity with approximately 20% reduction in cell viability.

Further confirmation of siRNA delivery was shown by fluorescent imaging with fluorescently labeled siRNA. This allowed for viewing of the amount of siRNA used within the cells for each formulation (**Figure 2.5**). Compared with the non-treatment and free siRNA incubated cells, both TNA formulations showed siRNA within the cell. However, cells incubated with 3P complexes showed a much larger fluorescent intensity through confocal microscopy than those incubated with 2P indicating that 3P was able to increase the amount of siRNA that would be trafficked into the cell.

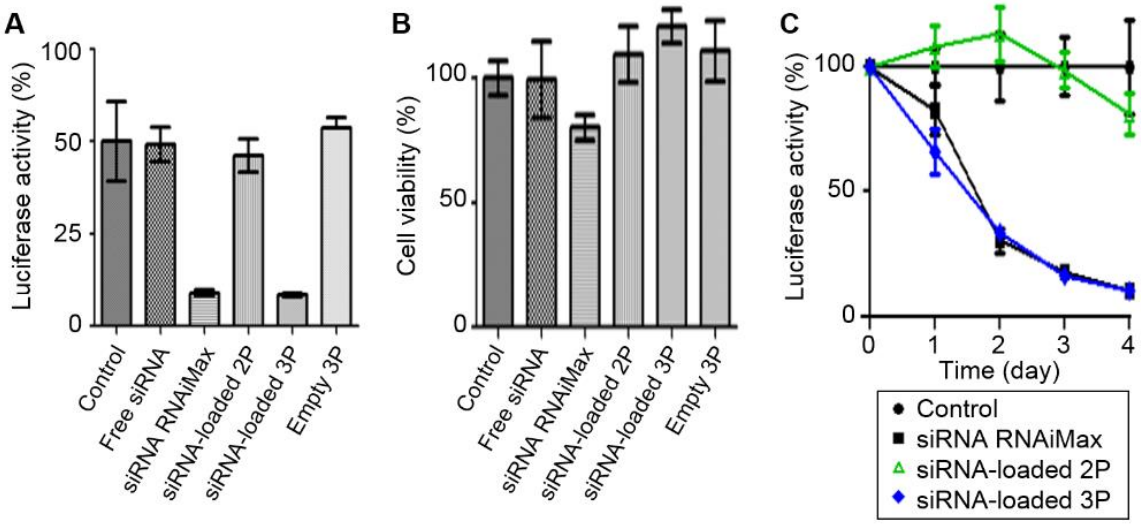


**Figure 2.4. Transfection efficiency and toxicity of TNAs.**

A human colon cancer HT-29 cell line stably expressing a luciferase reporter gene was transfected with TNAs to monitor luciferase activity (A) and cell viability (B) after 72 hours of incubation. Transfection profiles over a 4-day period were taken to determine long-term gene silencing effects of TNAs (C).

### 2.3.3. Hydrophobic modification of nanoassembly core increases intracellular siRNA delivery and endosomal escape

Because of PAL's ability to interact with cellular membranes, it was necessary to determine if the 3P particle was entering the cell through an endocytotic pathway or through membrane disruption (**Figure 2.6**). To observe this, cells were incubated with TNA complexes containing fluorescent siRNA at 4 °C and 37 °C. At 4 °C endocytosis is significantly reduced whereas at 37 °C cells operate under normal conditions. By comparing intracellular uptake of TNAs at these temperatures the importance of an endocytotic pathway in TNA uptake can be elucidated. The results show larger fluorescent intensity for those cells incubated at 37 °C, indicating that TNAs enter the cell through endocytosis in a greater amount than non-specific membrane disruption as seen with other cationic polymers and PAL-conjugated bPEI.

Intracellular fluorescent imaging was further used to elucidate TNA complex intracellular distribution and siRNA release, following cell internalization (**Figure 2.7**). First, siRNA release from the TNAs was examined. Fluorescein labeled TNA complexes with dylight-547 labeled siRNA were incubated with cells for 48 hours. 2P was colocalized with siRNA in a greater amount compared to 3P, which would result in minimal siRNA being released into the cells. Minimal siRNA release would result in low or no transfection occurring and this correlates well with the previous in vitro results. 3P's lower colocalization would be expected with its lack of complex formation.

Next, endosomal escape (**Figure 2.7**) by the TNA complexes was examined. Fluorescein labeled TNA complexes were incubated with cells similarly and dyed with a lysosome stain. 2P complexes colocalized in lysosomes and 3P complexes showed less lysosomal colocalization. These results suggest 2P did not escape endosomes as efficiently as 3P and 2P's reduced transfection efficiency was attributed to less endosomal escape.

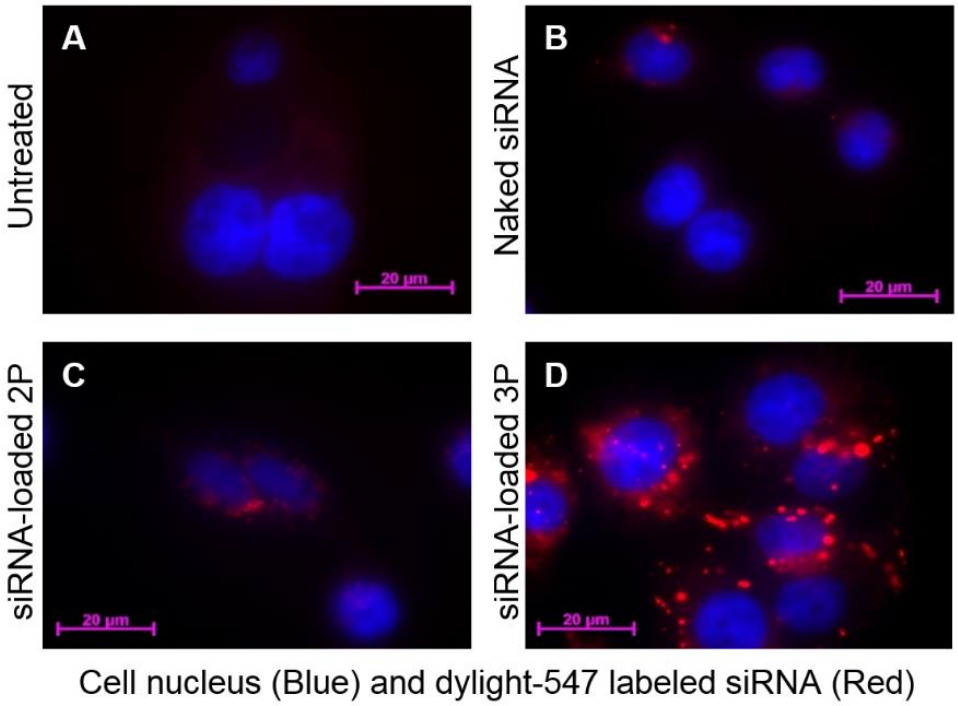


**Figure 2.5. Fluorescent microscopy.**

HT29 cells were incubated with TNAs (1 mg/mL) containing dylight-547 labeled siRNA (72 nM) to confirm intracellular delivery of siRNA at 48 hours post-transfection, following the treatment of cells with PBS (A), naked siRNA (B), 2P complexes (C), and 3P complexes (D).

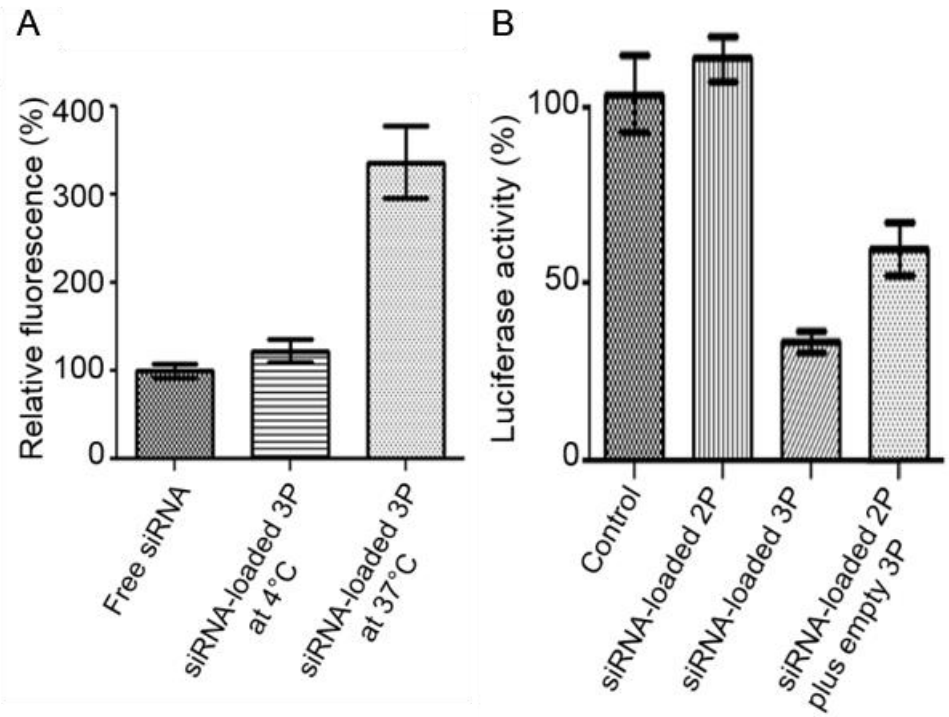


**Figure 2.6. Elucidation of siRNA transfection mechanisms for TNAs.**

Cells were treated with siRNA-loaded TNAs at an incubation temperature that endocytosis is active (37 °C) or suppressed (4 °C) to determine the intracellular uptake mechanism for TNAs (A). Cancer cells treated with siRNA-loaded 2P were incubated with empty 3P at 24 hours post transfection to demonstrate a unique property of 3P that enhances siRNA transfection alone or in combination with 2P (B).

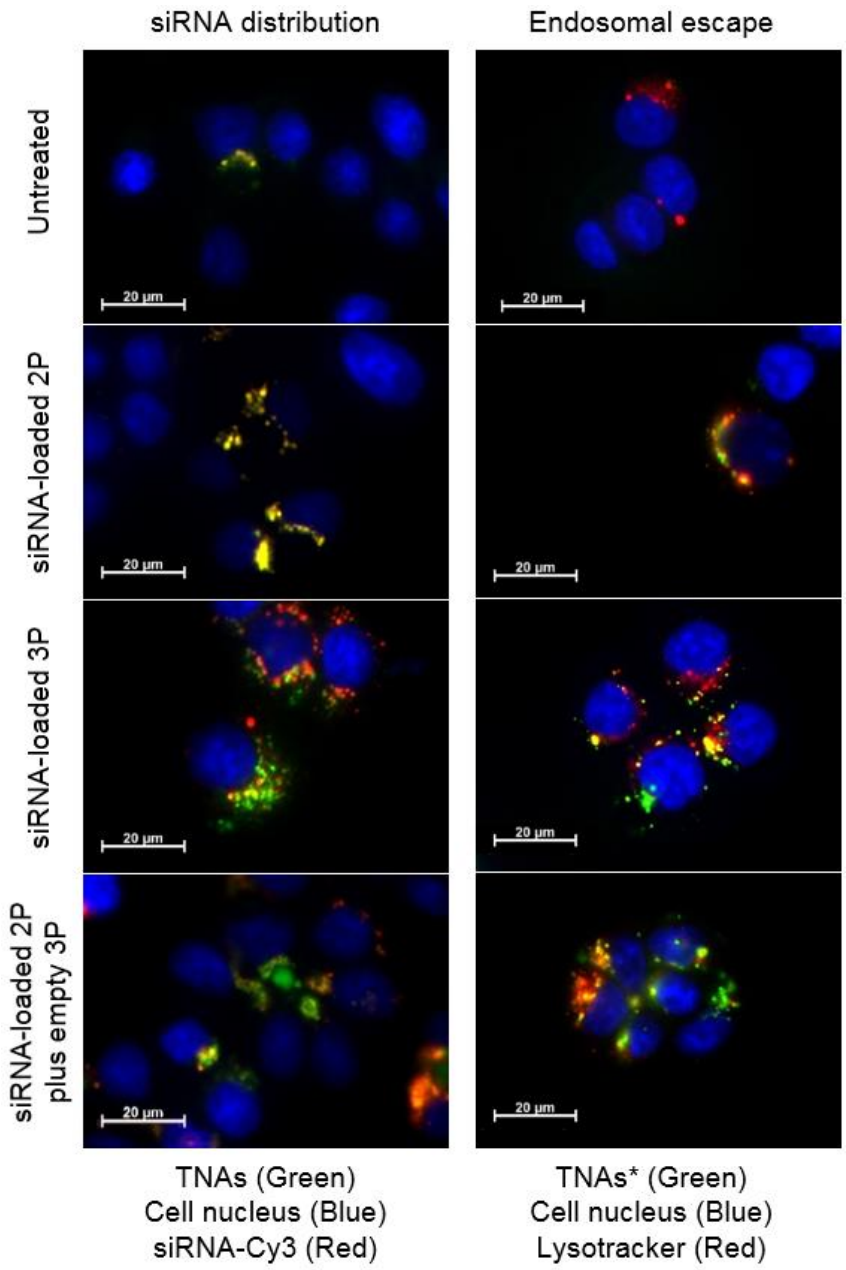


**Figure 2.7. Intracellular distributions of siRNA-loaded TNAs.**

Fluorescence images of cells were taken at 48 hours post-transfection to determine the release of siRNA from TNAs as well as endosomal escape of TNAs during transfection. *TNAs were entrapped with non-labeled, anti-luciferase siRNA to avoid fluorescence signal interference between the siRNA and Lysotracker.

### 2.3.4. Combined dosage of hydrophobic modified and unmodified TNA decreases colocalization of siRNA in endosomes

A combinatorial approach to TNA transfection was examined to help elucidate 3P's role in transfection efficacy as well as attempt to protect siRNA while achieving transfection. 2P-siRNA complexes were incubated with cells for 24 hours and then empty 3P particles introduced (**Figure 2.6**). It was found that the addition of empty 3P did increase the transfection efficiency of 2P-siRNA complexes from 0% to 60%.

A closer look at the intracellular trafficking of this dosage was achieved through fluorescent microscopy. Colocalization between siRNA and particle was relatively less compared with 2P as shown in **Figure 2.7**. The combinatorial dosage also showed a relative reduction in colocalization between endosome and particle, indicating that particles and siRNA were escaping endosomes, previously not seen with 2P particles alone. This gave a greater indication that 3P has a greater endosomal escape capability compared with 2P and that it may lend it to other particles taken up by the cell concurrently.

### *2.3.5.* Modulating the hydrophobic substitution of TNA core increases transfection efficiency while decreasing siRNA/particle interactions

Because of the success of the 2P/3P combination approach, the ratio of PAL substitution on 3P was examined to find an optimal ratio where 3P could form complexes with siRNA. This would enable 3P to protect cells so that a less complicated approach could be taken compared to the combination 2P/3P described in the previous section. Two additional TNAs were synthesized by aiming for 15% and 25% palmitoylation of

2P, named 3P low and 3P mid, respectively. The amounts of primary amines remaining in the core of 3P low and 3P mid were determined by a fluorescamine assay (**Figure 2.8**). The assay indicated that palmitoylation was achieved at differing levels compared with the initial 3P particle. Gel electrophoresis was performed to confirm siRNA complexation with 3P low and 3P mid. 3P low achieved complexation between 0.5 mg/ml and 1.0 mg/ml, significantly lower than the original 3P at 72 nM siRNA concentration. 3P mid began to form partial complexes at 1 mg/ml but required a higher polymer concentration for complete complexation.

To examine the effect of palmitoylation on transfection efficiency, cells were incubated with each form of 3P complexes with siRNA for 72 hours. Though 3P low was able to maintain a complex with siRNA, it did not find more than 20% transfection efficiency but the partial complexes formed by 3P mid increased transfection efficiency further. This showed a positive correlation between PAL content on 3P and transfection efficiency as well as provided insight into PAL's role on transfection.

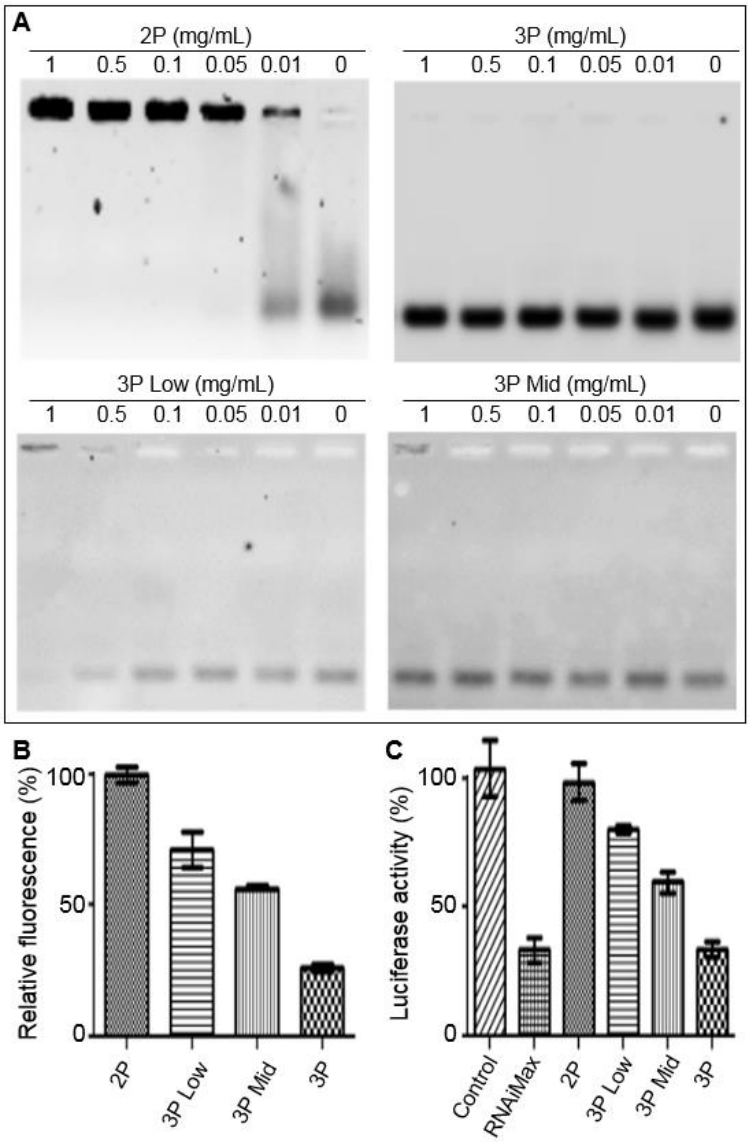


**Figure 2.8. Complex formation and siRNA transfection of TNAs with varying PAL contents in the core.**

TNAs were confirmed to entrap siRNA less efficiently as the amount of PAL conjugated in the core increased, which were determined by gel electrophoresis (A) and fluorescamine assay (B), respectively. Conversely, siRNA-loaded TNAs transfected cells more efficiently during a 72-hour period as the amount of PAL in the core increased (C).

## 2.4. Discussion

siRNA therapy has shown much promise in the treatment of genetic diseases, such as cancer, at the *in vitro* level by reducing expression levels of proteins currently unable to be target by drugs. However, few formulations evaluated *in vitro* have moved to the *in vivo* level or clinical trials. Most of the issues encountered in moving to *in vivo* involve lack of stability in the bloodstream which ultimately lead to low transfection efficiency. Many formulations have attempted to address these issues by using a linked, or crosslinked[119-120], polymer system or a hydrophobic core[121] to stabilize both the particle and its complex with siRNA. Here we have taken tethered nanoassemblies (TNAs) which consist of a unimolecular pegylated PEI system (2P) and modified its core to include a hydrophobic region (3P) to examine its effects on stability and transfection efficiency as well as elucidate its effect on improving the system as a siRNA delivery vehicle.

Delivery vehicles for siRNA therapy must focus on 3 factors effected by complex stability: delivery of the siRNA to its target site, protection of the siRNA from degradation, and release of the siRNA into the cytoplasm of the cell. Both physical properties of the particle and thermodynamic properties of the TNA/siRNA complex can determine if it will meet these criteria and improve its chance at becoming a working *in vivo* system[122]. In terms of physicochemical properties, both particles have beneficial surface charge and size for in vivo delivery. Pegylation reduced surface charge to a neutral state and increased the empty particle diameter was between 20-40 nm which is beneficial for enhanced circulation time and decreasing off-target interactions[122-123].

Although both particles had similar physical properties, only 2P was able to form a stable complex with siRNA. 2P was shown to bind strongly to siRNA and protect it from

degradation. Tight binding, as indicated by the complexes resistance to competing anions, would typically indicate an effective particle[124]. Resistance to competing anions is indicative of the vehicle being capable of maintaining it's complex with siRNA in the blood stream when presented with other negatively charged moieties[107]. However, if the complexes are too stable then it is troubling from a therapeutic perspective as the complexes may have difficulty releasing siRNA inside targeted cells[125]. In contrast, 3P was unable to form complexes at concentrations lower than 50 mg/ml or protect siRNA from degradation. This result was surprising because 3P was found to have active primary amines present in formulation, as indicated by the fluorescamine assay, but it required more than 100 times the amount of particle to show even slight complexation. The ratio of active amines to siRNA for complexation differed between 2P and 3P, indicating that the addition of PAL to the nanoparticle core can interfere with free primary amines possibly by condensing in the core around active amines to block their interaction with siRNA. This indicates hydrophobic modification to the core of TNAs causes a decrease in complex stability.

The result contradicted our initial hypothesis as PAL was expected to increase stability of the TNA/siRNA complex rather than reduce it. Though the primary amines may be blocked from interacting with siRNA by the hydrophobic group, it would not affect the fluorescamine interaction since the hydrophobic nature of fluorescamine, its size, and the presence of organic solvent may allow for fluorescamine to reach the amine groups in 3Ps core. It is unclear if the addition of organic solvent during siRNA complexation would allow stable complex formation with 3P. Despite its lack of complex formation, 3P was able to transfect cells with much greater efficiency than 2P. Again, this

would appear to contradict traditional thinking that a strong complex is necessary for effective transfection. This must mean that 3P is moving siRNA into the cell more effectively than 2P, as we see a greater amount of siRNA within the cell after dosages. Two pathways are common for cellular internalization of nanoparticles: endosomal pathway and membrane disruption[126]. Membrane disruption occurs when a lipid fuses with a membrane to create holes or help push through them. This has been seen with other lipid containing nanoparticles, such as liposomes and micelles[127-128]. As the lipid portion of 3P should be localized to the core and protected by a PEG shell, an endosomal pathway is the most likely of these two pathways. After experimentation, it was confirmed that endocytosis was the major pathway of TNA uptake (**Figure 2.6**).

Considering that the TNAs enter the cell via endocytosis, endosomal escape of the TNAs would be crucial to delivering the siRNA to the cytoplasm of the cell. Without a mechanism to remove the TNA/siRNA complex from the endosome, transfection efficiency would be greatly reduced. While there are many mechanisms for this, bPEI is hypothesized to exhibit the proton sponge effect[129]. The proton sponge effect is a type of hydrogen ion buffering where the hydrogen ions and chloride ions entering the endosome are absorbed by the amines within bPEI. This causes more and more ions to be pumped in the endosome in order to lower the pH, to become a lysosome. Eventually the endosome swells and bursts, releasing the particle[130]. This is considered to be the main mechanism of endosomal escape for many cationic polymer systems[131-132]. Another mechanism is cellular membrane disruption through direct interaction between cationic bPEI and anionic lipid layers[125]. In this case, the mechanism of endosomal escape is unclear but PAL addition seemed to be key in assisting disruption of the endosome. The

colocalization images (**Figure 2.7**) showed that 2P remained within the lysosomes with its siRNA payload but 3P had little colocalization with either. This indicates that 2P has lost some of its natural endosomal escape property but addition of PAL returned an endosomal escape method, either by proton sponge or membrane disruption via PAL. This would show that PAL must play a major role in the 3P's transfection ability possible through endosomal escape enhancement. However, it is important to note that based on design PAL is presumed to be within the core of 3P but the discrepancy between the PDI value and GPC peak could indicate some weak hydrophobic interaction between particles. Aggregates between small numbers of particles would account for large PDI seen via DLS measurement (**Table 2.1**) and indicate a mild interaction with PAL between particles. This would not necessarily be seen in the GPC data due to shear stress and column interaction during measurement. Therefore, palmitate may be present in low amounts near the surface of the nanoparticle. Further study of how 3P delivered siRNA into the cell is necessary.

It must be noted that combination of both 2P and 3P nanoparticles would provide an effective siRNA delivery system where 2P complexes would protect the siRNA and empty 3P would assist in endosomal escape. Colocalization images provided evidence for this, showing less particles within the endosome and less siRNA within the particles. This also shows that 2P is able to release its siRNA once it is within the cytoplasm of the cell. However, the success of this 'combined' formulation may depend on the co-delivery efficiency of both particles, and therefore developing a single particulate system might be still a viable option. In this chapter, we have found that increasing lipophilicity of the core of siRNA TNA complexes with PAL would be beneficial to enhance siRNA

transfection, as others have seen. However, PAL's hindrance to siRNA loading still remains a major challenge to developing polymer nanoassemblies with a lipophilic core for future clinical applications. It may be possible to optimize transfection efficiency and siRNA loading in polymer nanoassemblies by utilizing alternate moieties as the effect of the hydrophobic group in enhancing siRNA transfection appeared evident.

## 2.5. Conclusions

In this chapter, TNAs were used to evaluate the effects of hydrophobic modification of the TNA core on TNA/siRNA complex stability and transfection of siRNA. The results showed that nanoassemblies with a hydrophilic, cationic core (2P) either bind siRNA too tightly to release their siRNA payload once inside the cell or are unable to escape the endosome. Both of these factors are crucial for an efficacious delivery system. However, TNAs with a hydrophobic, partially cationic core (3P) appeared to fail to form stable siRNA complexes but enhance target gene silencing presumably due to enhanced intracellular uptake and endosomal escape of siRNA. Further investigation demonstrated that a combined formulation of 2P and 3P was effective to protect siRNA and achieve effective transfection, which revealed that PAL conjugated in the core of nanoassemblies played an important role in determining the fate of siRNA-loaded nanoassemblies in the cell. Taken together, we conclude from this chapter that ionic and hydrophobic interactions should be considered concurrently in the design of siRNA delivery carriers to guarantee stability and transfection efficiency.

# Chapter 3: Effects of TNA shell modification on siRNA transfection

This work was adapted with permission from work published by the author in AIMS Bioengineering on November 16th, 2016[133].

## 3.1. Introduction

siRNA therapy holds promise as a method to treat genetic diseases through degradation of specific protein mRNAs, thereby reducing their expression[96, 134]. Reducing the expression of these targeted proteins allows for treatment of many different diseases, including those with few therapeutic options[135-137]. However, this therapy is hindered by a lack of stability in the bloodstream[98-99, 138] and incurs the need for a delivery vehicle in order to improve the therapy. Cationic polymers, such as polyethylenimine (PEI), have intrinsic properties that aid in their development as delivery vehicles by enhancing protection of siRNA and escape of endosomes resulting in high transfection effeciencies[102]. Cationic PEI interacts with anionic siRNA to form ionic complexes, offering protection from RNase degradation and renal clearance[105]. These siRNA/PEI complexes have a highly cationic surface charge which can be used to interact with cellular membranes, promoting uptake through endocytosis, and endosomal escape[139-140].

However, the surface charge of siRNA/PEI complexes can limit their applications *in vivo*. The cationic surface charge of siRNA complexes has induced toxicity and reduced stability of the particle in the bloodstream[73]. Additionally, the cationic surface charge can promote other anionic compounds to interact with the siRNA/PEI complexes which increases dissociation due to counter ions. This causes decreased complex stability resulting in the release of polymer and free siRNA before reaching their target site. Released polymers may disrupt cellular membranes and cause further toxicity, while siRNA would leave the body and not have therapeutic effects. To address these issues,

chemical modifications to cationic siRNA/PEI complexes are often made to neutralize the surface charge. A common modification to shield surface charge and stability of complexes is to chemically conjugate poly(ethylene glycol) (PEG), a biocompatible and non-ionic polymer, to cationic PEI chains[111]. In previous studies, chemical conjugation of PEG significantly reduced toxicity of PEI by avoiding uncontrolled aggregation/dissociation of the PEG-conjugated PEI and genetic cargos[141-142]. PEG prevents interactions of siRNA complexes with anionic materials in the bloodstream and cellular membranes by forming a neutral, hydrophilic shell around siRNA/PEI complexes[143]. Preventing interactions can lessen the toxicity and enhance the stability of PEI complexes compared to unmodified PEI complexes.

In the previous chapter, PEG-PEI-based nanoparticles (TNAs) for siRNA delivery were introduced[95]. The TNAs were < 30 nm in diameter with improved particle uniformity and stability. TNAs exhibited siRNA transfection comparable to a commercial reagent (RNAiMAX)[95]. However, it was found that the PEG-PEI (2P) TNA did not cause transfection which is not consistent with other groups findings[136, 144]. Covalent modification is common among PEI formulations as well as other cationic polymers however the size and attachment percentage varies considerably[145]. This variation of PEG density may alter the transfection efficiency of the PEI. This is evidenced by other reports that PEG decreases endosomal escape[146], which was observed in the previous chapter. Additionally, particle uniformity also effects PEG density. Commercially purchased PEI often contains small impurities (small molecule amine compounds) that are produced by hydrolysis and oxidation during storage. These PEI contaminants can form a mixture of PEG-PEI particles and polymer chains varying in PEG density across particles.

Based on these factors, we hypothesize that reduced siRNA transfection of PEG-PEI particles is attributed to PEG density. Summarized in **Figure 3.1**, this chapter focuses on PEG molecular weight (PEG MW), PEG substitution rate (PEG%), and PEI impurities as factors influencing PEG densities for siRNA/PEI complexes, and aims to elucidate how these factors would influence siRNA transfection in a model human colon cancer cell line (HT29). Towards the aim, a library of siRNA/PEG-PEI complexes was created with varying PEG densities. PEG density was varied by changing the PEG MW and PEG%. siRNA complexes were synthesized using PEG-conjugated PEI nanoparticles made from PEI as purchased (PEG-PEI) or PEI purified by dialysis (PEG-PEI-d). Transfection efficiency of siRNA/PEG-PEI and siRNA/PEG-PEI-d complexes were measured with anti-luciferase siRNA in HT29 stably expressing the luciferase reporter gene.

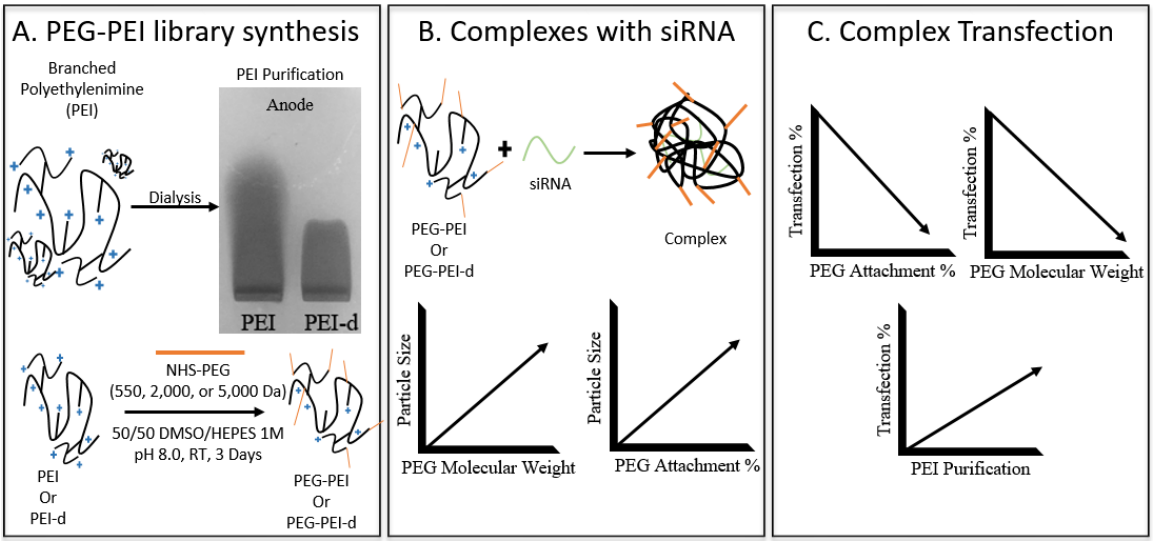


**Figure 3.1. PEG density analysis.**

Synthesis of PEG-PEI library from PEI and purified PEI (PEI-d) as seen by the gel electrophoresis image (A). Hypothetical PEG density effect on PEG-PEI complexes (B). Hypothetical PEG Density effect on PEG-PEI transfection (C).

## 3.2. Materials and Methods

### 3.2.1. Materials and Cells

PEI (25 kDa, branched) was purchased from Sigma Aldrich. PEGs (550 Da, 2 kDa, and 5 kDa α-methoxy-ω-NHS activated, NHS-PEG) were purchased from NOF America. HEPES buffer (pH 8.0, 1 M), NuSieve agarose GTG, dialysis membrane with molecular weight cutoff (MWCO) of 100 kDa, deuterated DMSO, Opti-MEM, SimplyBlue SafeStain, and phosphate buffered saline (PBS 1X) were purchased from Fisher Scientific (Waltham, MA). Anti-Luciferase siRNA was synthesized with the sequence of 5'-GUUGGCACCAGCAGCGCACUU-3. A human colon cancer cell line (HT29) was from American Type Culture Collection (ATCC). HT29 cells were grown using McCoy's 5A with 10% fetal bovine serum (FBS) according to ATCC recommendations. Cells were cultured in a humidified environment with 5% $CO_2$ at 37 °C

### 3.2.2. Synthesis of TNAs of varying PEG substitutions and PEI backbones

We first purified PEI by dialysis (100 kDa MWCO) against water for 2 days. The dialyzed PEI (PEI-d) was collected by lyophilization. PEI and PEI-d (20 µL of a 10 mg/mL) were run on a 2% agarose gel at 120 V for 1 hour to verify the removal of small impurities. The gel was stained with SimplyBlue SafeStain overnight and destained in water for 6 hours. PEG-PEI (or PEG-PEI-d) particles were then synthesized by reacting NHS-PEG with PEI (or PEI-d) in a 1:1 mixture of DMSO:HEPES buffer (1 M) for 3 days at room temperature. Molar ratios of NHS-PEG:PEI were 3:1, 15:1, or 40:1 for 1%, 5%, and 10% (denoted as PEG% of PEI). The reactants were dialyzed against water (100K

MWCO) to remove free PEG and other impurities. PEG-PEI and PEG-PEI-d particles were collected by lyophilization.

PEG-PEI and PEG-PEI-d particles were analyzed via 1H-NMR to obtain the PEG%. Each PEG-PEI (5 mg) was added to deuterated DMSO (500 μL) and run in an NMR (400 MHz Varian NMR). To determine the PEG%, peak areas were compared between the PEI main chain (CH2, 2.6 ~ 3.4 ppm) and PEG conjugated to PEI (CH2, 3.6 ppm). The peak area comparisons determined the molar ratios between PEG chains and primary amines of PEI (214 in average), which were converted to the percent substitution of PEG on PEI. The PEG-PEI and PEG-PEI-d forming unimolecular nanoparticles were analyzed for purity and uniformity by gel permeation chromatography (GPC, Asahipak GF-7M column, 0.5 mL/min, 40 °C, PBS mobile phase).

### 3.2.3. Quantification of size and surface charge of TNAs and complexes

The surface charge and diameter of the particles were determined by measuring zeta potential and dynamic light scattering (DLS, Zetasizer Nano, Malvern, UK). Aqueous solutions of PEG-PEI particles were mixed with siRNA according to their minimum complexation ratio, found in section 3.2.4, for 30 minutes at room temperature. PEG-PEI complexes and empty polymer at a concentration of 1 mg/ml (500 μL) were loaded into disposable zeta cuvettes and analyzed for particle diameter via DLS measurement (Zetasizer Nano, Malvern, UK) and then zeta potential in the same cuvette.

### 3.2.4. Complex formation of TNAs with siRNA

A solution of PEG-PEI particle (1 mg/mL) was mixed with a solution of siRNA in PBS to create a final concentration of particle ranging from 0 to 100 μg/mL polymer

mixed with 72 nM siRNA. PEG-PEI particles and siRNA were mixed at room temperature for 30 minutes. The mixing ratio is described as the N/P ratio, where N is amines on PEI and P is the phosphate groups on siRNA. siRNA/PEG-PEI complexes at varying N/P ratios were analyzed by gel electrophoresis (1% agarose gel, 20 μL loading per well, 120V, 1 hour). The gels were stained with ethidium bromide and imaged with Typhoon GLA 9500 (GE Healthcare, Logan, UT).

### 3.2.5. *In vitro* transfection efficiency and toxicity of TNAs

Cells were seeded in a white 96 well cell culture plate (5,000 cells/well, 100 μL Opti-MEM) and incubated for 24 hours prior to experiments. A solution of each polymer was solubilized in Opti-MEM at 1000X the concentration at which the polymer formed complexes with siRNA (determined by gel electrophoresis). One hundred microliters of polymer dilutions (500X, 200X, and 10X) were added to 100 μL of 720 nM siRNA solution. The mixtures were incubated at room temperature for 30 minutes. Cell culture media (20 μL) in each well was replaced with 20 μL PEG-PEI/siRNA or PEI/siRNA complexes (n = 4). The N/P ratios were 1, 20, 50, and 100 for each well. The plates were incubated for 72 hours, and luciferin (100 μL, 0.1 mg/ml in PBS) was added to each well for luminescence measurement via a GloMax luminometer (Promega). To measure cell viability, a resazurin solution (10 μL, 1 mM) was added to each well. The plates were incubated for 3 hours and live cells were counted on a fluorescent plate reader (SpectraMax M5, Molecular Devices, 560Ex/590Em). The luciferase readings were normalized to cell viability to obtain the percentage of luciferase activity remaining after treatment.

## 3.3. Results

### 3.3.1. Increasing PEG corona density increases particle size and decreases surface charge

PEG-PEI nanoparticles were successfully synthesized by using 25 kDa PEI and PEG with varying molecular weights. A library of PEG-PEI particles with varying PEG densities. NMR confirmed successful modification of two parameters for the particles: PEG MW (550, 2,000, and 5,000 Da) and PEG substitution percent (1, 5, 10%). **Table 3.1** summarizes the synthesis conditions including PEG% aimed and obtained. PEG-PEI particles were characterized by GPC (**Figure 3.2**) and DLS (**Table 3.1**). The GPC shows the removal of free PEG from the PEG-PEI particles. DLS revealed that the diameters of empty particles ranged from 4 nm to over 30 nm. PEG MW and PEG% were considered collectively to determine PEG density on PEG-PEI particles.

PEG MW and PEG substitution rate influenced PEG density directly, and particle diameter increased as PEG density increased. Particles increased their diameter as PEG MW and PEG% increased. A similar trend was observed with the surface charge of the particles. PEG-PEI with low PEG MW and PEG% (e.g., 550 Da or 2 kDa with 1% PEG substitution) showed positive surface charge. The surface charge decreased as PEG MW and PEG% increased, while the larger molecular weight PEGs shielded surface charge better at lower PEG%. **Table 3.1** summarizes particle diameters of PEG-PEI particles forming complexes with siRNA at their minimum complexation ratios (found in section 3.3.3). PEG-PEI particles increased diameter after complexation but less so as PEG corona density increased.

**Table 3.1. Characterization of PEG-PEI and PEG-PEI-d Library**

| Particle Name | PEG MW (Da) | PEG% Aimed | Actual PEG% | | PDI | | Surface Charge (mV) | | Diameter (nm ± SD) | | Diameter after siRNA Complexation (nm ± SD) | |
|---|---|---|---|---|---|---|---|---|---|---|---|---|
| | PEI/PEI-d | PEI/PEI-d | PEI | PEI-d | PEI | PEI-d | PEI | PEI-d | PEI | PEI-d | PEI | PEI-d |
| N/A | 0 | 0 | 0 | 0 | 0.78 | 0.56 | 44.02 | 42.63 | 4.02 ± 0.97 | 4.53 ± 0.59 | 89.69 ± 5.34 | 72.34 ± 9.21 |
| 550-1 | 550 | 0.01 | 0.01 | 0.01 | 0.24 | 0.33 | 9.01 | 2.84 | 6.81 ± 1.69 | 7.21 ± 2.37 | 12.34 ± 2.15 | 14.41 ± 1.54 |
| 550-5 | 550 | 0.05 | 0.062 | 0.055 | 0.23 | 0.3 | 12.4 | 3.29 | 6.86 ± 1.54 | 6.42 ± 1.1 | 11.24 ± 5.23 | 13.68 ± 3.45 |
| 550-10 | 550 | 0.1 | 0.115 | 0.112 | 0.39 | 0.45 | -1.02 | 2.58 | 9.52 ± 2.42 | 9.89 ± 1.67 | 16.78 ± 2.21 | 18.36 ± 2.1 |
| 2K-1 | 2000 | 0.01 | 0.011 | 0.009 | 0.56 | 0.28 | 19.6 | -0.48 | 9.7 ± 1.5 | 8.04 ± 2.02 | 15.14 ± 3.48 | 15.45 ± 4.78 |
| 2K-5 | 2000 | 0.05 | 0.049 | 0.055 | 0.32 | 0.35 | 9.91 | 4.95 | 12.15 ± 3.28 | 17.14 ± 4.23 | 18.25 ± 4.11 | 18.36 ± 2.61 |
| 2K-10 | 2000 | 0.1 | 0.105 | 0.093 | 0.36 | 0.57 | 7.84 | 2.13 | 14.52 ± 4.03 | 23.14 ± 5.2 | 17.58 ± 2.25 | 22.95 ± 6.51 |
| 5K-1 | 5000 | 0.01 | 0.01 | 0.01 | 0.3 | 0.45 | 1.91 | 2.68 | 7.11 ± 1.7 | 14.25 ± 2.77 | 12.57 ± 1.56 | 19.21 ± 1.26 |
| 5K-5 | 5000 | 0.05 | 0.048 | 0.051 | 0.32 | 0.41 | 1.06 | 1.21 | 12.93 ± 2.08 | 20.15 ± 5.33 | 15.24 ± 4.12 | 21.34 ± 6.36 |
| 5K-10 | 5000 | 0.1 | 0.097 | 0.095 | 0.4 | 0.31 | 0.37 | 0.11 | 13.41 ± 2.8 | 33.87 ± 10.02 | 20.83 ± 3.22 | 31.25 ± 5.22 |

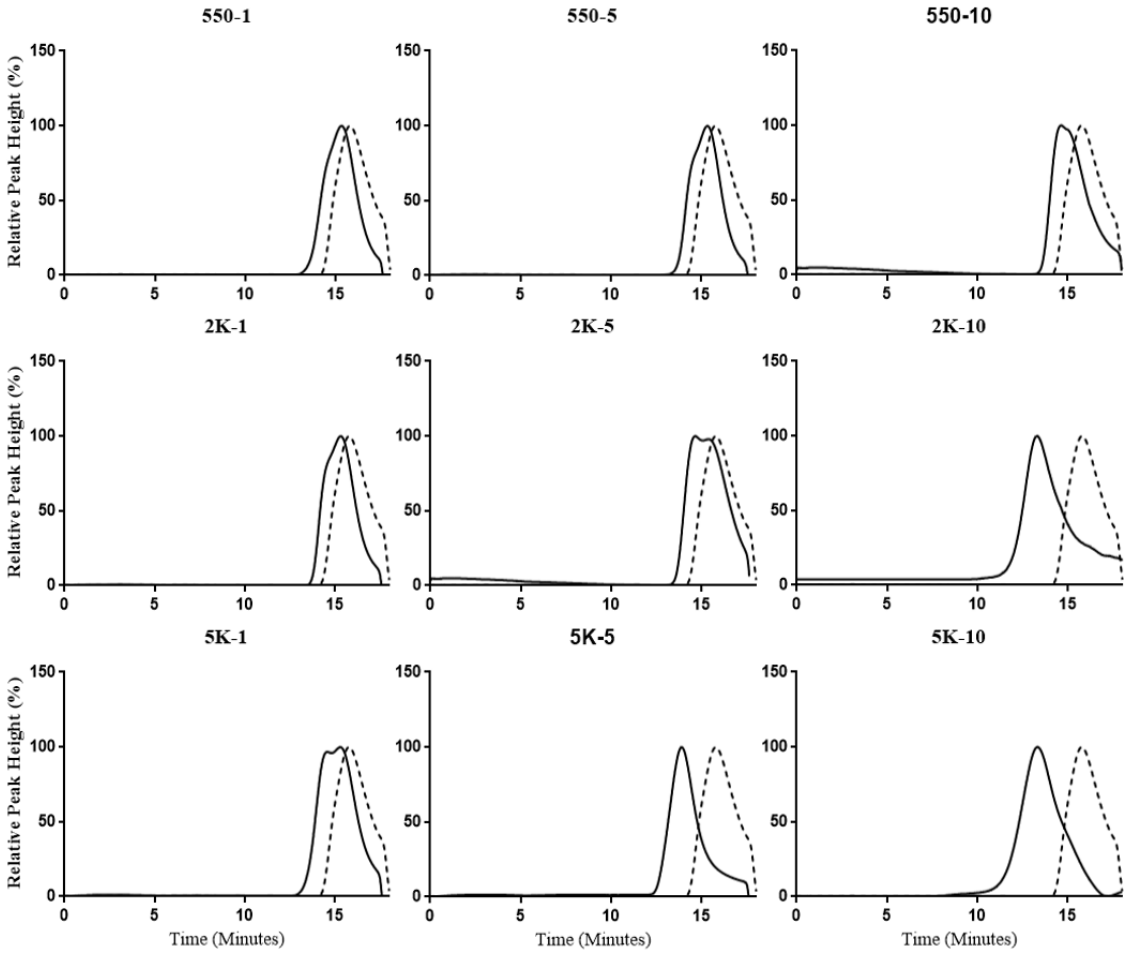


**Figure 3.2. Gel permeation chromatograms of PEG-PEI particles.**

Gel permeation chromatography (GPC) of PEG-PEI particles in the created library. Dashed chromatograms are PEI and solid chromatograms are PEG-PEI.

### 3.3.2. Increased polymer homogeneity of TNAs increases particle size and decrease number of polymer chains used in complexation

PEG-PEI-d was synthesized from a dialyzed version of a 25 kDa PEI which can reduce the PEI impurities involved in siRNA/TNA complexation. Gel electrophoresis (**Figure 3.1A, insert**) confirms that a portion of smaller molecular weight PEI chains were removed after dialysis. Cationic PEIs traveled toward the anode, yet undialyzed PEI showed a broader smear on the gel than PEI-d. These results indicate that PEI contains short molecular weight contaminants and its average molecular weight (25 kDa) may be misleading to determine the accurate polymer charge density. In contrast, PEI-d showed a single band with no smudge, demonstrating the removal of small molecular weight PEI chains and other impurities after dialysis. A library of particles mirroring the extent of pegylation of PEI based particles was synthesized from the PEI-d polymer and summarized in **Table 3.1.**

PEI-d based particles had similarly uniform size distributions as the PEI based particles (**Figure 3.3**). An increase in particle diameter compared to the PEI based particles was observed after pegylation (**Table 3.1**). The PEI-d based particles had consistently larger particle diameters at higher PEG corona densities. Additionally, complexes formed between PEI-d based particles and siRNA did not exhibit swelling in particle diameter compared to their empty diameter. Typically, swelling of a polymer complex occurs due to multiple polymer strands entrapping the siRNA. This lack of swelling indicates less polymer strands are involved during complexation.

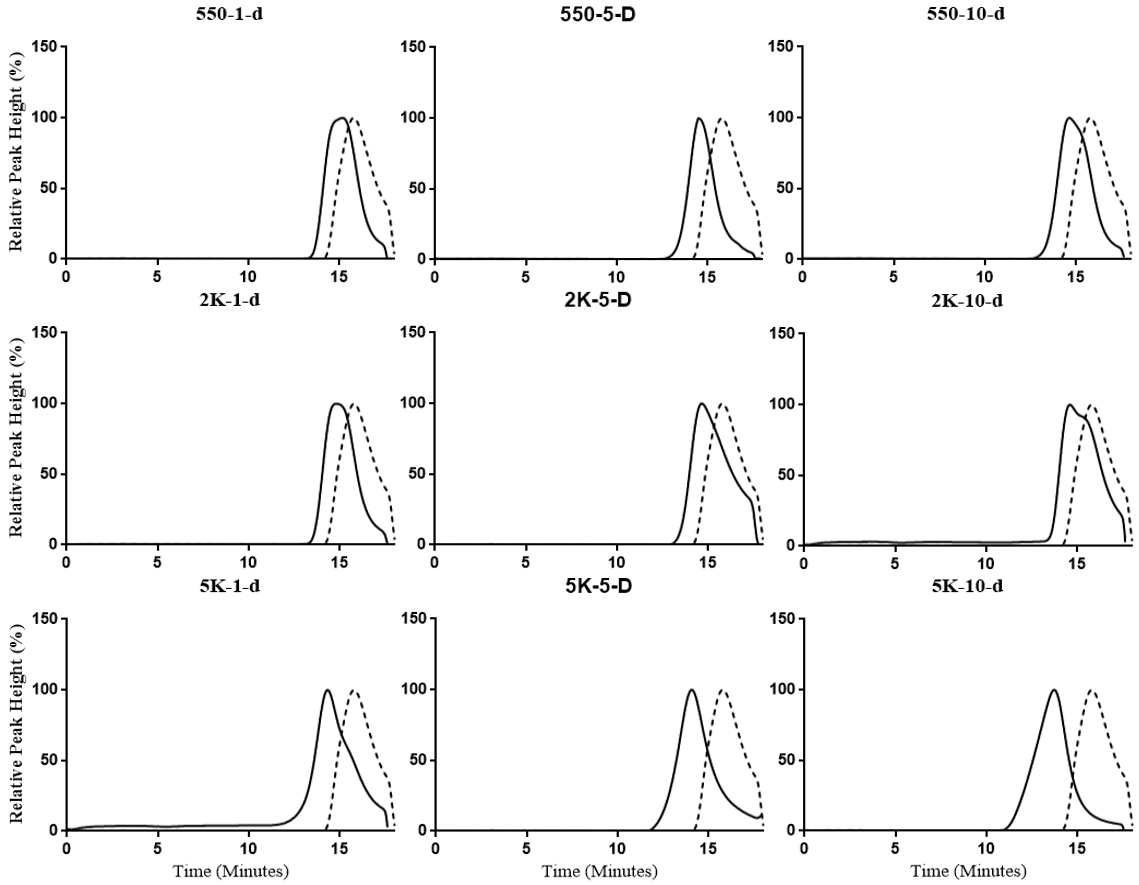


**Figure 3.3 Gel permeation chromatography of PEG-PEI-d particles.**

Gel permeation chromatography (GPC) of PEG-PEI-d particles created. Dashed chromatograms are PEI and solid chromatograms are PEG-PEI-d.

### 3.3.3. Increased PEG corona density increases particle/siRNA complexation ratio

Gel electrophoresis revealed that PEG-PEI and PEG-PEI-d particles increased the minimum amount of polymer necessary to form complexes with a set amount of siRNA (72 nM), which will be referred to as the minimum complexation ratio, as their PEG density increased. At the minimum complexation ratio, PEG-PEI neutralized the charge (a theoretical N/P = 1) and retained siRNA in the well of the gel (**Figure 3.4** and **3.5**, black boxes). These results indicate that PEG conjugation reduces primary amines from PEI and requires more PEG-PEI particles to retain the same amount of siRNA within complexes. In theory, a 10% 5 kDa PEG substitution (5K-10) would increase average molecular weight of the product from 25 kDa (PEI with no PEG) to approximately 130 kDa (520% increase), and approximately 6 times more 5K-10 particles (572%) would be needed to match the number of primary amines on unmodified PEI forming complexes with siRNA at N/P =1. However, our observations revealed that the actual increase in 5K-10 mass required for complexation was ~800% (**Figure 3.4**). It should be noted that these gels are reproducible as several preliminary gels had to be done in order to narrow down the polymer concentration range for each PEG-PEI. Though some variability in the minimum complex ratio can occur, this does not negate the observed effect of pegylation density on the PEG-PEI polymers. These results indicate that PEG-PEI and PEG-PEI-d particles would require greater amounts of polymer than theoretical estimation to form siRNA complexes as PEG density increased.

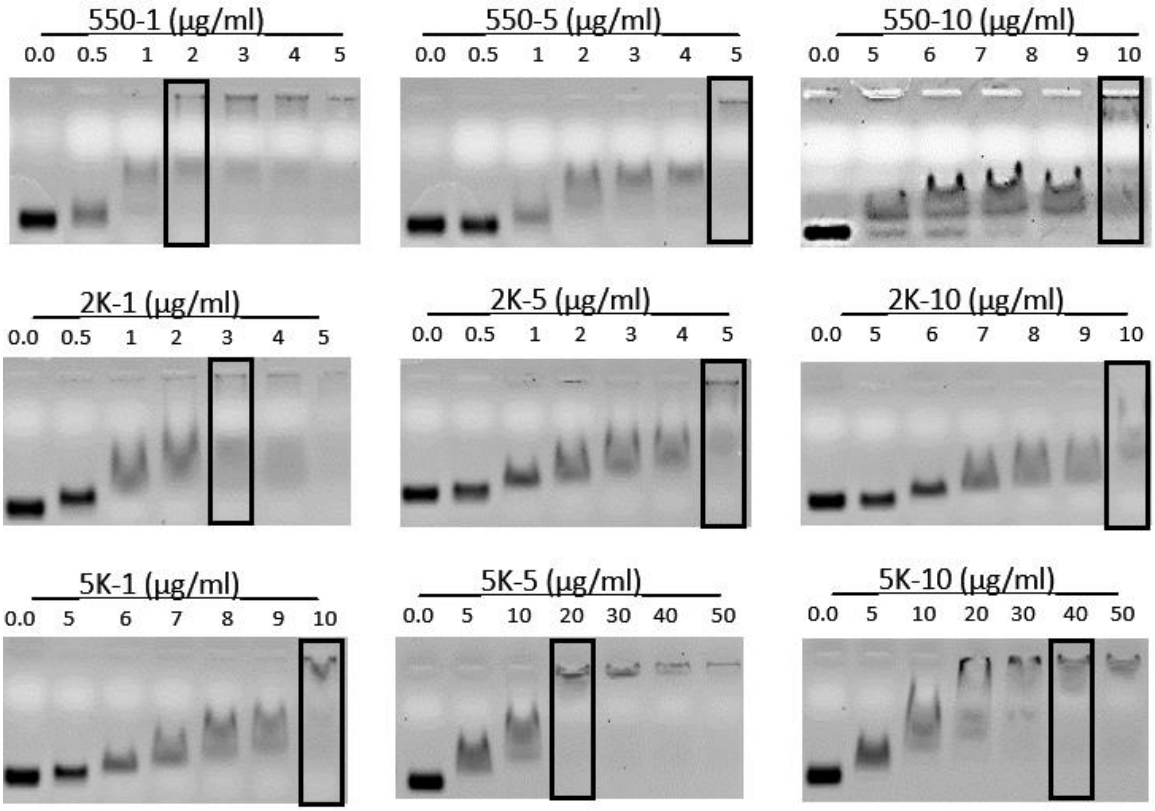


**Figure 3.4. siRNA complexation of PEG-PEI particles.**

Gel electrophoresis images of PEG-PEI run on a 1% agarose gel. siRNA at 72 nM was allowed to complex for 30 minutes with varying concentrations of PEG-PEI. The mixture was run on the gel and stained with ethidium bromide to image. The boxes indicate at which point the PEG-PEI forms a complete complex with siRNA.

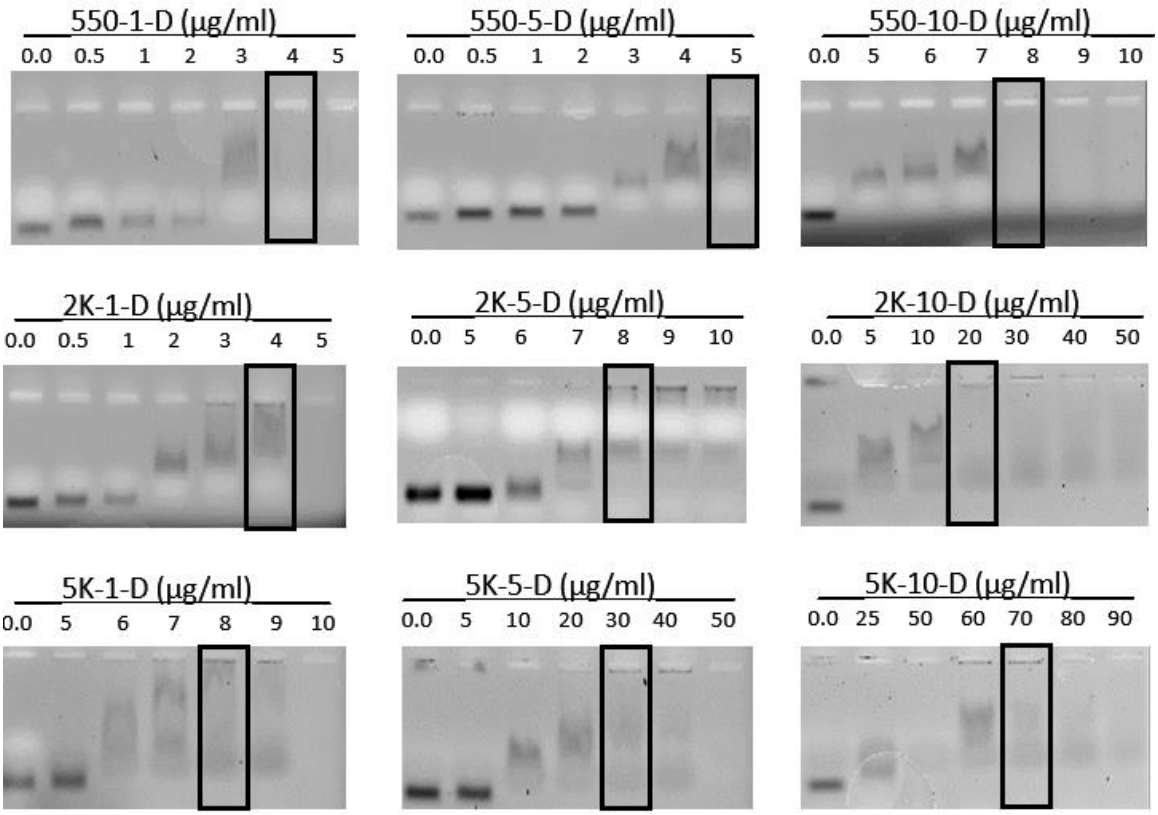


**Figure 3.5. siRNA complexation of PEG-PEI-d particles.**

Gel electrophoresis images of PEG-PEI-d run on a 1% agarose gel. siRNA at 72 nM was allowed to complex for 30 minutes with varying concentrations of PEG-PEI. The mixture was run on the gel and stained with ethidium bromide to image. The boxes indicate at which point the PEG-PEI-d forms a complete complex with siRNA.

### *3.3.4.* PEG corona density decreases siRNA transfection efficiency

**Figure 3.6** summarizes transfection efficacy of PEG-PEI particles with anti-luciferase siRNA at varying N/P ratios. As PEG% increased, the maximal transfection efficacy decreased in the PEG-PEIs containing 2 kDa and 5 kDa PEG. The PEG-PEIs containing 550 Da PEG with 1% and 5% PEG substitution retained transfection efficiency. However, PEG-PEIs with 10% PEG substitution increased the N/P ratio to achieve maximal transfection efficiency. Combining the two trends revealed that increasing PEG density decreased overall transfection efficiency of siRNA/PEG-PEI complexes. Low PEG density exhibited a positive effect on the complexes by reaching the maximal transfection efficiency of the unmodified PEI at a lower N/P ratio. It should be noted that transfection efficiency does not is not above ~75% for any of the formulations tested. This may be due to the cells susceptibility to siRNA or a factor of the siRNA concentration.

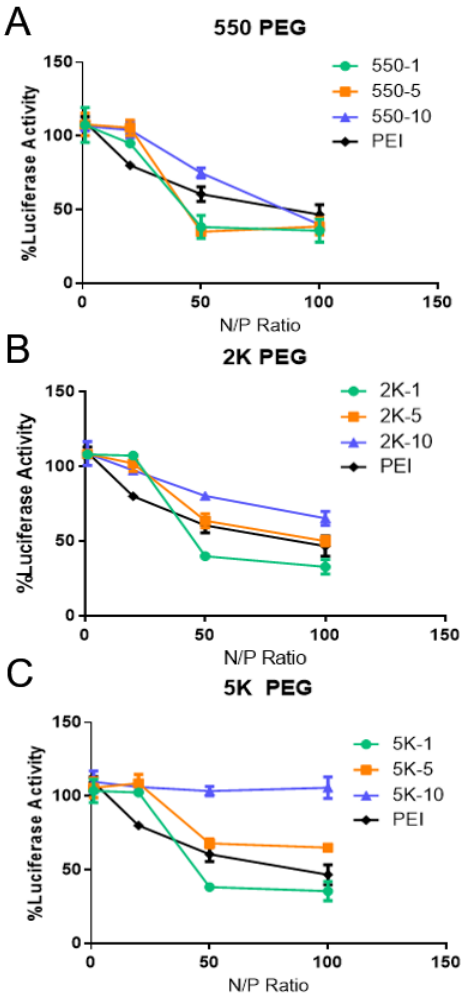


**Figure 3.6. Effect of PEG density on transfection efficacy of siRNA/PEG-PEI complexes.**

550 Da (A), 2 KDa (B), or 5 KDa (C) PEG-PEI complexes with anti-luciferase siRNA (72 nM) at varying N/P ratios (experimentally determined by gel electrophoresis) are incubated HT29 colorectal cancer cells stably expressing luciferase for 72 hours. The luciferase activity was normalized to cell viability.

### *3.3.5.* Increased polymer homogeneity decreases necessary complexation ratio to achieve maximum siRNA transfection

**Figure 3.7** shows the effects of the PEG-PEI-d on transfection efficiency at varying N/P ratios. Similar to PEG-PEI particles, PEG-PEI-d decreased the maximal transfection efficacy as PEG% increased, while PEG MW showed no negative effects on transfection at low PEG%. However, PEG-PEI-d showed maximal transfection at a lower N/P ratio than PEG-PEI (20 vs 50). This effect was reduced as the PEG density was increased.

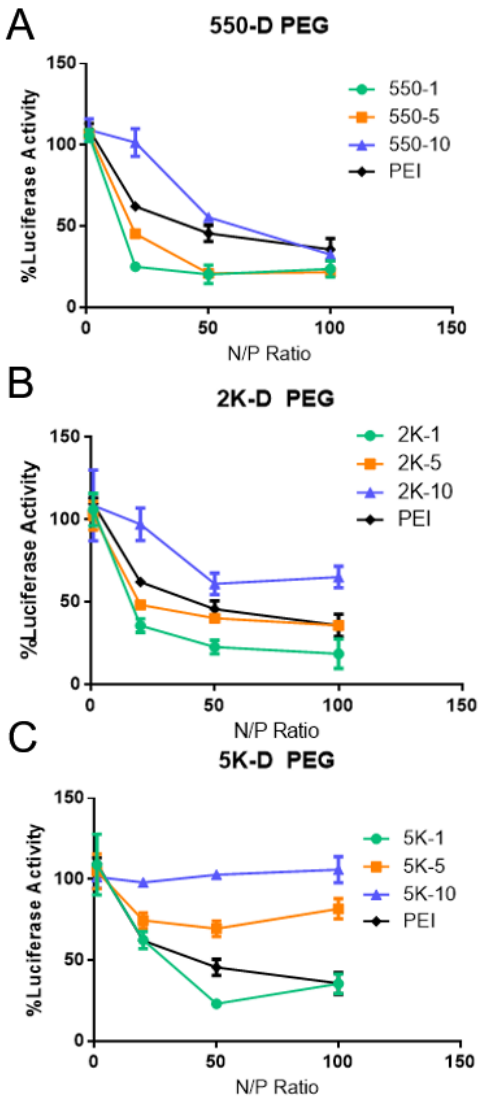


**Figure 3.7. Effect of PEG density on transfection efficacy of siRNA/PEG-PEI-d Complexes.**

550 Da (A), 2 KDa (B), or 5 KDa (C) PEG-PEI-d complexes with anti-luciferase siRNA (72 nM) at varying N/P ratios (experimentally determined by gel electrophoresis) are incubated HT29 colorectal cancer cells stably expressing luciferase for 72 hours. The luciferase activity was normalized to cell viability.

## 3.4. Discussion

PEI is a well-studied cationic polymer used in gene delivery, including siRNA delivery, because it can readily form ionic complexes with genetic material to improve stability of the genetic cargo in the blood stream. However, clinical applications of the siRNA/PEI complexes are often held back by complex instability and toxicity[147]. The toxicity of siRNA/PEI complexes is mainly attributed to the cationic surface charge disrupting anionic cellular membranes[148]. A common method of reducing surface charge of PEI/siRNA complexes is covalently attaching PEG to PEI[149], forming a PEG shell. PEG is available in many different molecular weights and thus can create PEIs with a variety of PEG densities[150]. In the previous chapter, we prepared nanoparticles from PEG-conjugated PEI (PEG-PEI) for siRNA delivery[95] and found that their transfection efficiency was significantly reduced, presumably due to variations of PEG density. However, the effects of PEG density on physicochemical properties and transfection efficiency of siRNA/PEG-PEI complexes were elusive. Therefore, this chapter elucidates how PEG density affects transfection efficiency of siRNA/PEG-PEI complexes by investigating three factors that influence PEG density on PEI (PEG MW, PEG% and PEI impurities).

Increased PEG MW was found to weaken siRNA/PEG-PEI complex stability and lower transfection efficacy. These results indicated that increasing PEG MW increased the amount of PEG-PEI required to form complexes (**Figure 3.4 and 3.5**). Our initial speculation was that the increased amount of PEG-PEI was due to increased molecular weight of the polymer after PEG attachment. PEG conjugation reduces the weight percentage of primary amines on PEI, and thus requires more polymer to form complexes

with siRNA and neutralize the charge. Therefore, we used the reduced weight percentage of primary amines to predict the increase in the weight ratio between PEG-PEI and siRNA to form complexes. For example, if PEI's primary amines are reduced by 20%, 20% additional polymer is needed to form complexes. However, our data shows that PEG-PEIs containing 2 kDa and 5 kDa PEG need more polymer than predicted to form these complexes. This may be due to the PEG chains blocking siRNA from interacting with the amines of PEI, similarly to how PAL may act when attached to 3P proposed in chapter 2.

Larger PEG chains (2 kDa or 5 kDa) would block cationic sites on PEI more effectively than shorter chains due to increased flexibility, as evidenced by the reduction of surface charge as the PEG chain length was increased (**Table 3.1**). Since both PEI and PEG are hydrophilic, the polymers may entangle rather than form a distinct core and shell system like nanoparticles containing hydrophobic polymers[113, 151]. This entanglement would block the cationic sites from interacting with the siRNA, but the effect would be lessened by smaller chain lengths of PEG, as confirmed by lower molecular weight PEG-PEIs (**Figure 3.4 and 3.5**). Additionally, blockage of amine groups would reduce interaction with cellular membranes and endosomes. This may result in lowered transfection efficiency responsible for unsuccessful transfection of the PEG-PEI used in the previous chapter. PEG/PEI entanglement could further decrease complex stability as the interact with water at the surface of the nanoparticle. This interaction would cause the TNA to constantly alter its conformation, which would change the conformation of the core and may release siRNA prematurely.

Lowering PEG% increased PEG-PEI/siRNA interactions and retained transfection efficacy of the complex. Reducing the PEG% reduced the minimum amount of polymer required for complex formation regardless of PEG MW (**Figure 3.4 and 3.5**). Lower PEG% would reduce the number of PEG chains blocking cationic moieties from interaction with both siRNA and cellular membranes. This was supported by observing increased surface charge after reduction of PEG% (**Table 3.1**). Complexes with lower PEG% achieved greater transfection efficiency than those with higher PEG% (**Figure 3.6 and 3.7**). In fact, complexes with relatively low PEG% and low PEG MW increased transfection beyond the unmodified PEI control. This result agrees with others findings that PEG-PEI can be more efficacious than PEI[152]. It should be noted that as PEG MW increases, the disparity in transfection efficiency between PEG% also increases. This is likely the result of PEG composing a larger weight percentage of the complex and further blocking interactions with cellular membranes. For example, when complexes are synthesized with 10 % attachment of 5 KDa PEG, their weight percentage of PEG is ~81%. The PEG weight percentage will be ~30% if the complexes have 1% attachment of the same PEG. This increase in weight percentage of PEG on the polymer correlates with a larger PEG shell. These trends show the importance of PEG% to influence the interactions between siRNA and PEI. While the exact mechanism by which PEG chain length reduces transfection is unknown, it is speculated that either the complex is less stable[145, 153] or unable to escape the endosome[86, 154]. Additionally, this gives further evidence as to why the 2P from the previous chapter did not cause transfection.

Impurities in PEI were confirmed to alter the physicochemical properties of complexes and reduce transfection efficacy at low N/P ratios and thereby alter PEG shell

density. PEI stocks that are purchased commercially often include smaller molecular weight PEIs that are the result of polymer degradation and synthesis byproducts. Dialysis of the PEI stock used in the synthesis of these PEG-PEIs was able to successfully remove a portion of these impurities (**Figure 3.1A**). Removing these residual impurities increased the proportional molecular weight of the PEI and the homogeneity of the stock (PEI-d). After synthesis of PEG-PEIs using the PEI-d stock (PEG-PEI-d), physicochemical properties of PEG-PEI-d differed from PEG-PEI mainly in particle diameter before and after complexation with siRNA (**Table 3.1**). The increased particle diameter is likely due to the increased proportion of larger cationic polymer chains in PEG-PEI-d. Particle diameter swelling after complexation was also reduced which indicates fewer PEG-PEI-d chains were involved complex formation. Fewer chains involved in complex formation increases the homogeneity of the PEG shell surrounding the particle as well as the overall homogeneity of the complexes. In PEG-PEI particles, the small PEI impurities can take part in siRNA complexation and increase the amount of PEG-PEI needed to neutralize the charge of siRNA and increase weight percentage of PEG. Therefore, PEG-PEI complexes would have greater PEG content, which is beneficial to reduce the surface charge yet disadvantageous to improving transfection. This speculation is supported by PEG-PEI-d complexes that showed transfection efficacy similar to PEG-PEI complexes yet transfected cells at a lower N/P ratio.

## 3.5. Conclusions

In this chapter, pegylation density of TNA/siRNA complexes, influenced by factors including PEG molecular weight, PEG attachment percentage, and PEI impurities, significantly alters transfection efficiency of these complexes. PEG density correlated negatively with transfection efficiency of TNAs as low PEG density increased transfection efficiency and high PEG density removed transfection ability from the particles. This effect also demonstrates why the PEG-PEI (2P) from chapter 2 was unable to transfect cells. Additionally, the removal of PEI impurities increased the overall transfection efficiency of all complexes at lower N/P ratios. Our findings demonstrate the importance of PEG length, PEG attachment percentage, and removal of PEI impurities in improving transfection efficacy of siRNA carriers using PEG-PEI. These results may be applicable to other cationic polymers forming complexes with siRNA and interacting with cellular membranes in a similar way to PEI, such as poly(lysine) and chitosan derivatives, and thus provide valuable insights for future development of more effective and much safer siRNA carriers.

# Chapter 4: Hydrophobic Modifications to TNAs and Non-Specific Reduction of Reporter Protein Concentrations.

This chapter is adapted from work published in the International Journal of Pharmaceutics on June 15th, 2017[155]. I would like to extend a special acknowledgement to Dr. Tadahide Izumi who helped with western blotting of the high molecular weight luciferase. I would also like to acknowledge Dr. Piotr Rychahou who helped with cell lines and luciferase western blotting methods.

## 4.1. Introduction

Small interfering RNA (siRNA) can suppress mutated genes generating proteins which are currently unable to be targeted by small molecule drugs and thus provide a new therapy for genetic diseases including cancer [25, 156-157]. However, siRNA often shows low transfection *in vivo* due to poor delivery efficiency[158]. To improve delivery of siRNA to target sites, polymer-based non-viral gene vectors have been developed, which include ionic complexes between anionic siRNA and cationic polyethyleneimine (PEI)[75, 147]. siRNA/PEI complexes have achieved successful gene silencing in various human cells *in vitro*, but they are unstable in the body[105]. Polyethyleneglycol (PEG) is frequently used to stabilize siRNA/PEI complexes[121, 159]. The hydrophilic PEG chains surrounding siRNA/PEI complexes can shield the particle charge and prevent protein adsorption. The siRNA/PEI complexes can be further modified with hydrophobic excipients and other additives for improving stability and fine-tuning release of siRNA[111].

Based on this background, we developed siRNA delivery vectors in the previous chapters by using tethered nanoassemblies (TNAs) made from PEG, PEI, and hydrophobic pendant groups such as palmitate (PAL)[95]. TNAs are unimolecular assemblies of 30 nm diameter particles having cationic polymer backbone to which PEG and a hydrophobic moiety can be covalently conjugated. In previous chapters, we

reported that these TNAs enhanced siRNA transfection in a human colorectal cancer HT29 cell line as functions of PEG composition and PAL modification. These TNAs displayed siRNA transfection efficiency comparable to PEG-PEI formulations developed by other research groups[136, 160] as well as commercially available transfection reagents such as RNAiMAX. Upon further investigation of hydrophobically modified TNAs, subsequent batches of PEG-PEI appeared to substantially change siRNA transfection efficiency although the mechanism remained elusive[95]. However, further study of the hydrophobic modification to PEG-PEI also revealed that the resulting PEG-PEI-PAL TNA (3P) unexpectedly reduced luciferase expression in cells even in the absence of siRNA, called the false positive effect.

The false positive effect on siRNA transfection increases the difficulty in evaluating and predicting *in vivo* performance of PEG-PEI based non-viral gene vectors for future studies and clinical applications. Protein reporter assays are commonly used to evaluate the transfection efficiency of the siRNA/PEG-PEI complex, and luciferase is a widely-used reporter protein that offer a quick method for measuring siRNA-mediated gene silencing in living cells[18, 161-162]. Luciferase protein activity is correlated to the amount of luciferase protein in the cell following siRNA transfection by measuring luminescence using luminogenic substrate [163]. Luciferase has a short half-life in live cells, less than 3 hours[164], which makes it ideal for determining long-term siRNA transfection efficiency. Any protein left within the cell after incubation with siRNA/PEG-PEI complexes would be produced after the siRNA has had a chance to take effect. However, this would not account for protein that has been denatured or had its expression reduced by other means. If PEG-PEI can interfere with the luciferase reporter assay this way, it would explain

siRNA transfection efficiency varying among product batches. Another possible reason for inconsistent siRNA transfection of PEG-PEI is the cellular stress response triggered by siRNA/PEG-PEI complexes. Off target effects of siRNA have been demonstrated[63, 73], yet little is known if and how PEG-PEI would induce non-specific gene silencing during siRNA transfection.

Our previous findings suggest that the addition of hydrophobic pendant groups to TNAs would influence intracellular luciferase expression by either directly interacting with cells or indirectly disrupting the protein synthesis process[95, 133]. Therefore, this chapter aims to elucidate the false positive effect of hydrophobically modified TNAs on siRNA transfection by using TNAs made from combinations of PEG, PEI, poly(L-lysine) (PLL), palmitate (PAL), and deoxycholate (DOC): PEG-PEI (2P), PEG-PEI-PAL (3P), PEG-PLL (2P'), PEG-PLL-PAL (3P'), and PEG-PEI-DOC (2PD) as shown in **Figure 4.1**. These PEG-PEI TNAs (+/- siRNA) are characterized by *in vitro* siRNA transfection, cell viability, toxicity and immunoblotting in a human colorectal cancer cell line stably overexpressing luciferase (HT29/Luc). Raman spectroscopy is also employed to investigate interactions between hydrophobic pendant groups conjugated to the TNA core and compounds outside the particles. To investigate the cellular stress caused by TNAs, assays determining total protein count, ATP concentration, and cellular membrane porosity are used. Data obtained from these experiments are analyzed to determine the effects of hydrophobic groups and polymer scaffold condensation on false transfection of siRNA/PEG-PEI complexes. Understanding these unexpected outcomes of covalent modification to cationic polymers is crucial for future design of siRNA delivery vehicle development.

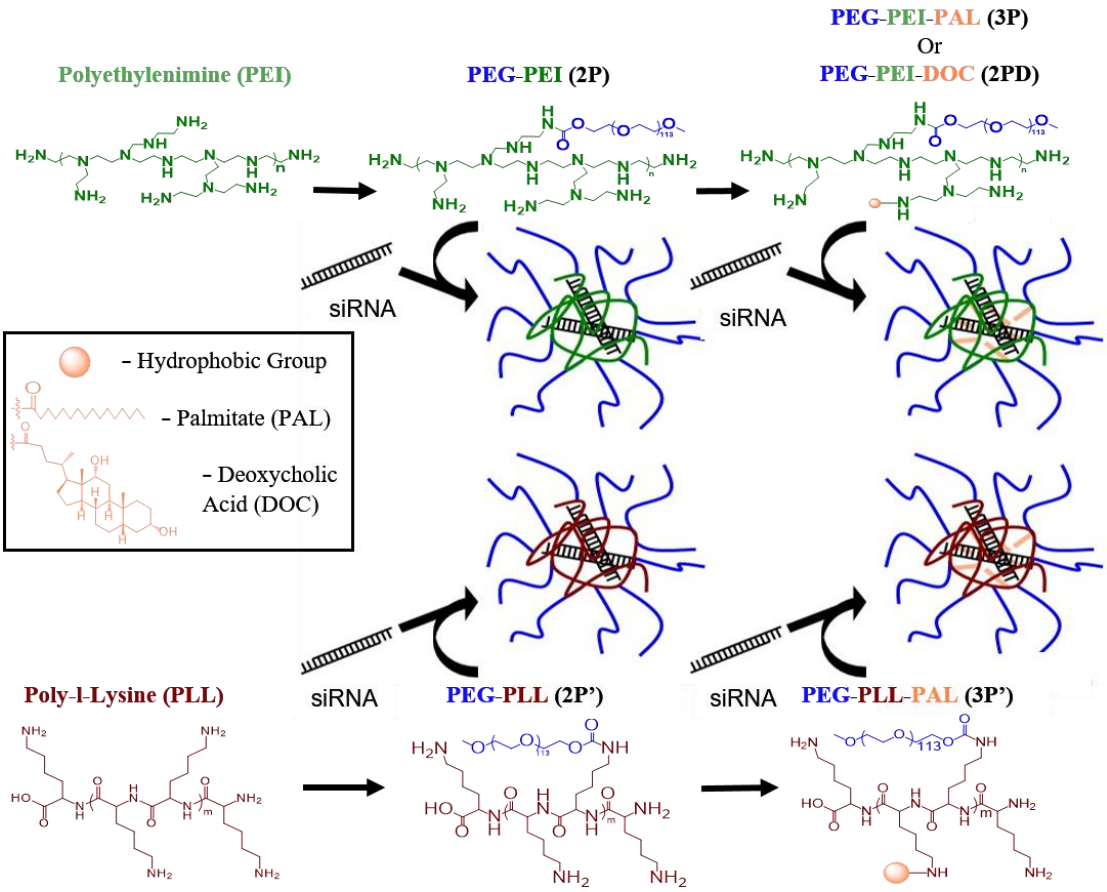


**Figure 4.1: TNA Scheme**

Progression of TNA development from backbone polymer (PEI or PLL) to subsequent random covalent modification with PEG and hydrophobic moiety (DOC or PAL) and finally their complexes with siRNA.

## 4.2. Materials and Methods

### 4.2.1. Materials and Cells

PEG (5 kDa, α-methoxy-ω-NHS ester activated) was purchased from NanoCS (New York, NY). Branched PEI (bPEI), deoxycholate (DOC), N-hydroxy succinimide, 4-dimethylaminopyridine, 1-ethyl-3-(3-dimethyl aminopropyl) carbodiimide hydrochloride (EDC HCl), palmitoyl chloride, resazurin sodium salt, sulforhodamine B based *in vitro* toxicology assay kit (TOX6), and poly(L-lysine) (PLL, 30-70 kDa) were purchased from Sigma Aldrich (St. Louis, MO). RNAiMAX, 4-12% NuPAGE Bis-Tris precast gels, HEPES buffer (pH 8.0, 1 M), MES buffer (0.1 M, pH 5.0), RIPA buffer, pyridine, NuSieve GTG agarose, dialysis membrane with molecular cut-off (MWCO) of 6-8 and 100 kDa, and other organic solvents were purchased from Fisher Scientific (Waltham, MA). siRNA (5'-GUUGGCACCAGCAGCGCACUU-3') was purchased from GE Dharmacon (Lafayette, CO). Opti-MEM was purchased from Life Technologies (Carlsbad, CA). Mitochondrial ToxGlo™ assay kit and Bradford assay kit were purchased from Promega (Madison, WI). McCoy's 5A, 0.05% trypsin/EDTA, and phosphate buffered saline (PBS) were from GE Healthcare (Logan, UT). Fetal bovine serum (FBS) was purchased from Atlanta Biologicals (Flowery Branch, GA).

HT29 human colon cancer cell line was purchased from American Type Culture Collection (ATCC, Manassas, VA), and subsequently transfected to establish a cell-line stably expressing firefly luciferase (HT29/Luc). Cells were cultured at logarithmic growth in a humidified environment with 5% $CO_2$ at 37 °C in McCoy's 5A media supplemented with 10% FBS according to ATCC recommendations.

### 4.2.2. Synthesis of TNAs with different backbones and hydrophobic moieties

TNAs with a PEI backbone (2P and 3P) were synthesized from 25 kDa bPEI, 5 kDa NHS-activated PEG, and palmitoyl chloride as previously reported[95]. In this chapter, 2P was further modified with DOC through covalent conjugation to the PEI backbone. Briefly, DOC was mixed with NHS, EDC, and DMAP in a 5:5:0.2 molar ratio in MES buffer (0.1 M, pH 5.0). 2P was then added to the mixture in a 1:100 molar ratio of 2P:DOC at room temperature. After 48 hours, the product was purified by dialysis and freeze drying to collect 2PD.

TNAs with a PLL backbone (2P' and 3P') were prepared from 30-70 kDa PLL with 5 kDa NHS-activated PEG and palmitoyl chloride as previously reported[165]. 2P' was synthesized by reacting PLL with NHS-activated PEG in water:DMSO:pyridine mixture at ratios of 2:1:1. The solution was mixed for 72 hours at room temperature. 2P' was further modified with palmitoyl chloride to create 3P'. 2P' was dissolved in THF at 40 °C and palmitoyl chloride was added in a 1.1:1 molar ratio palmitate:2P'. After 15 minutes of mixing, pyridine in a 2:1 molar ratio of pyridine:palmitate was added as a HCl scavenger. The solution was reacted for additional 2 hours and purified by ether precipitation and dialysis. The product was collected by freeze drying.

Purity and molecular weight uniformity of TNAs were determined by gel permeation chromatography (GPC, Asahipak GF-7M column, 2 mg/mL, DMF mobile phase, 0.5 mL/min, 40 °C). Diameter and surface charge were determined by dynamic light scattering (DLS) and zeta potential measurements using Zetasizer Nano (Malvern, UK).

### 4.2.3. Determination of minimum complexation ratios of TNAs and siRNA

TNAs at varying concentrations (0-1 mg/mL) were mixed with 2 µg/mL siRNA solutions in Opti-MEM at a 1:1 ratio and allowed to equilibrate for 30 minutes. Each mixture (20 µL) was then loaded on to a 1% agarose gel and run at 100 volts for 60 minutes at room temperature in TAE (Tris-Acetate 0.04 M, EDTA 0.001M) buffer. The gel was stained with 100 ng/mL ethidium bromide in a TAE buffer and rinsed 3 times with deionized water. The gel was imaged using Typhoon GLA 9500 (GE Healthcare, Logan, UT) fluorescent imager with an ethidium bromide filter set.

### 4.2.4. *In vitro* transfection and toxicity efficiency of TNAs

Cells were plated at 5,000 cells per well into white opaque 96 well plates and incubated for 24 hours. After 24 hours, TNA solutions were prepared by adding 100 µL of 10 mg/mL TNA solutions to 100 µL of 10 µg/mL siRNA solution or 100 µL of Opti-MEM. Naked siRNA controls were created with 200 µL of siRNA solutions at 5 µg/mL. Opti-MEM (200 µL) was used as the blank control. RNAiMAX controls were created by mixing 5 µL of RNAiMAX with 95 µL of Opti-MEM and then either 100 µL of Opti-MEM or 100 µL of 10 µg/mL siRNA solution for the empty RNAiMAX control or siRNA-loaded RNAiMAX control, respectively. Complexes were formed by incubating the mixtures for 30 minutes at room temperature, except the RNAiMAX control that was incubated for 5 minutes as instructed by the manufacturer. From each well, 20 µL of solutions were replaced with their respective complex solutions or controls (n = 6) to yield 1 mg/mL of TNA and 1 µg/mL siRNA in the well. The plate was incubated for 72 hours and then read for bioluminescent intensity using GloMax luminometer. The substrate was 100 µL of 0.1 mg/mL luciferin solution in PBS. Luminescent intensity was

collected for 10 seconds and reported as percentage of luciferase activity with respect to control wells. The data was normalized to cell viability (described below) to account for cell death in the reduction of the luciferase signal.

Three cell viability assays were used in this chapter to consider different aspects of cell health. The first assay was a resazurin assay, which measures mitochondrial activity in live cells. 10 µL of a 1 mM resazurin solution was added to each well and incubated for 3 hours. The plate was read on SpectraMax M5 (Molecular Devices) fluorescent plate reader at excitation/emission of 560/590 nm. The readings were subtracted from blank controls and reported as percentage of viable cells.

The second assay was a sulforhodamine B assay for the quantification of cellular proteins in live cells. Briefly, cells were fixed with 30 µL/well of provided TCA solution at 4 °C for 1 hour. After media removal and air drying, 20 µL/well of sulforhodamine B solution was added and allowed to stain for 30 minutes. The stain was then removed, washed with 1% acetic acid solution, and air dried. 100 µL/well of 10 mM Tris base solution was added and incubated for 5 minutes at room temperature. Absorbance was measured at 565 nm excitation and 690 nm emission with a SpectraMax M5 (Molecular Devices) fluorescent plate reader. The absorbance at 690 nm is subtracted from the absorbance at 565 nm to determine percent viable cells with respect to controls.

The third assay was for monitoring cell membrane integrity and mitochondrial activity of cultured cells, which were measured with the Mitochondrial ToxGlo assay kit per manufacturer's instruction. Briefly, 20 µL/well of the provided bis-AAF-R110 solution was added to the plate and incubated at 37 °C for 30 minutes. Fluorescence was measured at excitation/emission of 495/520 nm using a SpectraMax M5 (Molecular

Devices) fluorescent plate reader. Then, 100 µL/well of the provided ATP detection reagent was added to the plate and read for luminescence with GloMax luminometer. The values were compared to their respective controls (untreated wells) and reported as percentages of the control.

### 4.2.5. Analysis of Luciferase Protein Expression Levels *in vitro*

Cells were plated at 50,000 cells/well in a 12 well clear plate. 24 hours later, 200 µL of media were replaced with 200 µL of Opti-MEM, empty TNAs, or siRNA/TNA complexes. After a 72-hour incubation at 37 °C, cells were lysed with a RIPA buffer and assayed for protein content with a Bradford assay kit (Promega). 100 µg of protein for each sample were subjected to electrophoresis through a 4-12% NuPAGE Bis-Tris precast gel. Afterwards, the proteins were transferred to a nitrocellulose membrane. Primary antibodies used to treat the membranes were anti-luciferase and anti-beta-actin (Cell Signaling Technologies). After washing, the membranes were exposed to IgG-horseradish peroxidase conjugate secondary antibodies for 1 hour and developed with an ECL Western blotting substrate (Promega and SCBT). To detect the slow-migrating firefly luciferase protein in SDS/PAGE, cells were incubated with the 2P, 2P', 3P, and 3P' for 72 h as described above, and further incubated in the presence of MG132 (40 µM) for 6 h. The protein extracts were run in SDS/PAGE and transferred to PVDF membranes, which were cut above the intact firefly luciferase protein to exclude the intact protein in the membrane, and blotted with the rabbit polyclonal anti-firefly luciferase antibody (Promega). The blot was developed with SuperSignal West Femto (Pierce, Thermofisher), and the signals were analyzed in ChemiDoc Imaging Systems (Bio-Rad).

### 4.2.6. Activity of luciferase protein after pre-incubation with TNAs

20 µL of 10 mg/mL TNA solutions or RNAiMAX solution were incubated for 10 minutes in wells of a white 96 well plate (n = 6). Each well contained 80 µL/well of PBS with luciferase proteins to obtain 1 mg/mL TNA and 5 ng/mL of luciferase. 100 µL of 0.1 mg/mL luciferin solution in PBS were added to each well and read using GloMax luminometer with an integration time of 10 seconds. Similarly, 2 mL of 10 mg/mL TNA solutions or RNAiMAX solution were mixed for 30 minutes with 8 mL of 0.125 mg/mL luciferin solution. 100 µL of this solution was then injected using GloMax luminometer into each well of a white 96 well plate containing 100 µL/well of 5 ng/mL luciferase in PBS. Luminescence was measured and integrated for 10 seconds. Data is reported as RLU values.

### 4.2.7. Observed interactions of TNAs and components with siRNA through Raman spectroscopy

Raman spectroscopy was conducted in the solid state using a Nicolet iS 50 FTIR with a Raman module (Thermo Fisher Scientific, Waltham, MA). The samples were prepared on a 48 well metal plate. 100 µL of a 10 mg/mL solution of each sample was added to a well. To analyze individual components of 3P and TNAs, 100 µL of water was added to each well. For physical mixtures of components, 100 µL of a 10 mg/mL solution of the respective component was added to the well. 1 µL of a 1 mg/mL siRNA solution or 1 µL of water was added to each well. The loaded metal plate was put at room temp for 30 minutes to acclimate all samples. The plate was then transferred to dry ice and the

samples were frozen. The frozen samples were then freeze dried overnight and then read on the Raman. Data was collected and deconvoluted using the Omnic Spectra Software suite (Thermo Fisher Scientific, Waltham, Mass.).

## 4.3. Results

### 4.3.1. Hydrophobic moiety in the TNA core has greater influence on luciferase expression reduction than TNA condensation

Total five TNAs (2P, 3P, 2PD, 2P', and 3P') were synthesized to investigate the effects of backbone condensation (PEI vs PLL) and hydrophobic groups (PAL vs DOC) on siRNA transfection. Both PEI-based (2P, 3P, and 2PD) and PLL-based (2P' and 3P') TNAs were found uniform in size and contained no impurities as confirmed by GPC analysis (**Figure 4.2 A & B, Figure S1**). DLS measurements showed that all TNAs were 30-35 nm with 2P, 3P, 2PD, 2P', and 3P' having diameters of 29.5, 34.3, 28.9, 31.2, and 33.4 nm respectively. Zeta potential measurements had all particles with neutral surface charge. The siRNA uptake of each particle is shown in **Figure 4.2 C & D and Figure S1 B**. 3P had the highest complexation ratio (mass of particle needed to completely complex with 1 µg of siRNA) of 1.0 mg per 1 µg of siRNA. This concentration of particle (1 mg/mL) was chosen along with 1 µg/mL of siRNA to be used for further testing of each complex.

Approximately 38% of the HT29 cells stably expressed a firefly luciferase protein, which was sufficient to quantify bioluminescence of cells treated with anti-luciferase siRNA. The reduction of the bioluminescent signal when cells are dosed with the luciferin substrate typically correlate with siRNA delivery efficacy. To further investigate

the unexpected reductions in luciferase expressions (or false positives in siRNA transfection), cells were dosed with 1 mg/mL TNAs with and without anti-luciferase siRNA for 72 hours. **Figure 4.3A** shows a reduction in luciferase protein of HT29 close to 50% when treating cells with 3P, and near 40% when treated with 2PD regardless of the presence of siRNA. Western blots also show a reduction in cellular luciferase concentration after treatment with 2PD and 3P (**Figure 4.3B**). 2P remains unable to reduce the luciferase expression, which is consistent with previous findings. None of these particles showed significant toxicity on a resazurin assay. These results confirm that both PLA and DOC induce the false positive effects. Replacing the TNA backbone with PLL from PEI yielded similar results (**Figure 4.4**). 2P' was unable to reduce luciferase expression just as 2P. However, 3P' reduced the expression of luciferase by approximately 25% regardless of the presence of siRNA. Interestingly, 3P' shows a false positive but not to the same extent as 3P.

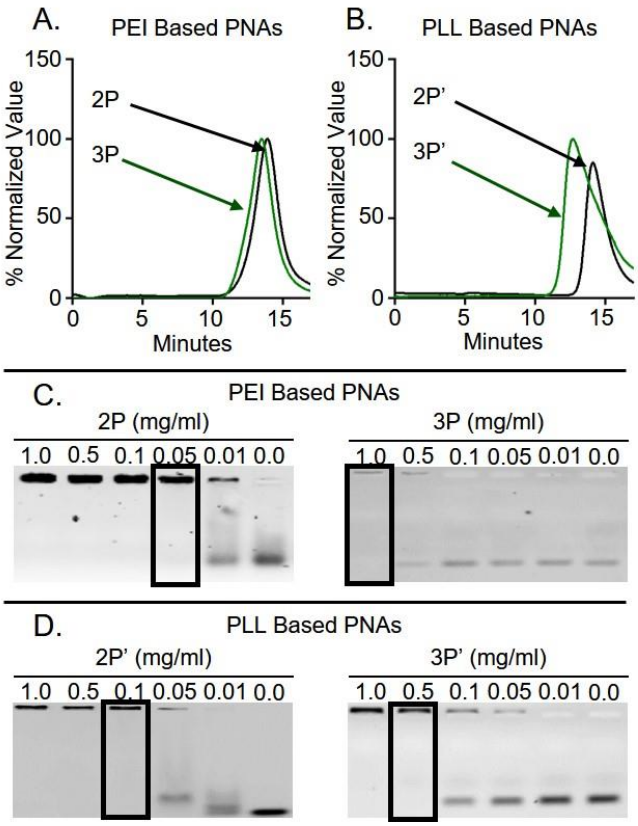


**Figure 4.2: Characterization of TNAs**

Gel permeation chromatography (GPC) spectra shows particle uniformity and purity of PEI based TNAs (A) where black chromatograph represents 2P and green represents 3P and PLL based TNAs (B) where black chromatograph represents 2P' and green represents 3P'. Gel electrophoresis of PEI based TNA/siRNA mixtures (C) and PLL based TNA/siRNA mixtures (D) with 72 nM siRNA and varying concentrations of TNA to determine the ratio of TNA to siRNA needed to form complexes (black boxes).

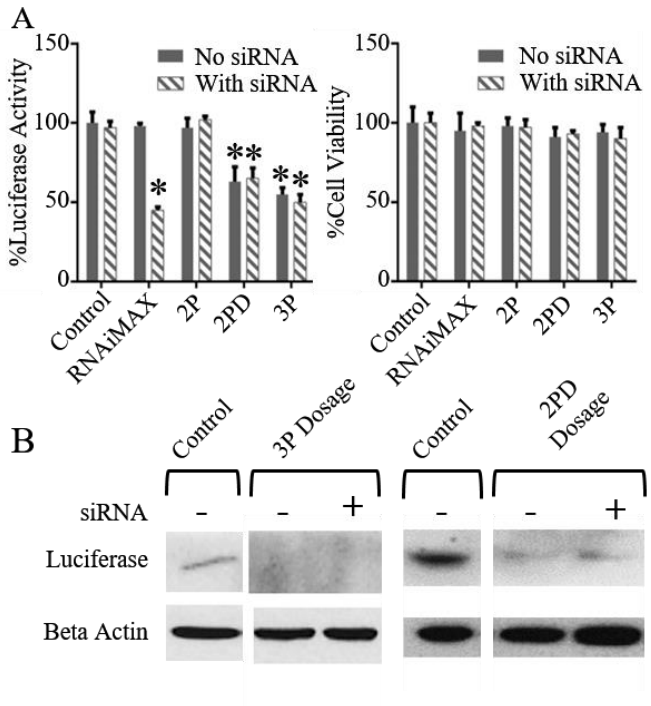


**Figure 4.3: TNA *in vitro* Luciferase Reduction**

A: luminometric assay of luciferase (left) and viability assay (right) after 72-hour incubation with each particle. Dark grey bars represent each condition without siRNA and light grey bars represent condition with 1 µg/mL anti-luciferase siRNA. B: Western blotting results after 72-hour incubation with 3P and 2PD including an untreated control. siRNA in each condition is represented by N (no siRNA present) or L (anti-luciferase siRNA, 1 µg/mL). * denotes that the column is significantly different from the control condition ($p<0.01$)

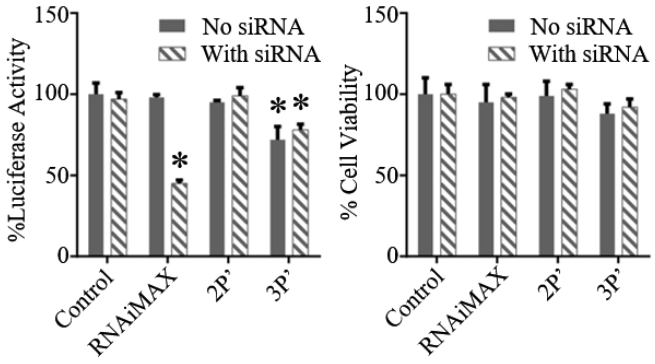


**Figure 4.4: PLL Based TNA *in vitro* Luciferase Reduction**

luminometric assay of luciferase (left) and mitochondrial activity viability assay (right) after 72-hour incubation with each particle at a concentration of 1 mg/mL. Grey bars represent each condition without siRNA and striped bars represent condition with anti-luciferase 1 μg/mL siRNA. * denotes that the column is significantly different from the control condition ($p<0.01$)

### 4.3.2. Luciferase activity is unaffected by TNA interactions with either luciferase or luciferin

Although the luciferase assay is a good indicator of protein activity within the cell, it cannot distinguish between proteins that have lost activity and proteins that decrease in number. Previous western blots confirmed a reduction in luciferase protein after incubation with 3P and 2PD, yet contributions to loss of luciferase activity from interference with TNAs still need to be considered. To test for direct TNA-protein interaction, TNAs were incubated with luciferase for 10 minutes at room temperature and then probed changes in luminescence level. As shown in **Figure 4.5A**, no reduction in luciferase activity was observed. In fact, 2PD and 3P even increased protein activity slightly. When TNAs were incubated with luciferin before adding luciferase only 2P reduced the protein activity under this condition (**Figure 4.5B**), although it did not show false positives in the *in vitro* assays. These results indicate that the TNAs with hydrophobic moieties do not reduce luciferase activity through direct interactions with luciferase or luciferin.

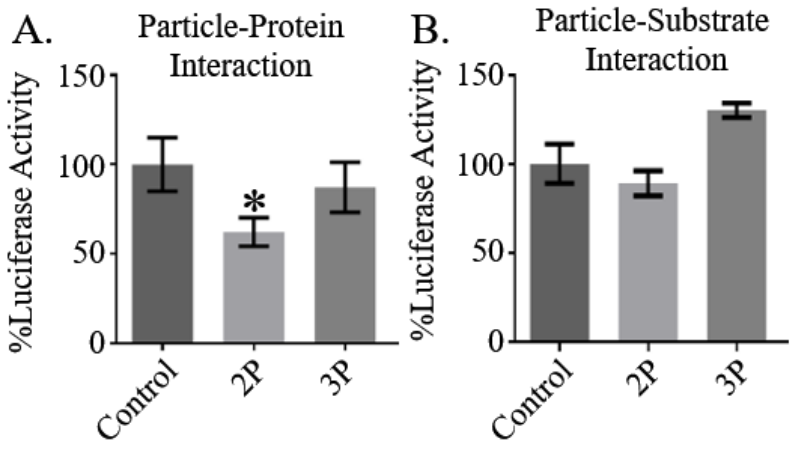


**Figure 4.5: Direct TNA/Protein and TNA/Substrate Interactions**

A: Interaction between TNAs and Luciferase protein was observed by incubating the protein and TNA together for 10 minutes. Then luciferin solution was added to the well and a luminescence reading was taken. The readings were normalized to the control well of luciferase protein alone. B: TNA and Luciferin (substrate to luciferase) direct interaction was observed by 30-minute incubation of TNA and Luciferin before an injection of luciferase solution was added to the well. A luminescence reading was taken and the values normalized to the control well which did not contain TNAs.

### 4.3.3. Raman spectroscopy indicates that hydrophobic moieties contribute to TNA's interaction with siRNA

To better understand how palmitate could interact with other cellular components and induce cell stress, Raman spectroscopy of 2P, 3P, and each of their individual components was conducted (**Figure 4.6**). Each component was allowed to interact with siRNA, which does not appear on the Raman spectra (**Figure S2**), while their spectra were compared for change in vibrational intensity. Interactions between siRNA with PEG or PAL were minor but the interaction between PEI and siRNA was more pronounced. However, physical mixtures of PAL/PEI and PAL/PEG showed unexpected interactions with siRNA. PEG/PAL showed a large change in vibrational intensity although neither component showed significant interaction with siRNA on their own. PEI/PAL increased its vibrational intensity, which indicates that the polymers are more mobile in the presence of siRNA. Raman spectra of 2P and 3P with siRNA slightly changed after the addition of siRNA although the exact influence of PAL in these interactions could not be determined.

To account for any variance in measurement of the polymers, PEG polymer was analyzed under a number of conditions to determine what effect sample conditions would have on the measurements taken. **Figure S3** indicates that samples of PEG taken from the same stock and analyzed in succession would have different peak intensities but the number and location of peaks would be the same. Referencing peak intensity to the largest peak of the of the spectra determined that these peaks were all in the same ratio (**Figure S4**), which supports why the Raman spectra in **Figure 4.6** use normalized intensity**. Figure S5** indicates that Raman spectra of the same sample over a few hours

have very minor changes. Though the Raman spectra of the polymer samples were all taken in succession, no experiment took longer than 2 hours to perform and therefore peak changes between samples should not have occurred.

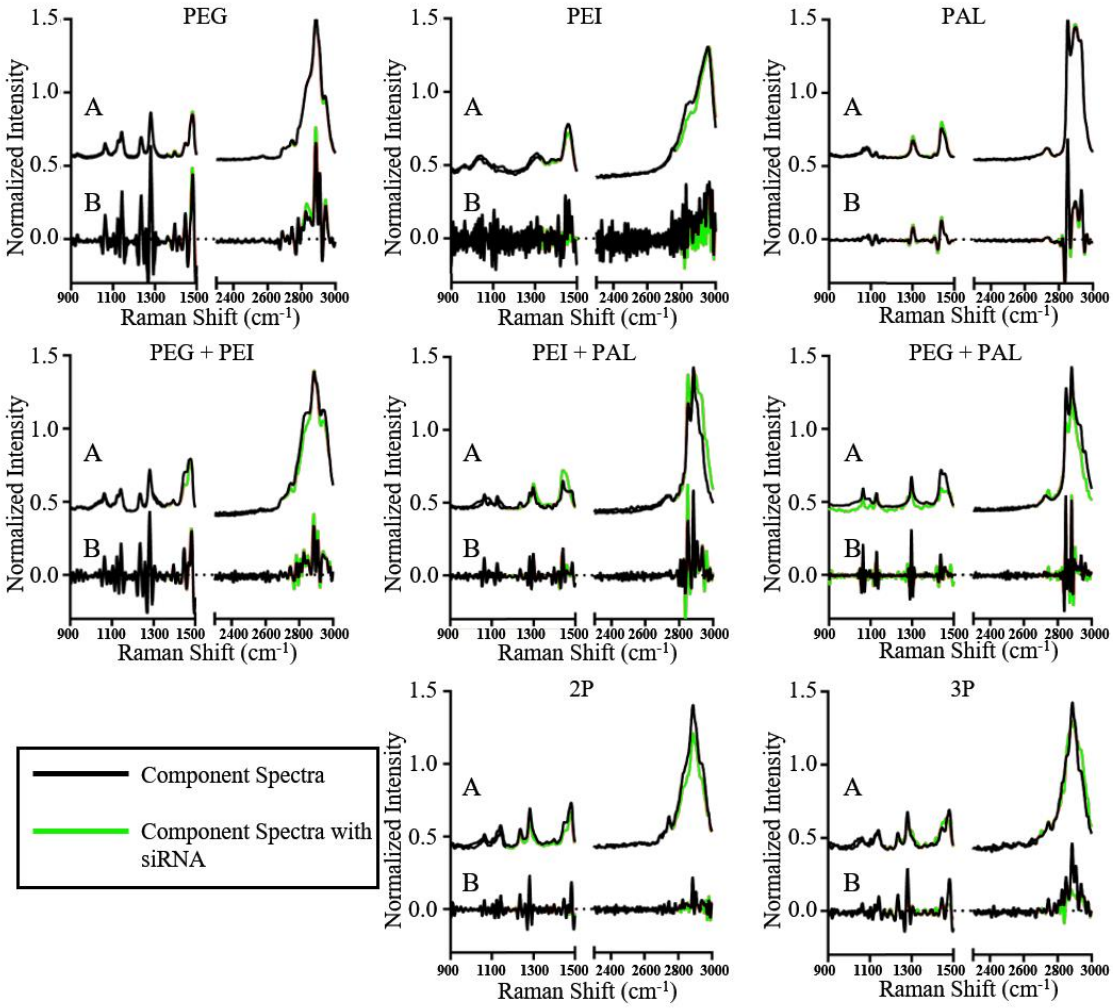


**Figure 4.6: Raman Spectroscopy of TNAs and Their Components**

Raman spectrographs of each component of TNAs, a physical mixture or components, and fully formed TNAs. Spectrograph A is the raw form of the Raman shift and spectrograph B is the deconvoluted raw spectra. Green lines indicate components or TNAs mixed with siRNA and black lines indicate components or TNAs alone.

### 4.3.4. Hydrophobically modified TNAs reduce protein expression, membrane integrity, and ATP concentration but retained mitochondrial activity

Resazurin cell viability assay was used to determine levels of live cells after incubation of TNAs. The resazurin assay measures redox activity within the cell, but this process does not represent a complete picture of cell health. Changes in ATP content, total protein amount, and cell membrane porosity were also investigated to determine the presence of cellular stress. **Figure 4.7** shows differences among these cytotoxicity assays. 3P did not have a significant impact on redox activity in the cell but ATP and total protein levels in the cells greatly decreased. Additionally, membrane porosity decreased with incubation of 3P.

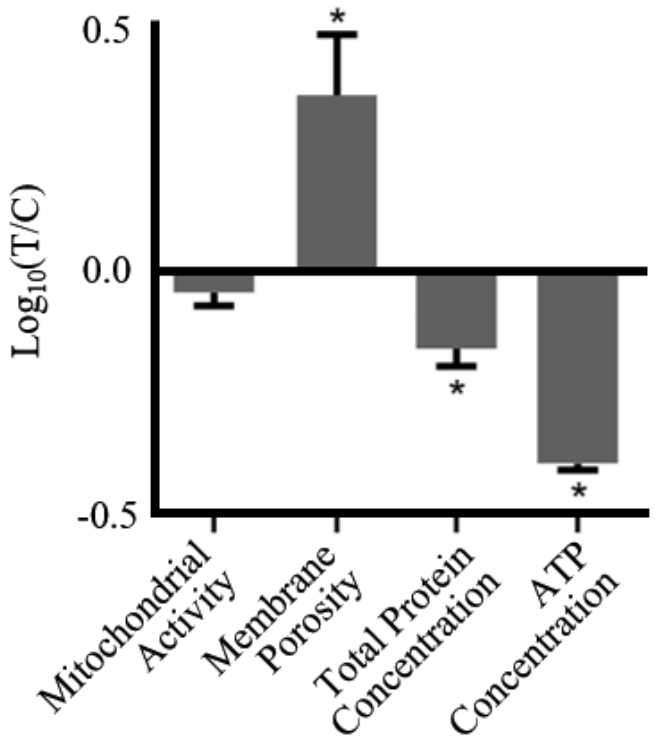


**Figure 4.7: Alternative Cell Health Markers After Incubation with 3P**

Four cell viability markers were examined to elucidate cell stress occurring within cells after 72-hour incubation with empty 3P complexes at 1 mg/mL. Mitochondrial activity was analyzed using the resazurin assay, total protein count was determined using the Sulforhodamine B assay, total ATP count was done using a luminometric assay in HT29 cells that did not express luciferase, and membrane integrity was analyzed by an assay that measured the cells ability to reduce Bis-AAF-R110 which can only be reduced from inside the cell. Values were plotted as the log of the ratio between the cells dosed with 3P and the control cells. Values statistically different from 0 are denoted by (*) ($p<0.01$)

### 4.3.5. TNAs increased ubiquitination and degradation of luciferase

Western blotting determined the extent of ubiquitination of luciferase to gain a better understanding of the fate of the luciferase protein after TNA treatment. Western blot analysis of cells dosed for 72 hours with 2P, 2P', 3P, and 3P' and an additional 6 hours with MG132 proteasome inhibitor confirmed the presence of both intact luciferase and ubiquitinated luciferase (**Figure 4.8**). The proteasome inhibitor prevents the degradation of ubiquitinated luciferase so that it can be visualized on the blot. **Figure 4.8 A** shows the reductions in luciferase concentration previously seen with 3P and 3P' and displays little effect by the proteasome inhibitor MG132. Initially ubiquitinated luciferase decreased in cells dosed with 3P and 3P', but its corresponding bands increased upon addition of the proteasome inhibitor (**Figure 4.8B**). All TNAs induced an increase in ubiquitination of luciferase while 3P and 3P' caused the highest increase in this band comparatively. This indicates that 3P and 3P' increase ubiquitination of luciferase and they may also increase proteasome activity.

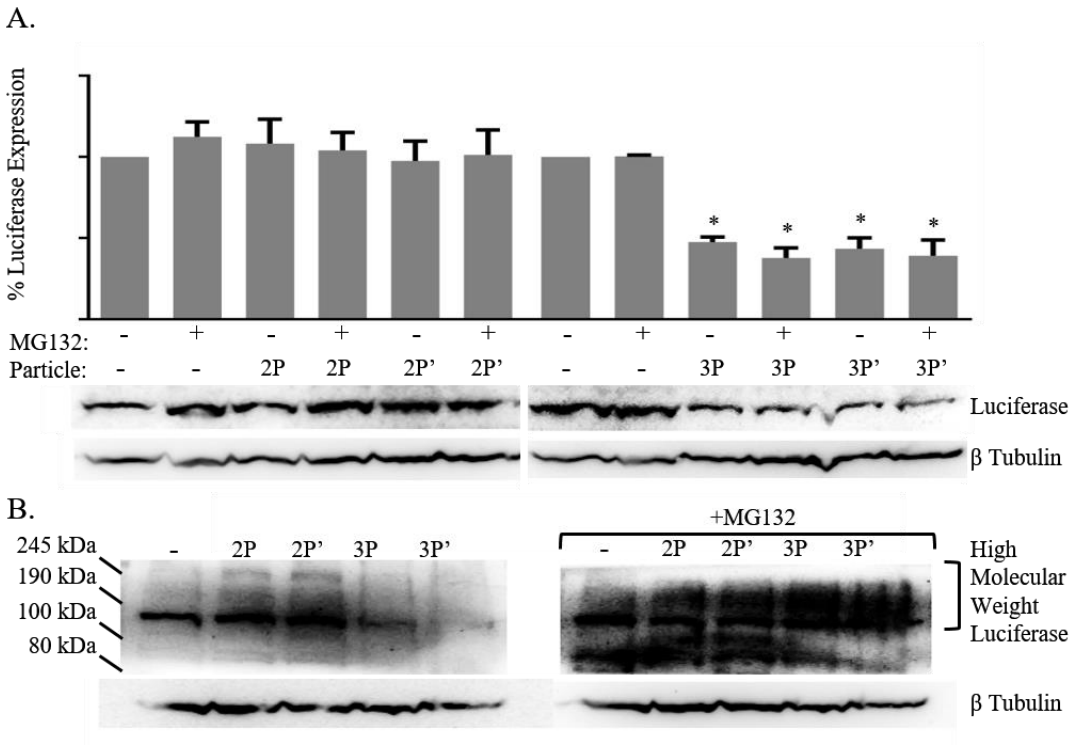


**Figure 4.8: TNA Induced Ubiquitination of Luciferase**

Western blots detailed the expression of (A) luciferase, and (B) high molecular weight luciferase after 72h dosage of TNAs in HT-29-luc cells. Bar graphs represent quantification of luciferase/beta tubulin ratio from western blot and are presented as the expression percentage of luciferase compared with the untreated control. Additionally, cells were dosed as indicated with MG132 proteasome inhibitor for 6h before cell lysis. Cellular expression of luciferase was compared with beta tubulin. * denotes that the column is significantly different from the no particle, no MG132 condition ($p<0.01$)

## 4.4. Discussion

In chapter 2, PEG-PEI TNAs were investigated to improve siRNA delivery by modulating complex stability through addition of palmitate, a hydrophobic moiety[95]. Although those TNAs modified with a hydrophobic group PAL (3P) caused increased transfection, their complex stability was lowered. In further investigation of how these TNAs were able to accomplish this effect, an siRNA-independent reduction of luciferase in cells treated 3P was observed in luciferase assays for transfection efficiency (**Figure 4.3**), referred to as a false positive effect. These false positives can be detrimental in developing siRNA-based therapeutic options that require specific gene silencing for targeted gene therapy. Therefore, this chapter further investigated potential causes for the unexpected protein reduction by using TNAs made from PEG-PEI with different hydrophobic pendant groups (PAL vs DOC) and polymer backbone (PEI vs PLL).

Structural differences in hydrophobic groups may influence false positives caused by TNAs differently. TNAs attached with rigid bile acid DOC (2PD) and the flexible fatty acid PAL (3P) pendant groups were investigated as these hydrophobic groups are structurally different. 2PD observed a reduction of luciferase activity slightly less than 3P, indicating that the false positive effect is not unique to palmitate. However, it is unknown if the decreased protein activity is due to inactivated protein or reduced cellular concentration of luciferase because the assay does not differentiate between the two conditions. To observe any loss of activity of luciferase due to TNA interaction, TNAs were incubated with free luciferase protein or free luciferin substrate before addition of the other component. Since neither 3P nor 2PD reduced the activity of luciferase, the protein concentration should be lower in the cell. Western blotting supported this

speculation, indicating that 3P and 2PD reduced luciferase protein concentrations. This determined that the false positive transfection is due to reduced cellular protein concentration brought on by the hydrophobic moiety.

Another factor that may affect the false positive effect is composition of the cationic backbone which influences the TNA's secondary structure formation. Secondary structure refers to the folding or condensing of the polymer structure either on its own or in the presence of anionic groups. This can influence the location of components within the TNA's core. Linear PLL, another well studied cationic polymer for gene transfection, replaced branched PEI as the backbone for TNAs, creating 2P' and 3P'. These particles were similar in size and surface charge to PEI based TNAs. The false positive effect was observed in 3P' but initially to a lesser extent than 3P. While changing the backbone structure mildly decreased the false positive effect, it did not eliminate it. This indicates that the contribution of the backbone structure to the false positive effect is significantly less than that of the hydrophobic moiety.

Raman spectroscopy offers another method to better understand PALs influence on false positives by examining PAL's influence on TNA interaction. Raman spectroscopy measures the vibrational energy of chemical bonds in a compound which can determine the influence of TNA components on interactions with other compounds[166-168]. These bond vibrations are unique and will change by either shifting their energy spectrum or reducing signal intensity depending on interactions or conformation of TNA components. Raman spectroscopy showed the differences in vibrational energies after the interaction between siRNA and components of 3P, their physical mixtures, and finally the complete TNAs. Initially, the Raman spectra detected minor intensity reductions when siRNA

interacted with each separate component of 3P (PEG, PEI, and PAL). However, physical mixtures of components containing PAL (PAL/PEI and PAL/PEG) showed larger vibrational intensity changes than the components. The changes indicated that the PAL had influence over the conformation or interaction of the components. When each component is tethered in a TNA, the vibrational changes are more intense in some areas as siRNA interacts with TNAs. Even if the PAL and siRNA are not directly interacting, PAL may influence the way 3P condenses around the siRNA, which would further alter the particle conformation and disrupt vibrational energies. While this is not a strong correlation, it gives evidence that the inclusion of PAL in the TNA does influence the TNA condensation when it comes in to contact with other compounds.

PAL influence over TNA interaction with cellular components could induce cell stress without significant cytotoxicity. Cell stress is a condition where cell metabolism, protein concentration, and gene expression may be altered to combat cellular damage or sudden changes in environment[169]. Though cell stress often leads to cytotoxicity, it can still be present without inducing significant toxicity and can be overlooked by some cellular viability assays. The viability assay used in conjunction with the transfection assays was a resazurin based assay which is a widely-used method for determining cell viability in mammalian cells[170]. Resazurin is reduced to a fluorescent molecule, resorufin, in the cell indicating redox activity which correlates with cell viability. This assay focuses on cell metabolism and does not account for other indicators of cell health. Three other markers of cell health were examined to obtain a more complete picture of cell health: total protein concentration in cells, ATP production, and membrane porosity. Cells dosed with 3P exhibited less total protein, lower ATP concentration, and more

porous membranes than those of the control group. Lowered total protein production does indicate cell death has occurred but the amount of cell death indicated in **Figure 4.7** would not completely account for the reduced luciferase concentration. More porous membranes and lowered ATP production[171] are significant signs of cell stress and adds further evidence that 3P is not completely harmless to the cell. These factors support that 3P has an adverse effect on the cells that leads to cell stress but the specific cause of the stress is uncertain.

Core components of hydrophobically modified TNAs have been known to cause cell stress in other formulations which may give possible mechanisms to cell stress induced by 3P. Free PAL can cause cell stress and autophagy through endoplasmic reticulum stress[172], free radical formation[173], toll like receptor activation[174], caspase mediated apoptosis[175], and glucose metabolism reduction[176]. Lipids attached to cationic head groups have been shown to increase enzyme inhibition inside cells, a result of both cationic and lipophilic regions[177]. Additionally, cationic polymers and some lipids can reduce protein expression and increased protein degradation due to cell stress[178-181]. However, it should be noted that these cell stress mechanisms are due to free components either alone or removed from their respective nanoparticles. The purification methods used during TNA synthesis removed all free hydrophobic groups and the hydrophobic moieties to the PEI backbone are stable so that no free hydrophobic groups would be present in formulation. However, the chemically conjugated hydrophobic moieties may be able to interact with cellular components in a similar way to these free hydrophobic groups. Although these formulations differ from TNAs, they present possible

mechanisms by which hydrophobic moieties can cause cellular stress through interaction with the cell.

3P induced cell stress may produce false positives by causing fluctuation of cellular protein concentration, including luciferase. One mechanism of protein reduction in the cell is increased ubiquitination of proteins, which increases their proteasome degradation. Protein ubiquitination occurs normally in the cell as part of the ubiquitination-proteasome pathway but is increased in times of stress or when certain pathways are activated, such as autophagy[182]. Western blotting confirmed an increase in the molecular weight of luciferase inside cells dosed with hydrophobically modified TNAs. Although this is not direct evidence of luciferase ubiquitination, an increase in molecular weight of a protein can often be the result of ubiquitination. Additionally, hydrophobic groups may cause oxidative and endoplasmic reticulum stress which has been shown to increase protein ubiquitination[183-184]. These stresses can also lead to regulated cell death which would increase protein ubiquitination[185] as well. Although the exact cellular mechanism inducing the luciferase reduction is unknown, this gives a plausible mechanism for the interactions hydrophobically modified TNAs are generating in the cell.

Based on the results of this chapter, we propose that the hydrophobically modified TNAs can interact with cellular components by allowing hydrophobic groups to influence TNA interactions with compounds outside of the nanoparticle. The data suggests that the hydrophobic group is most influential, compared with backbone structure, in generating the false positive. To achieve this, the hydrophobic component would be required to interact near the surface of the TNA. TNAs exist as a single polymer, core/shell systems regardless of the presence of siRNA, as discussed in chapter 3, and empty TNAs should

behave similarly to complexed TNAs. Hydrophobic moieties are housed in the core of the TNA and the PEG shell should prevent their interaction while the TNA maintains its secondary structure, or folded state. However, TNAs could be in a state of equilibrium between the folded and unfolded states. The addition of PEG and PAL will drive the equilibrium toward the folded state, forming a core/shell environment, but a small percentage of the unfolded state will persist. This unfolded state may allow the PAL to interact with cellular components, possibly causing endoplasmic reticulum stress.

While this mechanism accounts for interactions outside the TNA, the TNA may additionally interact with cellular components reaching its core. TNAs may also capture molecules needed for cellular metabolism, such as ATP or other important cellular process cofactors, which are small enough to enter the particle core. Entrapping these important cellular molecules would have induced cellular stress causing non-specific reduction in luciferase. In particular, 3P has both cationic and hydrophobic regions, and thus they can attract coenzymes like ATP through both ionic and hydrophobic interactions. After the coenzyme is charge neutralized, they may be entrapped in TNAs further strongly by hydrophobic interactions. We previously confirmed that TNAs altered drug release patterns in the presence of hydrophobic excipients outside of the TNAs, yet these hydrophobic excipients were not found to enter the TNA but weakly bound the surface of the TNA[186]. Therefore, binding of cofactors to the surface or inside the TNA is possible and can cause cell stress. Further investigation into these mechanisms is ongoing and will be reported in future studies.

## 4.5. Conclusions

This chapter demonstrates a false positive outcome of the luciferase based transfection efficiency assay induced by siRNA/TNA complexes modified with hydrophobic pendant groups. This effect was not specific to any hydrophobic group tested and may be triggered by other groups and factors including polymer composition, conformation, and complex stability. Altering the condensation mechanism of the TNA based on backbone linearity appeared to reduce this effect but was unable to eliminate it. Additionally, the hydrophobic moieties of the TNA appeared to induce some mechanism of cell stress. This stress likely caused the over-ubiquitination and degradation of luciferase. The exact cellular mechanism which induces this effect remains elusive but these results clearly indicate that the hydrophobic core components of the TNAs can induce false positive results in the luciferase based transfection efficiency assay. These findings provide a valuable insight into designing non-viral gene vectors made from PEG-PEI and potentially other types of cationic polymers.

## 4.6. Limitations of Observations

It should be noted that while the data in this chapter provides evidence for the conclusions being made, there are limitations to what the data can concretely tell us. We concluded that cellular stress is likely inducing an over ubiquitination of the luciferase protein as shown by the increased luciferase molecular weight. While the western blots and the viability assays point in the direction of this conclusion, it is more suggestive than conclusive. Future experimentation can elaborate on these findings in order to strengthen these conclusions. The viability assays indicate declining cell health but cellular stress can be more concretely measured through reactive oxidative species detection or

generalized oxidative stress assays. Comparing these results and the luciferase concentrations to a total cell count would also yield a more concrete characterization of normalization of cellular viability assays and cellular luciferase activity. Additionally, the western blot data shows an increase in high molecular weight luciferase which may indicate increased ubiquitination but overall ubiquitination can be measured on a western blot. Proteasome activity can be assayed separately which would further indicate any upregulation of the ubiquitin-proteasome pathway. Overall, the data in this chapter supports our conclusions but key control experiments would strengthen our findings.

# Chapter 5: Conclusions

## 5.1. Core components of TNAs influence siRNA/TNA complex stability and transfection efficiency

In this work, the effects of hydrophobic core modification on transfection efficiency and TNA/siRNA complex stability were examined. It was found that increasing hydrophobic content of the core can increase transfection efficiency but at the cost of reduced complex stability. The hydrophobically modified TNAs were unable to protect siRNA from degradation as the siRNA's interaction with the amines present in the core of the TNA is likely blocked by the hydrophobic moiety. These hydrophobic groups had significant effects outside the core by increasing the endosomal escape ability of the TNA.

The hydrophobic moiety used in the TNA did not initially interfere with the transfection evaluation assays but upon subsequent batches it began to cause false positives in the assay. A luciferase based assay was used in all parts of this work to evaluate transfection efficiency of the TNAs. However, subsequent batches of hydrophobically modified TNAs caused a reduction in luciferase activity relative to the control without siRNA being present. This effect was not specific to the type of hydrophobic moiety used and it was determined that the hydrophobic moiety was causing cellular stress that wasn't observed using the mitochondrial activity assay. The reduction of luciferase was likely caused by over-ubiquitination and subsequent rapid degradation of the protein brought on by cellular stress caused by the hydrophobically modified TNAs. This work reinforces the necessity of proper controls to account for unexpected results such as this and calls attention to the inclusion of hydrophobic groups in unimolecular nanoparticle systems.

Although hydrophobic core modification of TNAs shows beneficial properties, such as increased endosomal escape and transfection efficiency, proper selection of these groups is crucial to siRNA delivery vehicle design. In this work, it was demonstrated that the core components of TNAs can have negative effects outside of the TNA. Proper selection of core components will help to reduce their negative effects and improve overall efficacy of the TNA. Though these effects were observed using a unimolecular PEI based nanoparticle, these results should be applicable to other cationic polymer based delivery vehicles that interact with siRNA as a single polymer and improve delivery vehicle design.

## 5.2. PEG shell density effects transfection efficiency and complex stability

This work demonstrated that PEG shell density influenced the overall transfection efficiency of the TNAs. In chapter 2, PEG-PEI (2P) was not found to transfect cells though other groups have had success with this formulation. Decreasing the pegylation density of the 2P increased its transfection efficiency past that of unmodified PEI. This was observed by altering all factors effecting shell composition including PEG molecular weight, PEG attachment percentage, and reduced PEI impurities in the synthesis stock. Additionally, reducing the PEI impurities also decreased the number of polymers involved in siRNA/TNA complex formation. This further increased the unimolecularity and stability of the complex.

The effect of pegylation density on transfection efficiency and stability of the TNA complexes indicates that future particle design should limit the shell density in order to delivery vehicle efficacy. The results of this work indicated that some pegylation density was beneficial to the transfection efficiency of the TNA. Additionally, complexes were

more unimolecular after a moderate amount of pegylation and removal of PEI impurities. To obtain these beneficial effects, particle design needs to include a consistent and balanced shell density for the most efficacious delivery vehicle. Considering that pegylation is one of the most common shell modifications nanoparticles, these findings may also be applicable to other cationic polymer based delivery vehicles.

## 5.3. Future Directions

The data presented in this document shows a number of the complexities and problems with developing a cationic nanoparticle based siRNA delivery system. While the effects of modifications to the TNA on siRNA transfection were determined by this work, siRNA transfection issues made it difficult to examine the effects further. The TNA in its current form must reduce its pegylation percentage in order to deliver siRNA more efficaciously *in vitro* and control the location of the hydrophobic moiety in the core. Additionally, issues with hydrophobic modification of TNAs needs more elucidation. Therefore, the design of the TNA needs to be altered in order to examine the effects of improve the delivery of siRNA and

TNAs can be redesigned while being true to their underlying values: a stable system that can form unimolecular complexes with siRNA. A unimolecular system can be formed using a single large polymer linked to itself or many smaller polymers linked together. Linking multiple smaller PEI polymers through crosslinking would create a more rigid core where hydrophobic component would be more tightly sequestered. This would help control or even eliminate the issues seen in this work from the hydrophobic group. The crosslinked TNA could then be pegylated at a lower percentage compared to the original TNAs. The resulting TNA could then be used to investigate the effect of

different hydrophobic moieties and attachment percentages on siRNA/TNA stability and transfection efficacy. Ideally, the resulting TNAs could be examined for siRNA/TNA stability using isothermal calorimetry in order to obtain a more succinct measure of binding stability. The results of these studies would generate more information on the effects of TNA/siRNA binding stability on transfection efficiency to produce a more efficacious siRNA delivery vehicle and further their design.

The issues seen with hydrophobic modification also warrant further study and elucidation. While this work provides evidence that the hydrophobic groups increase ubiquitination of our reporter protein, it is unknown exactly what effect the hydrophobic group has on the cell. Multiple cell lines should be investigated to determine how broad this effect is as well as other protein concentration assays to determine the overall ubiquitination of proteins in the cell and proteasome activity. The viability assays should be compared to total cell counts in order to give a more succinct term of specific cell health factors per cell. Further elucidation of the pathways that the hydrophobic groups activate, through western blotting or RT-PCR, would help identify the cause of the cellular stress. This direction would allow for better choices of TNA core components and control or reporter proteins. Understanding this effect will be valuable for the future of siRNA delivery vehicle design.

## Supplemental Figures

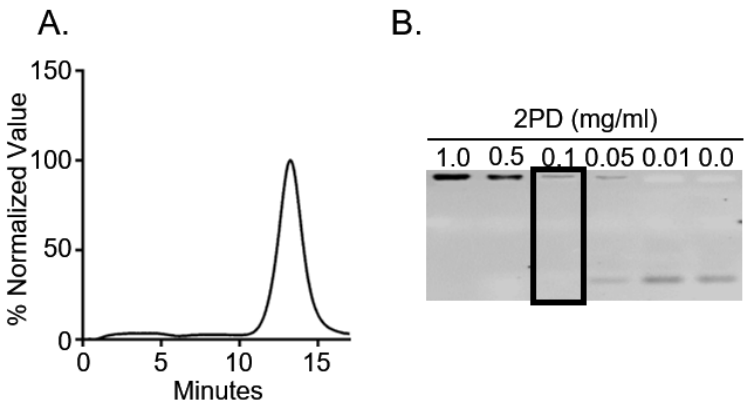


**Figure S1: Characterization of 2PD TNA**

A: Gel permeation chromatography (GPC) spectra shows particle uniformity and purity of 2PD B: Gel electrophoresis of 2PD with 72 nM siRNA and varying concentrations of TNA to determine the ratio of 2PD to siRNA needed to form complexes (black box).

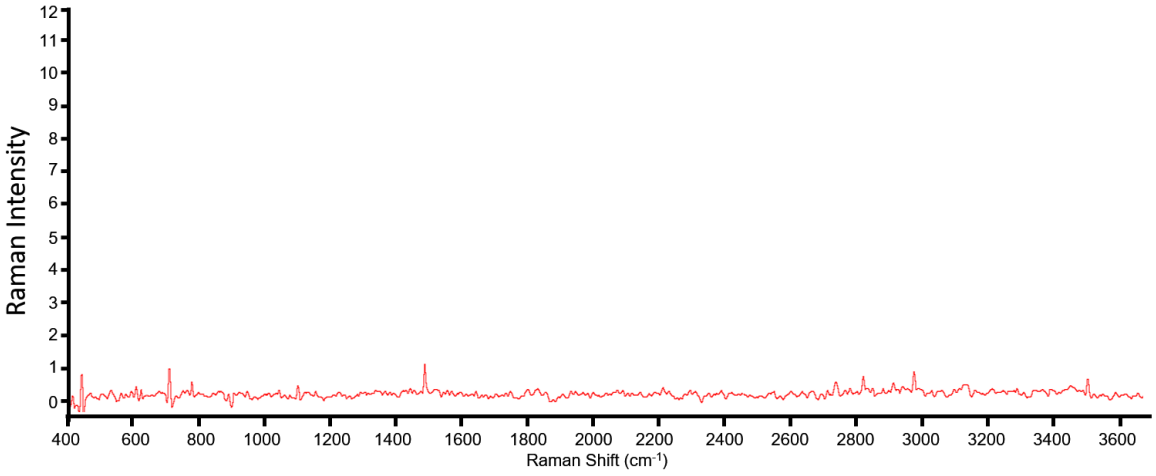


**Figure S2: Raman spectra of siRNA**

The same amount of siRNA used in Raman experiments described in section 4.2.3 was freeze dried to a well on the Raman sample plate. The subsequent Raman spectra of siRNA shows very minor peaks. The peaks of siRNA will not interfere with the peaks of Raman samples containing siRNA as the Raman intensity of these peaks are very low.

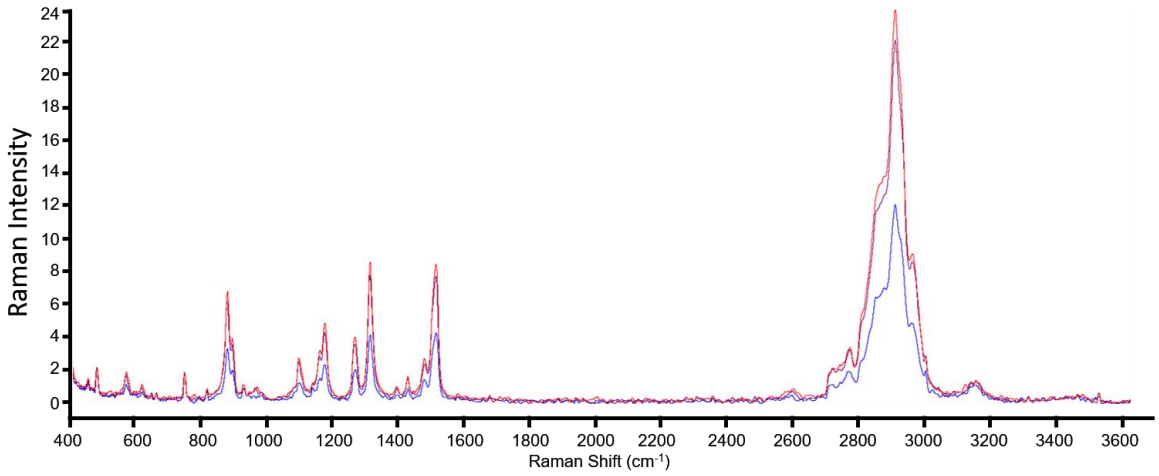


**Figure S3: Raman spectra comparison of multiple PEG samples**

Raman spectra of PEG from 3 separate wells of the sample plate. 100 uL of a 10 mg/ml aqueous solution of 5 kDa molecular weight PEG was freeze dried in three separate wells of the Raman sample plate. Raman spectra was taken of each well in succession. Each color represents a different well. Although peak heights change between runs, the numbers and position of peaks did not.

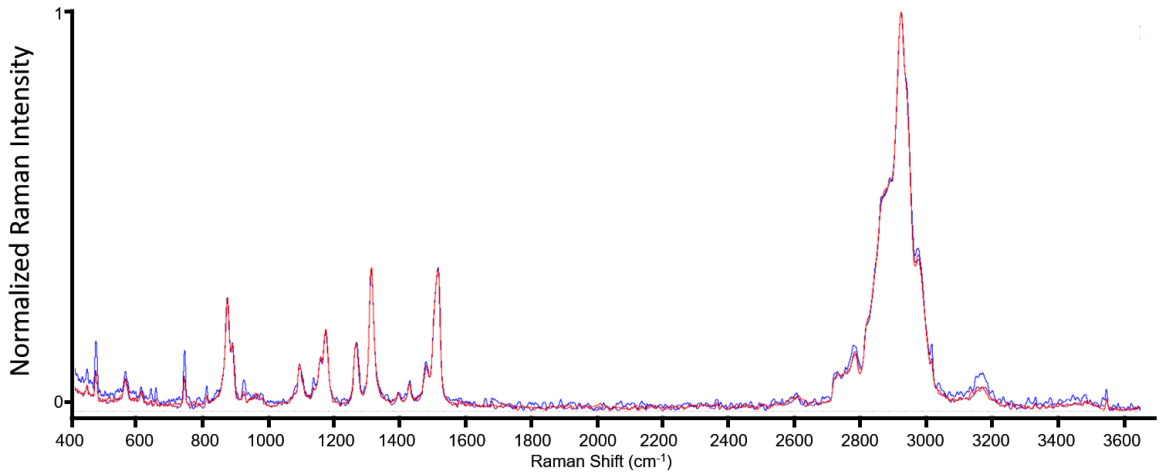


**Figure S4: Normalized Raman spectra comparison of multiple PEG samples**

Normalized Raman spectra of PEG from figure S2. The Raman spectra of each PEG from figure S2 was normalized to its highest peak. The overlaid spectra show that peak ratios and heights match between wells of the same sample. Each color indicates a different well.

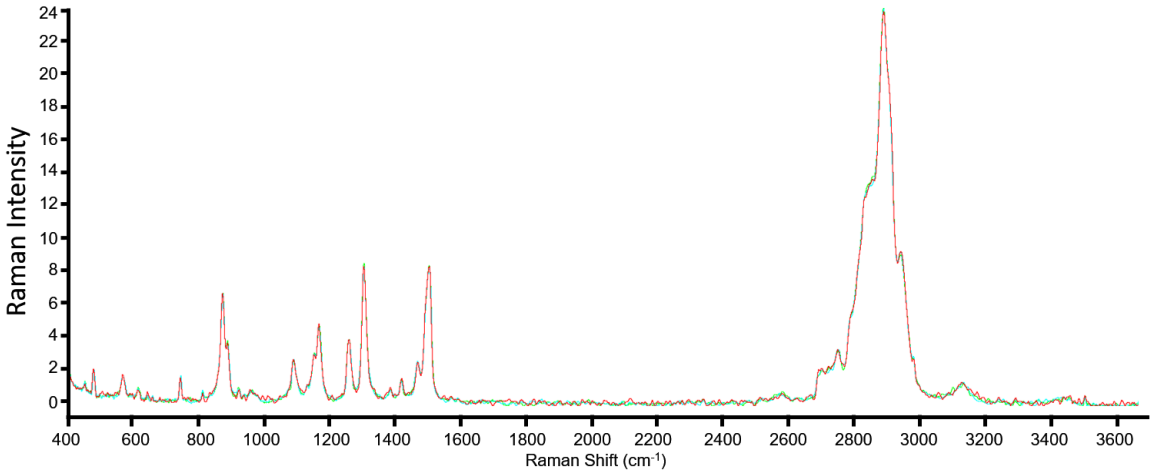


**Figure S5: Multiple Raman spectra comparison of single PEG sample**

Raman spectra of PEG taken at 3 different time points. 100 uL of a 10 mg/ml aqueous solution of 5 kDa molecular weight PEG was freeze dried in one well of the Raman sample plate. Raman spectra was taken of the same well 3 separate times with a 1 hour interval between each run. Each color represents a different run. The peaks show minor differences between each run.

## References


1. Hanahan, D.; Weinberg, R. A., The hallmarks of cancer. *Cell* **2000,** *100* (1), 57-70.

2. Hanahan, D.; Weinberg, R. A., Hallmarks of cancer: the next generation. *Cell* **2011,** *144*, 646-74.

3. Pecot, C. V.; Calin, G. A.; Coleman, R. L.; Lopez-Berestein, G.; Sood, A. K., RNA interference in the clinic: challenges and future directions. *Nat Rev Cancer* **2011,** *11* (1), 59-67.

4. Patil, S. D.; Rhodes, D. G.; Burgess, D. J., DNA-based therapeutics and DNA delivery systems: a comprehensive review. *AAPS J* **2005,** *7* (1), E61-77.

5. Friedmann, T. R., R., Gene therapy for human genetic disease? *Science* **1973**, 949-55.

6. Brewster, L. P.; Brey, E. M.; Greisler, H. P., Cardiovascular gene delivery: The good road is awaiting. *Adv Drug Deliv Rev* **2006,** *58* (4), 604-29.

7. Ohlfest, J. R.; Demorest, Z. L.; Motooka, Y.; Vengco, I.; Oh, S.; Chen, E.; Scappaticci, F. A.; Saplis, R. J.; Ekker, S. C.; Low, W. C.; Freese, A. B.; Largaespada, D. A., Combinatorial antiangiogenic gene therapy by nonviral gene transfer using the sleeping beauty transposon causes tumor regression and improves survival in mice bearing intracranial human glioblastoma. *Mol Ther* **2005,** *12* (5), 778-88.

8. Uherek, C.; Wels, W., DNA-carrier proteins for targeted gene delivery. *Adv Drug Deliv Rev* **2000,** *44* (2-3), 153-66.

9. Hackett, P. B.; Ekker, S. C.; Largaespada, D. A.; McIvor, R. S., Sleeping beauty transposon-mediated gene therapy for prolonged expression. *Adv Genet* **2005,** *54*, 189-232.

10. Kormann, M. S.; Hasenpusch, G.; Aneja, M. K.; Nica, G.; Flemmer, A. W.; Herber-Jonat, S.; Huppmann, M.; Mays, L. E.; Illenyi, M.; Schams, A.; Griese, M.; Bittmann, I.; Handgretinger, R.; Hartl, D.; Rosenecker, J.; Rudolph, C., Expression of therapeutic proteins after delivery of chemically modified mRNA in mice. *Nat Biotechnol* **2011,** *29* (2), 154-7.

11. Bangel-Ruland, N.; Tomczak, K.; Fernandez Fernandez, E.; Leier, G.; Leciejewski, B.; Rudolph, C.; Rosenecker, J.; Weber, W. M., Cystic fibrosis transmembrane conductance regulator-mRNA delivery: a novel alternative for cystic fibrosis gene therapy. *J Gene Med* **2013,** *15* (11-12), 414-26.

12. Lundin, K. E.; Gissberg, O.; Smith, C. I., Oligonucleotide Therapies: The Past and the Present. *Hum Gene Ther* **2015,** *26* (8), 475-85.

13. Stephenson, M. L.; Zamecnik, P. C., Inhibition of Rous sarcoma viral RNA translation by a specific oligodeoxyribonucleotide. *Proc Natl Acad Sci U S A* **1978,** *75* (1), 285-8.

14. Kole, R.; Krainer, A. R.; Altman, S., RNA therapeutics: beyond RNA interference and antisense oligonucleotides. *Nat Rev Drug Discov* **2012,** *11* (2), 125-40.

15. Fire, A., RNA-triggered gene silencing. *Trends in Genetics* **1999,** *15*, 358-363.

16. Fire, A.; Xu, S.; Montgomery, M.; Kostas, S., Potent and specific genetic interference by double-stranded RNA in Caenorhabditis elegans. *nature* **1998,** *391*, 806-811.

17. Hannon, G. J., RNA interference. *Nature* **2002,** *418* (6894), 244-51.

18. Bartlett, D. W.; Davis, M. E., Insights into the kinetics of siRNA-mediated gene silencing from live-cell and live-animal bioluminescent imaging. *Nucleic acids research* **2006,** *34*, 322-33.

19. Sunaga, N.; Shames, D. S.; Girard, L.; Peyton, M.; Larsen, J. E.; Imai, H.; Soh, J.; Sato, M.; Yanagitani, N.; Kaira, K.; Xie, Y.; Gazdar, A. F.; Mori, M.; Minna, J. D., Knockdown of oncogenic KRAS in non-small cell lung cancers suppresses tumor growth and sensitizes tumor cells to targeted therapy. *Mol Cancer Ther* **2011,** *10* (2), 336-46.

20. Freire, J. M.; Rego de Figueiredo, I.; Valle, J.; Veiga, A. S.; Andreu, D.; Enguita, F. J.; Castanho, M. A., siRNA-cell-penetrating peptides complexes as a combinatorial therapy against chronic myeloid leukemia using BV173 cell line as model. *J Control Release* **2017,** *245*, 127-136.

21. Bochicchio, S.; Dapas, B.; Russo, I.; Ciacci, C.; Piazza, O.; De Smedt, S.; Pottie, E.; Barba, A. A.; Grassi, G., In vitro and ex vivo delivery of tailored siRNA-nanoliposomes for E2F1 silencing as a potential therapy for colorectal cancer. *Int J Pharm* **2017**.

22. Rengaswamy, V.; Zimmer, D.; Suss, R.; Rossler, J., RGD liposome-protamine-siRNA (LPR) nanoparticles targeting PAX3-FOXO1 for alveolar rhabdomyosarcoma therapy. *J Control Release* **2016,** *235*, 319-27.

23. Layzer, J. M.; McCaffrey, A. P.; Tanner, A. K.; Huang, Z.; Kay, M. A.; Sullenger, B. A., In vivo activity of nuclease-resistant siRNAs. *RNA* **2004,** *10* (5), 766-71.

24. Xu, C.-f.; Wang, J., Delivery systems for siRNA drug development in cancer therapy. *Asian Journal of Pharmaceutical Sciences* **2015,** *10* (1), 1-12.

25. Wittrup, A.; Lieberman, J., Knocking down disease: a progress report on siRNA therapeutics. *Nat Rev Genet* **2015,** *16* (9), 543-52.

26. Chiu, Y. L.; Rana, T. M., siRNA function in RNAi: a chemical modification analysis. *RNA* **2003,** *9* (9), 1034-48.

27. Harborth, J.; Elbashir, S. M.; Vandenburgh, K.; Manninga, H.; Scaringe, S. A.; Weber, K.; Tuschl, T., Sequence, chemical, and structural variation of small interfering RNAs and short hairpin RNAs and the effect on mammalian gene silencing. *Antisense Nucleic Acid Drug Dev* **2003,** *13* (2), 83-105.

28. Czauderna, F.; Fechtner, M.; Dames, S.; Aygun, H.; Klippel, A.; Pronk, G. J.; Giese, K.; Kaufmann, J., Structural variations and stabilising modifications of synthetic siRNAs in mammalian cells. *Nucleic Acids Res* **2003,** *31* (11), 2705-16.

29. Whitehead, K. A.; Langer, R.; Anderson, D. G., Knocking down barriers: advances in siRNA delivery. *Nat Rev Drug Discov* **2009,** *8* (2), 129-38.

30. Anderson, W. F., Prospects for human gene therapy in the born and unborn patient. *Clin Obstet Gynecol* **1986,** *29* (3), 586-94.

31. McManus, M. T.; Sharp, P. A., Gene silencing in mammals by small interfering RNAs. *Nat Rev Genet* **2002,** *3* (10), 737-47.

32. Mali, S., Delivery systems for gene therapy. *Indian J Hum Genet* **2013,** *19* (1), 3-8.

33. Yu, J. Y.; DeRuiter, S. L.; Turner, D. L., RNA interference by expression of short-interfering RNAs and hairpin RNAs in mammalian cells. *Proc Natl Acad Sci U S A* **2002,** *99* (9), 6047-52.

34. Sibbald, B., Death but one unintended consequence of gene-therapy trial. *CMAJ* **2001,** *164* (11), 1612.

35. Thomas, C. E.; Ehrhardt, A.; Kay, M. A., Progress and problems with the use of viral vectors for gene therapy. *Nat Rev Genet* **2003,** *4* (5), 346-58.

36. Kim, H. J.; Kim, A.; Miyata, K.; Kataoka, K., Recent progress in development of siRNA delivery vehicles for cancer therapy. *Adv Drug Deliv Rev* **2016,** *104*, 61-77.

37. Sarett, S. M.; Nelson, C. E.; Duvall, C. L., Technologies for controlled, local delivery of siRNA. *J Control Release* **2015,** *218*, 94-113.

38. Zhang, S.; Zhao, Y.; Zhi, D.; Zhang, S., Non-viral vectors for the mediation of RNAi. *Bioorganic chemistry* **2012,** *40*, 10-8.

39. Singh, Y.; Tomar, S.; Khan, S.; Meher, J. G.; Pawar, V. K.; Raval, K.; Sharma, K.; Singh, P. K.; Chaurasia, M.; Surendar Reddy, B.; Chourasia, M. K., Bridging small interfering RNA with giant therapeutic outcomes using nanometric liposomes. *J Control Release* **2015,** *220* (Pt A), 368-87.

40. Ozpolat, B.; Sood, A. K.; Lopez-Berestein, G., Liposomal siRNA nanocarriers for cancer therapy. *Advanced drug delivery reviews* **2014,** *66*, 110-6.

41. Leung, A. K.; Tam, Y. Y.; Cullis, P. R., Lipid nanoparticles for short interfering RNA delivery. *Adv Genet* **2014,** *88*, 71-110.

42. Hope, M. J., Enhancing siRNA delivery by employing lipid nanoparticles. *Ther Deliv* **2014,** *5* (6), 663-73.

43. Semple, S. C.; Akinc, A.; Chen, J.; Sandhu, A. P.; Mui, B. L.; Cho, C. K.; Sah, D. W.; Stebbing, D.; Crosley, E. J.; Yaworski, E.; Hafez, I. M.; Dorkin, J. R.; Qin, J.; Lam, K.; Rajeev, K. G.; Wong, K. F.; Jeffs, L. B.; Nechev, L.; Eisenhardt, M. L.; Jayaraman, M.; Kazem, M.; Maier, M. A.; Srinivasulu, M.; Weinstein, M. J.; Chen, Q.; Alvarez, R.; Barros, S. A.; De, S.; Klimuk, S. K.; Borland, T.; Kosovrasti, V.; Cantley, W. L.; Tam, Y. K.; Manoharan, M.; Ciufolini, M. A.; Tracy, M. A.; de Fougerolles, A.; MacLachlan, I.; Cullis, P. R.; Madden, T. D.; Hope, M. J., Rational design of cationic lipids for siRNA delivery. *Nat Biotechnol* **2010,** *28* (2), 172-6.

44. Cheng, X.; Lee, R. J., The role of helper lipids in lipid nanoparticles (LNPs) designed for oligonucleotide delivery. *Adv Drug Deliv Rev* **2016,** *99* (Pt A), 129-37.

45. Watanabe, K.; Harada-Shiba, M.; Suzuki, A.; Gokuden, R.; Kurihara, R.; Sugao, Y.; Mori, T.; Katayama, Y.; Niidome, T., In vivo siRNA delivery with dendritic poly(L-lysine) for the treatment of hypercholesterolemia. *Mol Biosyst* **2009,** *5* (11), 1306-10.

46. Hobel, S.; Aigner, A., Polyethylenimine (PEI)/siRNA-mediated gene knockdown in vitro and in vivo. *Methods Mol Biol* **2010,** *623*, 283-97.

47. Boussif, O.; Lezoualc'h, F.; Zanta, M. A.; Mergny, M. D.; Scherman, D.; Demeneix, B.; Behr, J. P., A versatile vector for gene and oligonucleotide transfer into cells in culture and in vivo: polyethylenimine. *Proc Natl Acad Sci U S A* **1995,** *92* (16), 7297-301.

48. Singha, K.; Namgung, R.; Kim, W. J., Polymers in small-interfering RNA delivery. *Nucleic Acid Ther* **2011,** *21* (3), 133-47.

49. Rezvani Amin, Z.; Rahimizadeh, M.; Eshghi, H.; Dehshahri, A.; Ramezani, M., The effect of cationic charge density change on transfection efficiency of polyethylenimine. *Iran J Basic Med Sci* **2013,** *16* (2), 150-6.

50. Ma, D., Enhancing endosomal escape for nanoparticle mediated siRNA delivery. *Nanoscale* **2014,** *6* (12), 6415-25.

51. Sun, X.; Zhang, N., Cationic polymer optimization for efficient gene delivery. *Mini Rev Med Chem* **2010,** *10* (2), 108-25.

52. Gary, D. J.; Puri, N.; Won, Y. Y., Polymer-based siRNA delivery: perspectives on the fundamental and phenomenological distinctions from polymer-based DNA delivery. *J Control Release* **2007,** *121* (1-2), 64-73.

53. Ziebarth, J. D.; Wang, Y., Understanding the protonation behavior of linear polyethylenimine in solutions through Monte Carlo simulations. *Biomacromolecules* **2010,** *11* (1), 29-38.

54. Ding, Y.; Jiang, Z.; Saha, K.; Kim, C. S.; Kim, S. T.; Landis, R. F.; Rotello, V. M., Gold nanoparticles for nucleic acid delivery. *Mol Ther* **2014,** *22* (6), 1075-83.

55. Yang, S.; May, S., Release of cationic polymer-DNA complexes from the endosome: A theoretical investigation of the proton sponge hypothesis. *J Chem Phys* **2008,** *129* (18), 185105.

56. Hong, S.; Leroueil, P. R.; Janus, E. K.; Peters, J. L.; Kober, M. M.; Islam, M. T.; Orr, B. G.; Baker, J. R., Jr.; Banaszak Holl, M. M., Interaction of polycationic polymers with supported lipid bilayers and cells: nanoscale hole formation and enhanced membrane permeability. *Bioconjug Chem* **2006,** *17* (3), 728-34.

57. Benjaminsen, R. V.; Mattebjerg, M. A.; Henriksen, J. R.; Moghimi, S. M.; Andresen, T. L., The possible "proton sponge " effect of polyethylenimine (PEI) does not include change in lysosomal pH. *Mol Ther* **2013,** *21* (1), 149-57.

58. Gauthier, M. A.; Gibson, M. I.; Klok, H. A., Synthesis of functional polymers by post-polymerization modification. *Angew Chem Int Ed Engl* **2009,** *48* (1), 48-58.

59. Figueroa, E. R.; Lin, A. Y.; Yan, J.; Luo, L.; Foster, A. E.; Drezek, R. A., Optimization of PAMAM-gold nanoparticle conjugation for gene therapy. *Biomaterials* **2014,** *35* (5), 1725-34.

60. Kievit, F. M.; Zhang, M., Cancer nanotheranostics: improving imaging and therapy by targeted delivery across biological barriers. *Adv Mater* **2011,** *23* (36), H217-47.

61. Choi, H. S.; Liu, W.; Misra, P.; Tanaka, E.; Zimmer, J. P.; Itty Ipe, B.; Bawendi, M. G.; Frangioni, J. V., Renal clearance of quantum dots. *Nat Biotechnol* **2007,** *25* (10), 1165-70.

62. Ward, C. M.; Read, M. L.; Seymour, L. W., Systemic circulation of poly(L-lysine)/DNA vectors is influenced by polycation molecular weight and type of DNA: differential circulation in mice and rats and the implications for human gene therapy. *Blood* **2001,** *97* (8), 2221-9.

63. Xue, H. Y.; Liu, S.; Wong, H. L., Nanotoxicity: a key obstacle to clinical translation of siRNA-based nanomedicine. *Nanomedicine (Lond)* **2014,** *9* (2), 295-312.

64. Fischer, D.; Bieber, T.; Li, Y.; Elsasser, H. P.; Kissel, T., A novel non-viral vector for DNA delivery based on low molecular weight, branched polyethylenimine: effect of molecular weight on transfection efficiency and cytotoxicity. *Pharm Res* **1999,** *16* (8), 1273-9.

65. Godbey, W. T.; Wu, K. K.; Mikos, A. G., Poly(ethylenimine)-mediated gene delivery affects endothelial cell function and viability. *Biomaterials* **2001,** *22* (5), 471-80.

66. Park, T. G.; Jeong, J. H.; Kim, S. W., Current status of polymeric gene delivery systems. *Adv Drug Deliv Rev* **2006,** *58* (4), 467-86.

67. Jeong, J. H.; Kim, S. W.; Park, T. G., Molecular design of functional polymers for gene therapy. *Progress in Polymer Science* **2007,** *32* (11), 1239-1274.

68. Rehman, Z.; Zuhorn, I. S.; Hoekstra, D., How cationic lipids transfer nucleic acids into cells and across cellular membranes: recent advances. *J Control Release* **2013,** *166* (1), 46-56.

69. Toy, R.; Roy, K., Engineering nanoparticles to overcome barriers to immunotherapy. *Bioengineering & Translational Medicine* **2016,** *1* (1), 47-62.

70. Burke, R. S.; Pun, S. H., Extracellular barriers to in Vivo PEI and PEGylated PEI polyplex-mediated gene delivery to the liver. *Bioconjug Chem* **2008,** *19* (3), 693-704.

71. Plank, C.; Mechtler, K.; Szoka, F. C., Jr.; Wagner, E., Activation of the complement system by synthetic DNA complexes: a potential barrier for intravenous gene delivery. *Hum Gene Ther* **1996,** *7* (12), 1437-46.

72. Chollet, P.; Favrot, M. C.; Hurbin, A.; Coll, J. L., Side-effects of a systemic injection of linear polyethylenimine-DNA complexes. *J Gene Med* **2002,** *4* (1), 84-91.

73. Lv, H.; Zhang, S.; Wang, B.; Cui, S.; Yan, J., Toxicity of cationic lipids and cationic polymers in gene delivery. *Journal of controlled release : official journal of the Controlled Release Society* **2006,** *114*, 100-9.

74. Merkel, O. M.; Beyerle, A.; Beckmann, B. M.; Zheng, M.; Hartmann, R. K.; Stöger, T.; Kissel, T. H., Polymer-related off-target effects in non-viral siRNA delivery. *Biomaterials* **2011,** *32*, 2388-98.

75. Patil, Y.; Panyam, J., Polymeric nanoparticles for siRNA delivery and gene silencing. *International journal of pharmaceutics* **2009,** *367*, 195-203.

76. Moghimi, S. M.; Symonds, P.; Murray, J. C.; Hunter, A. C.; Debska, G.; Szewczyk, A., A two-stage poly(ethylenimine)-mediated cytotoxicity: implications for gene transfer/therapy. *Mol Ther* **2005,** *11* (6), 990-5.

77. Kircheis, R.; Schuller, S.; Brunner, S.; Ogris, M.; Heider, K. H.; Zauner, W.; Wagner, E., Polycation-based DNA complexes for tumor-targeted gene delivery in vivo. *J Gene Med* **1999,** *1* (2), 111-20.

78. Patnaik, S.; Aggarwal, A.; Nimesh, S.; Goel, A.; Ganguli, M.; Saini, N.; Singh, Y.; Gupta, K. C., PEI-alginate nanocomposites as efficient in vitro gene transfection agents. *J Control Release* **2006,** *114* (3), 398-409.

79. Maheshwari, A.; Mahato, R. I.; McGregor, J.; Han, S.; Samlowski, W. E.; Park, J. S.; Kim, S. W., Soluble biodegradable polymer-based cytokine gene delivery for cancer treatment. *Mol Ther* **2000,** *2* (2), 121-30.

80. Liu, Z.; Zhang, Z.; Zhou, C.; Jiao, Y., Hydrophobic modifications of cationic polymers for gene delivery. *Progress in Polymer Science* **2010,** *35*, 1144-1162.

81. Incani, V.; Lavasanifar, A.; Uludag, H., Lipid and hydrophobic modification of cationic carriers on route to superior gene vectors. *Soft Matter* **2010,** *6* (10), 2124-2138.

82. Kataoka, K.; Harada, A.; Nagasaki, Y., Block copolymer micelles for drug delivery: design, characterization and biological significance. *Adv Drug Deliv Rev* **2001,** *47* (1), 113-31.

83. Suk, J. S.; Xu, Q.; Kim, N.; Hanes, J.; Ensign, L. M., PEGylation as a strategy for improving nanoparticle-based drug and gene delivery. *Adv Drug Deliv Rev* **2016,** *99* (Pt A), 28-51.

84. Knop, K.; Hoogenboom, R.; Fischer, D.; Schubert, U. S., Poly(ethylene glycol) in drug delivery: pros and cons as well as potential alternatives. *Angewandte Chemie (International ed. in English)* **2010,** *49*, 6288-308.

85. Xie, Z.; Ji, Z.; Zhang, Z.; Gong, T.; Sun, X., Adenoviral vectors coated with cationic PEG derivatives for intravaginal vaccination against HIV-1. *Biomaterials* **2014,** *35* (27), 7896-908.

86. Mishra, S.; Webster, P.; Davis, M. E., PEGylation significantly affects cellular uptake and intracellular trafficking of non-viral gene delivery particles. *Eur J Cell Biol* **2004,** *83* (3), 97-111.

87. Hatakeyama, H.; Akita, H.; Harashima, H., A multifunctional envelope type nano device (MEND) for gene delivery to tumours based on the EPR effect: a strategy for overcoming the PEG dilemma. *Adv Drug Deliv Rev* **2011,** *63* (3), 152-60.

88. Abuchowski, A.; McCoy, J. R.; Palczuk, N. C.; van Es, T.; Davis, F. F., Effect of covalent attachment of polyethylene glycol on immunogenicity and circulating life of bovine liver catalase. *J Biol Chem* **1977,** *252* (11), 3582-6.

89. Merdan, T.; Kunath, K.; Petersen, H.; Bakowsky, U.; Voigt, K. H.; Kopecek, J.; Kissel, T., PEGylation of poly(ethylene imine) affects stability of complexes with

plasmid DNA under in vivo conditions in a dose-dependent manner after intravenous injection into mice. *Bioconjugate chemistry* **2005,** *16*, 785-92.

90. Masotti, A.; Moretti, F.; Mancini, F.; Russo, G.; Di Lauro, N.; Checchia, P.; Marianecci, C.; Carafa, M.; Santucci, E.; Ortaggi, G., Physicochemical and biological study of selected hydrophobic polyethylenimine-based polycationic liposomes and their complexes with DNA. *Bioorganic & medicinal chemistry* **2007,** *15* (3), 1504-15.

91. Kuhn, P. S.; Levin, Y.; Barbosa, M. C., Charge inversion in DNA–amphiphile complexes: possible application to gene therapy. *Physica A: Statistical Mechanics and its Applications* **1999,** *274* (1–2), 8-18.

92. Alshamsan, A.; Haddadi, A.; Incani, V.; Samuel, J.; Lavasanifar, A.; Uludag, H., Formulation and delivery of siRNA by oleic acid and stearic acid modified polyethylenimine. *Mol Pharm* **2009,** *6* (1), 121-33.

93. Wong, S. Y.; Pelet, J. M.; Putnam, D., Polymer systems for gene delivery—Past, present, and future. *Progress in Polymer Science* **2007,** *32* (8-9), 799-837.

94. Takigawa, D. Y.; Tirrell, D. A., Interactions of synthetic polymers with cell membranes and model membrane systems. Part 6. Disruption of phospholipid packing by branched poly(ethylenimine) derivatives. *Macromolecules* **1985,** *18* (3), 338-342.

95. Rheiner, S.; Rychahou, P.; Bae, Y., Effects of the Lipophilic Core of Polymer Nanoassemblies on Intracellular Delivery and Transfection of siRNA. *AIMS Biophysics* **2015,** *2* (3), 284-302.

96. Resnier, P.; Montier, T.; Mathieu, V.; Benoit, J.-P.; Passirani, C., A review of the current status of siRNA nanomedicines in the treatment of cancer. *Biomaterials* **2013,** *34*, 6429-43.

97. Oh, Y.-K.; Park, T. G., siRNA delivery systems for cancer treatment. *Advanced drug delivery reviews* **2009,** *61*, 850-62.

98. Aliabadi, H. M.; Landry, B.; Sun, C.; Tang, T.; Uludag, H., Supramolecular assemblies in functional siRNA delivery: where do we stand? *Biomaterials* **2012,** *33* (8), 2546-69.

99. Guo, P.; Coban, O.; Snead, N. M.; Trebley, J.; Hoeprich, S.; Guo, S.; Shu, Y., Engineering RNA for targeted siRNA delivery and medical application. *Advanced drug delivery reviews* **2010,** *62*, 650-66.

100. Sheikhi Mehrabadi, F.; Fischer, W.; Haag, R., Dendritic and lipid-based carriers for gene/siRNA delivery (a review). *Current Opinion in Solid State and Materials Science* **2012,** *16*, 310-322.

101. Gonzalez, H.; Hwang, S. J.; Davis, M. E., New class of polymers for the delivery of macromolecular therapeutics. *Bioconjugate chemistry* **1999,** *10*, 1068-74.

102. Zhang, S.; Zhao, B.; Jiang, H.; Wang, B.; Ma, B., Cationic lipids and polymers mediated vectors for delivery of siRNA. *Journal of controlled release : official journal of the Controlled Release Society* **2007,** *123*, 1-10.

103. Ballarín-González, B.; Ebbesen, M. F.; Howard, K. A., Polycation-based nanoparticles for RNAi-mediated cancer treatment. *Cancer letters* **2013**.

104. Grayson, A. C.; Doody, A. M.; Putnam, D., Biophysical and structural characterization of polyethylenimine-mediated siRNA delivery in vitro. *Pharm Res* **2006,** *23* (8), 1868-76.

105. Wightman, L.; Kircheis, R.; Rössler, V.; Carotta, S.; Ruzicka, R.; Kursa, M.; Wagner, E., Different behavior of branched and linear polyethylenimine for gene delivery in vitro and in vivo. *The journal of gene medicine* **2001,** *3*, 362-72.

106. Akhtar, S.; Benter, I., Toxicogenomics of non-viral drug delivery systems for RNAi: potential impact on siRNA-mediated gene silencing activity and specificity. *Advanced drug delivery reviews* **2007,** *59*, 164-82.

107. Zuckerman, J. E.; Choi, C. H. J.; Han, H.; Davis, M. E., Polycation-siRNA nanoparticles can disassemble at the kidney glomerular basement membrane. *Proceedings of the National Academy of Sciences of the United States of America* **2012,** *109*, 3137-42.

108. Nel, A. E.; Madler, L.; Velegol, D.; Xia, T.; Hoek, E. M.; Somasundaran, P.; Klaessig, F.; Castranova, V.; Thompson, M., Understanding biophysicochemical interactions at the nano-bio interface. *Nat Mater* **2009,** *8* (7), 543-57.

109. Albanese, A.; Tang, P. S.; Chan, W. C. W., The effect of nanoparticle size, shape, and surface chemistry on biological systems. *Annual review of biomedical engineering* **2012,** *14*, 1-16.

110. He, C.; Hu, Y.; Yin, L.; Tang, C.; Yin, C., Effects of particle size and surface charge on cellular uptake and biodistribution of polymeric nanoparticles. *Biomaterials* **2010,** *31*, 3657-66.

111. Zintchenko, A.; Philipp, A.; Dehshahri, A.; Wagner, E., Simple modifications of branched PEI lead to highly efficient siRNA carriers with low toxicity. *Bioconjugate chemistry* **2008,** *19*, 1448-55.

112. Pasche, S.; Voros, J.; Griesser, H. J.; Spencer, N. D.; Textor, M., Effects of ionic strength and surface charge on protein adsorption at PEGylated surfaces. *J Phys Chem B* **2005,** *109* (37), 17545-52.

113. Miteva, M.; Kirkbride, K. C.; Kilchrist, K. V.; Werfel, T. A.; Li, H.; Nelson, C. E.; Gupta, M. K.; Giorgio, T. D.; Duvall, C. L., Tuning PEGylation of mixed micelles to overcome intracellular and systemic siRNA delivery barriers. *Biomaterials* **2014**.

114. Zhu, C.; Jung, S.; Luo, S.; Meng, F.; Zhu, X.; Gwan, T.; Zhong, Z., Biomaterials Co-delivery of siRNA and paclitaxel into cancer cells by biodegradable cationic micelles based on PDMAEMA – PCL – PDMAEMA triblock copolymers. *Biomaterials* **2010,** *31*, 2408-2416.

115. Kim, D.; Lee, D.; Jang, Y. L.; Chae, S. Y.; Choi, D.; Jeong, J. H.; Kim, S. H., Facial amphipathic deoxycholic acid-modified polyethyleneimine for efficient MMP-2 siRNA delivery in vascular smooth muscle cells. *Eur J Pharm Biopharm* **2012,** *81* (1), 14-23.

116. Hong, J.; Ku, S. H.; Lee, M. S.; Jeong, J. H.; Mok, H.; Choi, D.; Kim, S. H., Cardiac RNAi therapy using RAGE siRNA/deoxycholic acid-modified polyethylenimine complexes for myocardial infarction. *Biomaterials* **2014,** *35*, 7562-73.

117. Patel, M. M.; Anchordoquy, T. J., Contribution of hydrophobicity to thermodynamics of ligand-DNA binding and DNA collapse. *Biophys J* **2005,** *88* (3), 2089-103.

118. Kim, H. J.; Miyata, K.; Nomoto, T.; Zheng, M.; Kim, A.; Liu, X.; Cabral, H.; Christie, R. J.; Nishiyama, N.; Kataoka, K., siRNA delivery from triblock copolymer micelles with spatially-ordered compartments of PEG shell, siRNA-loaded intermediate layer, and hydrophobic core. *Biomaterials* **2014,** *35* (15), 4548-56.

119. Matsumoto, S.; Christie, R. J.; Nishiyama, N.; Miyata, K.; Ishii, A.; Oba, M.; Koyama, H.; Yamasaki, Y.; Kataoka, K., Environment-responsive block copolymer micelles with a disulfide cross-linked core for enhanced siRNA delivery. *Biomacromolecules* **2009,** *10* (1), 119-27.

120. Xia, W.; Wang, P.; Lin, C.; Li, Z.; Gao, X.; Wang, G.; Zhao, X., Bioreducible polyethylenimine-delivered siRNA targeting human telomerase reverse transcriptase inhibits HepG2 cell growth in vitro and in vivo. *Journal of controlled release : official journal of the Controlled Release Society* **2012,** *157*, 427-36.

121. Nelson, C. E.; Kintzing, J. R.; Hanna, A.; Shannon, J. M.; Gupta, M. K.; Duvall, C. L.; Al, N. E. T., Balancing cationic and hydrophobic content of PEGylated siRNA polyplexes enhances endosome escape, stability, blood circulation time, and bioactivity in vivo. *ACS nano* **2013,** *7*, 8870-80.

122. Petros, R. a.; DeSimone, J. M., Strategies in the design of nanoparticles for therapeutic applications. *Nature reviews. Drug discovery* **2010,** *9*, 615-27.

123. Maeda, H.; Wu, J.; Sawa, T.; Matsumura, Y.; Hori, K., Tumor vascular permeability and the EPR effect in macromolecular therapeutics: a review. *J Control Release* **2000,** *65* (1-2), 271-84.

124. Holzerny, P.; Ajdini, B.; Heusermann, W.; Bruno, K.; Schuleit, M.; Meinel, L.; Keller, M., Biophysical properties of chitosan/siRNA polyplexes: profiling the

polymer/siRNA interactions and bioactivity. *Journal of controlled release : official journal of the Controlled Release Society* **2012,** *157*, 297-304.

125. Guo, G.; Zhou, L.; Chen, Z.; Chi, W.; Yang, X.; Wang, W.; Zhang, B., Alkane-modified low-molecular-weight polyethylenimine with enhanced gene silencing for siRNA delivery. *International journal of pharmaceutics* **2013,** *450*, 44-52.

126. Canton, I.; Battaglia, G., Endocytosis at the nanoscale. *Chemical Society Reviews* **2012**.

127. Noguchi, A.; Furuno, T.; Kawaura, C.; Nakanishi, M., Membrane fusion plays an important role in gene transfection mediated by cationic liposomes. *FEBS Lett* **1998,** *433* (1-2), 169-73.

128. Cevc, G.; Richardsen, H., Lipid vesicles and membrane fusion. *Advanced Drug Delivery Reviews* **1999,** *38*, 207-232.

129. Akinc, A.; Thomas, M.; Klibanov, A. M.; Langer, R., Exploring polyethylenimine-mediated DNA transfection and the proton sponge hypothesis. *J Gene Med* **2005,** *7* (5), 657-63.

130. Pack, D. W.; Hoffman, A. S.; Pun, S.; Stayton, P. S., Design and development of polymers for gene delivery. *Nat Rev Drug Discov* **2005,** *4* (7), 581-93.

131. Kurtulus, I.; Yilmaz, G.; Ucuncu, M.; Emrullahoglu, M.; Becer, C. R.; Bulmus, V., A new proton sponge polymer synthesized by RAFT polymerization for intracellular delivery of biotherapeutics. *Polymer Chemistry* **2014,** *5* (5), 1593-1604.

132. Richard, I.; Thibault, M.; De Crescenzo, G.; Buschmann, M. D.; Lavertu, M., Ionization behavior of chitosan and chitosan-DNA polyplexes indicate that chitosan has a similar capability to induce a proton-sponge effect as PEI. *Biomacromolecules* **2013,** *14* (6), 1732-40.

133. Rheiner, S.; Bae, Y., Increased poly(ethylene glycol) density decreases transfection efficacy of siRNA/poly(ethylene imine) complexes. *AIMS Bioengineering* **2016,** *3* (4), 454-467.

134. Lachelt, U.; Wagner, E., Nucleic Acid Therapeutics Using Polyplexes: A Journey of 50 Years (and Beyond). *Chem Rev* **2015,** *115* (19), 11043-78.

135. Choudhury, S. R.; Hudry, E.; Maguire, C. A.; Sena-Esteves, M.; Breakefield, X. O.; Grandi, P., Viral vectors for therapy of neurologic diseases. *Neuropharmacology* **2016**.

136. Liu, Y.; Liu, Z.; Wang, Y.; Liang, Y. R.; Wen, X.; Hu, J.; Yang, X.; Liu, J.; Xiao, S.; Cheng, D., Investigation of the performance of PEG-PEI/ROCK-II-siRNA complexes for Alzheimer's disease in vitro. *Brain Res* **2013,** *1490*, 43-51.

137. Aliabadi, H. M.; Maranchuk, R.; Kucharski, C.; Mahdipoor, P.; Hugh, J.; Uludağ, H., Effective response of doxorubicin-sensitive and -resistant breast cancer cells to combinational siRNA therapy. *Journal of controlled release : official journal of the Controlled Release Society* **2013,** *172*, 219-28.

138. Dominska, M.; Dykxhoorn, D. M., Breaking down the barriers: siRNA delivery and endosome escape. *J Cell Sci* **2010,** *123* (Pt 8), 1183-9.

139. Lee, S. J. S.-Y. S.; Huh, M. S.; Lee, S. J. S.-Y. S.; Lee, S. J. S.-Y. S.; Chung, H.; Park, J. H.; Oh, Y.-K.; Choi, K.; Kim, K.; Kwon, I. C., Stability and cellular uptake of polymerized siRNA (poly-siRNA)/polyethylenimine (PEI) complexes for efficient gene silencing. *Journal of controlled release : official journal of the Controlled Release Society* **2010,** *141*, 339-46.

140. Varkouhi, A. K.; Scholte, M.; Storm, G.; Haisma, H. J., Endosomal escape pathways for delivery of biologicals. *Journal of controlled release : official journal of the Controlled Release Society* **2011,** *151*, 220-8.

141. Wen, S.; Zheng, F.; Shen, M.; Shi, X., Surface modification and PEGylation of branched polyethyleneimine for improved biocompatibility. *Journal of Applied Polymer Science* **2013,** *128* (6), 3807-3813.

142. Ogris, M.; Steinlein, P.; Carotta, S.; Brunner, S.; Wagner, E., DNA/polyethylenimine transfection particles: influence of ligands, polymer size, and PEGylation on internalization and gene expression. *AAPS PharmSci* **2001,** *3* (3), E21.

143. Alexis, F.; Pridgen, E.; Molnar, L. K.; Farokhzad, O. C., Factors affecting the clearance and biodistribution of polymeric nanoparticles. *Mol Pharm* **2008,** *5* (4), 505-15.

144. Merkel, O. M.; Beyerle, A.; Librizzi, D.; Pfestroff, A.; Behr, T. M.; Sproat, B.; Barth, P. J.; Kissel, T., Nonviral siRNA delivery to the lung: investigation of PEG-PEI polyplexes and their in vivo performance. *Mol Pharm* **2009,** *6* (4), 1246-60.

145. Mao, S.; Neu, M.; Germershaus, O.; Merkel, O.; Sitterberg, J.; Bakowsky, U.; Kissel, T., Influence of polyethylene glycol chain length on the physicochemical and biological properties of poly(ethylene imine)-graft-poly(ethylene glycol) block copolymer/SiRNA polyplexes. *Bioconjugate chemistry* **2006,** *17*, 1209-18.

146. Walker, G. F.; Fella, C.; Pelisek, J.; Fahrmeir, J.; Boeckle, S.; Ogris, M.; Wagner, E., Toward synthetic viruses: endosomal pH-triggered deshielding of targeted polyplexes greatly enhances gene transfer in vitro and in vivo. *Mol Ther* **2005,** *11* (3), 418-25.

147. Pandey, A. P.; Sawant, K. K., Polyethylenimine: A versatile, multifunctional non-viral vector for nucleic acid delivery. *Mater Sci Eng C Mater Biol Appl* **2016,** *68*, 904-18.

148. Forsbach, A.; Müller, C.; Montino, C.; Kritzler, A.; Curdt, R.; Benahmed, A.; Jurk, M.; Vollmer, J., Impact of delivery systems on siRNA immune activation and RNA interference. *Immunology Letters* **2011,** *141*, 169-180.

149. Huang, F. W.; Wang, H. Y.; Li, C.; Wang, H. F.; Sun, Y. X.; Feng, J.; Zhang, X. Z.; Zhuo, R. X., PEGylated PEI-based biodegradable polymers as non-viral gene vectors. *Acta Biomater* **2010,** *6* (11), 4285-95.

150. Fitzsimmons, R. E.; Uludag, H., Specific effects of PEGylation on gene delivery efficacy of polyethylenimine: interplay between PEG substitution and N/P ratio. *Acta Biomater* **2012,** *8* (11), 3941-55.

151. Milla, P.; Dosio, F.; Cattel, L., PEGylation of proteins and liposomes: a powerful and flexible strategy to improve the drug delivery. *Curr Drug Metab* **2012,** *13* (1), 105-19.

152. Tang, G. P.; Zeng, J. M.; Gao, S. J.; Ma, Y. X.; Shi, L.; Li, Y.; Too, H. P.; Wang, S., Polyethylene glycol modified polyethylenimine for improved CNS gene transfer: effects of PEGylation extent. *Biomaterials* **2003,** *24* (13), 2351-62.

153. Petersen, H.; Fechner, P. M.; Martin, A. L.; Kunath, K.; Stolnik, S.; Roberts, C. J.; Fischer, D.; Davies, M. C.; Kissel, T., Polyethylenimine-graft-poly(ethylene glycol) copolymers: influence of copolymer block structure on DNA complexation and biological activities as gene delivery system. *Bioconjug Chem* **2002,** *13* (4), 845-54.

154. Holland, J. W.; Hui, C.; Cullis, P. R.; Madden, T. D., Poly(ethylene glycol)--lipid conjugates regulate the calcium-induced fusion of liposomes composed of phosphatidylethanolamine and phosphatidylserine. *Biochemistry* **1996,** *35* (8), 2618-24.

155. Rheiner, S.; Reichel, D.; Rychahou, P.; Izumi, T.; Yang, H.-S.; Bae, Y., Polymer nanoassemblies with hydrophobic pendant groups in the core induce false positive siRNA transfection in luciferase reporter assays. *International Journal of Pharmaceutics* **2017,** *528* (1–2), 536-546.

156. Lee, S. J.; Kim, M. J.; Kwon, I. C.; Roberts, T. M., Delivery strategies and potential targets for siRNA in major cancer types. *Adv Drug Deliv Rev* **2016,** *104*, 2-15.

157. Davis, M. E.; Zuckerman, J. E.; Choi, C. H.; Seligson, D.; Tolcher, A.; Alabi, C. A.; Yen, Y.; Heidel, J. D.; Ribas, A., Evidence of RNAi in humans from systemically administered siRNA via targeted nanoparticles. *Nature* **2010,** *464* (7291), 1067-70.

158. Kim, D. H.; Rossi, J. J., Strategies for silencing human disease using RNA interference. *Nat Rev Genet* **2007,** *8* (3), 173-84.

159. Malek, A.; Czubayko, F.; Aigner, A., PEG grafting of polyethylenimine (PEI) exerts different effects on DNA transfection and siRNA-induced gene targeting efficacy. *J Drug Target* **2008,** *16* (2), 124-39.

160. Fella, C.; Walker, G. F.; Ogris, M.; Wagner, E., Amine-reactive pyridylhydrazone-based PEG reagents for pH-reversible PEI polyplex shielding. *European journal of pharmaceutical sciences : official journal of the European Federation for Pharmaceutical Sciences* **2008,** *34* (4-5), 309-20.

161. Helmfors, H.; Eriksson, J.; Langel, U., Optimized luciferase assay for cell-penetrating peptide-mediated delivery of short oligonucleotides. *Anal Biochem* **2015,** *484*, 136-42.

162. Auld, D. S.; Thorne, N.; Nguyen, D. T.; Inglese, J., A specific mechanism for nonspecific activation in reporter-gene assays. *ACS Chem Biol* **2008,** *3* (8), 463-70.

163. Choy, G.; O'Connor, S.; Diehn, F. E.; Costouros, N.; Alexander, H. R.; Choyke, P.; Libutti, S. K., Comparison of noninvasive fluorescent and bioluminescent small animal optical imaging. *BioTechniques* **2003,** *35*, 1022-6, 1028-30.

164. Thorne, N.; Inglese, J.; Auld, D. S., Illuminating insights into firefly luciferase and other bioluminescent reporters used in chemical biology. *Chem Biol* **2010,** *17* (6), 646-57.

165. Reichel, D.; Lee, M. J.; Lee, W.; Kim, K. B.; Bae, Y., Tethered polymer nanoassemblies for sustained carfilzomib release and prolonged suppression of proteasome activity. *Ther Deliv* **2016,** *7* (10), 665-681.

166. Dootz, R.; Nie, J.; Du, B.; Herminghaus, S.; Pfohl, T., Raman and surface enhanced Raman microscopy of microstructured polyethylenimine/DNA multilayers. *Langmuir* **2006,** *22* (4), 1735-41.

167. York, S. S.; Boesch, S. E.; Wheeler, R. A.; Frech, R., Vibrational Assignments for High Molecular Weight Linear Polyethylenimine (LPEI) Based on Monomeric and Tetrameric Model Compounds. *Macromolecules* **2003,** *36* (19), 7348-7351.

168. Romero, G.; Estrela-Lopis, I.; Zhou, J.; Rojas, E.; Franco, A.; Espinel, C. S.; Fernández, A. G.; Gao, C.; Donath, E.; Moya, S. E., Surface Engineered Poly(lactide-co-glycolide) Nanoparticles for Intracellular Delivery: Uptake and Cytotoxicity—A Confocal Raman Microscopic Study. *Biomacromolecules* **2010,** *11* (11), 2993-2999.

169. Spriggs, K. A.; Bushell, M.; Willis, A. E., Translational regulation of gene expression during conditions of cell stress. *Mol Cell* **2010,** *40* (2), 228-37.

170. O'Brien, J.; Wilson, I.; Orton, T.; Pognan, F., Investigation of the Alamar Blue (resazurin) fluorescent dye for the assessment of mammalian cell cytotoxicity. *European Journal of Biochemistry* **2000,** *267* (17), 5421-5426.

171. Tiwari, B. S.; Belenghi, B.; Levine, A., Oxidative stress increased respiration and generation of reactive oxygen species, resulting in ATP depletion, opening of mitochondrial permeability transition, and programmed cell death. *Plant Physiol* **2002,** *128* (4), 1271-81.

172. Cunha, D. A.; Hekerman, P.; Ladrière, L.; Bazarra-Castro, A.; Ortis, F.; Wakeham, M. C.; Moore, F.; Rasschaert, J.; Cardozo, A. K.; Bellomo, E.; Overbergh, L.; Mathieu, C.; Lupi, R.; Hai, T.; Herchuelz, A.; Marchetti, P.; Rutter, G. A.; Eizirik, D. L.;

Cnop, M., Initiation and execution of lipotoxic ER stress in pancreatic β-cells. *Journal of Cell Science* **2008,** *121* (14), 2308.

173. Koyama, T.; Kume, S.; Koya, D.; Araki, S.-i.; Isshiki, K.; Chin-Kanasaki, M.; Sugimoto, T.; Haneda, M.; Sugaya, T.; Kashiwagi, A.; Maegawa, H.; Uzu, T., SIRT3 attenuates palmitate-induced ROS production and inflammation in proximal tubular cells. *Free Radical Biology and Medicine* **2011,** *51* (6), 1258-1267.

174. Suganami, T.; Tanimoto-Koyama, K.; Nishida, J.; Itoh, M.; Yuan, X.; Mizuarai, S.; Kotani, H.; Yamaoka, S.; Miyake, K.; Aoe, S.; Kamei, Y.; Ogawa, Y., Role of the Toll-like Receptor 4/NF-κB Pathway in Saturated Fatty Acid–Induced Inflammatory Changes in the Interaction Between Adipocytes and Macrophages. *Arteriosclerosis, Thrombosis, and Vascular Biology* **2006,** *27* (1), 84.

175. Listenberger, L. L.; Ory, D. S.; Schaffer, J. E., Palmitate-induced apoptosis can occur through a ceramide-independent pathway. *J Biol Chem* **2001,** *276* (18), 14890-5.

176. Alcazar, O.; Qiu-yue, Z.; Gine, E.; Tamarit-Rodriguez, J., Stimulation of islet protein kinase C translocation by palmitate requires metabolism of the fatty acid. *Diabetes* **1997,** *46* (7), 1153-8.

177. Aberle, A. M.; Tablin, F.; Zhu, J.; Walker, N. J.; Gruenert, D. C.; Nantz, M. H., A novel tetraester construct that reduces cationic lipid-associated cytotoxicity. Implications for the onset of cytotoxicity. *Biochemistry* **1998,** *37* (18), 6533-40.

178. Hollins, A. J.; Omidi, Y.; Benter, I. F.; Akhtar, S., Toxicogenomics of drug delivery systems: Exploiting delivery system-induced changes in target gene expression to enhance siRNA activity. *J Drug Target* **2007,** *15* (1), 83-8.

179. Omidi, Y.; Hollins, A. J.; Benboubetra, M.; Drayton, R.; Benter, I. F.; Akhtar, S., Toxicogenomics of non-viral vectors for gene therapy: a microarray study of lipofectin- and oligofectamine-induced gene expression changes in human epithelial cells. *J Drug Target* **2003,** *11* (6), 311-23.

180. Omidi, Y.; Hollins, A. J.; Drayton, R. M.; Akhtar, S., Polypropylenimine dendrimer-induced gene expression changes: the effect of complexation with DNA, dendrimer generation and cell type. *J Drug Target* **2005,** *13* (7), 431-43.

181. Ishii, M.; Maeda, A.; Tani, S.; Akagawa, M., Palmitate induces insulin resistance in human HepG2 hepatocytes by enhancing ubiquitination and proteasomal degradation of key insulin signaling molecules. *Arch Biochem Biophys* **2015,** *566*, 26-35.

182. Kirkin, V.; McEwan, D. G.; Novak, I.; Dikic, I., A role for ubiquitin in selective autophagy. *Mol Cell* **2009,** *34* (3), 259-69.

183. Yoshida, H., ER stress and diseases. *FEBS J* **2007,** *274* (3), 630-58.

184. Shang, F.; Taylor, A., Ubiquitin-proteasome pathway and cellular responses to oxidative stress. *Free Radic Biol Med* **2011,** *51* (1), 5-16.

185. Orlowski, R. Z., The role of the ubiquitin-proteasome pathway in apoptosis. *Cell Death Differ* **1999,** *6* (4), 303-13.

186. Reichel, D.; Bae, Y., Comparison of Dialysis- and Solvatofluorochromism-Based Methods to Determine Drug Release Rates from Polymer Nanoassemblies. *Pharmaceutical Research* **2016**, 1-14.

**Vita**

## EDUCATION

**B.S.E. in Chemical Engineering** August 2007 - May 2011

University of Iowa, Iowa City, Iowa

**Graduate Student in Pharmaceutical Sciences** August 2011 - Current

University of Kentucky, Lexington, KY

Advisor: Dr. Younsoo Bae

## PROFFESIONAL EXPERIENCE

**USDA NCAUR Internship, Peoria, IL June 2010 – July 2010**

**Alcon Laboratories Internship, Ft. Worth, TX, June 2009 - July 2009**

## FELLOWSHIPS

- Cancer and Nanotechnology Training Center (CNTC) Fellowship, University of Kentucky
    - February 2015 – September 2015

## PUBLICATIONS

- Jackson, M.A., Appell, M.D., Blackburn, J.A., **Rheiner, S.N.**, Berhow, M.A. 2011. The acrylation of glycerol: A precursor to functionalized lipids. Journal of the American Oil Chemists' Society. 89(4):713-719. DOI: 10.1007/s11746-011-1950-5.

- **Rheiner, S.**, Rychahou, P., Bae, Y., 2015. Effects of the Lipophilic Core of Polymer Nanoassemblies on Intracellular Delivery and Transfection of siRNA, AIMS Biophysics 2(3): 284-302, DOI: 10.3934/biophy.2015.3.284

- Yuhang Jiang, Phonepasong Arounleut, **Steven Rheiner**, Younsoo Bae, Alexander V. Kabanov, Carol Milligan, Devika S. Manickam, SOD1 nanozyme with reduced toxicity and MPS accumulation, Journal of Controlled Release, Volume 231, 10 June 2016, Pages 38-49, ISSN 0168-3659, http://dx.doi.org/10.1016/j.jconrel.2016.02.038.

- **Rheiner, S.**, Bae, Y., 2016. Increased poly(ethylene glycol) density decreases transfection efficacy of siRNA/poly(ethylene imine) complexes, AIMS Bioengineering 3(4):454-467, DOI: 10.3934/bioeng.2016.4.454

- **Steven Rheiner**, Derek Reichel, Piotr Rychahou, Tadahide Izumi, Hsin-Sheng Yang, Younsoo Bae, Polymer nanoassemblies with hydrophobic pendant groups in the core induce false positive siRNA transfection in luciferase reporter assays, International Journal of Pharmaceutics, Volume 528, Issues 1–2, 7 August 2017, Pages 536-546, ISSN 0378-5173, https://doi.org/10.1016/j.ijpharm.2017.06.056.

## PRESENTATIONS

- S. Rheiner, Y. Bae (2012) Cross-linked Nanoassemblies for Controlled siRNA Delivery. University of Kentucky PS Seminar Series, Lexington, KY.
- S. Rheiner, Y. Bae (2013) Crosslinked Nanoassemblies for Delivery of siRNA in Tumors. University of Kentucky PS Seminar Series, Lexington, KY.
- S. Rheiner, Y. Bae (2014) Polymer Tethered Nano-assemblies for siRNA Delivery. University of Kentucky PS Seminar Series, Lexington, KY.
- S. Rheiner, Y. Bae (2015) Controlled siRNA Delivery for Treatment of Cancer. University of Kentucky PS Seminar Series, Lexington, KY.
- S. Rheiner, Y. Bae (2015) Tethered Nanoassemblies for Enhanced siRNA Delivery *in vivo.* Cancer and Nanotechnology Training Center Seminar Series, Lexington, KY.
- S. Rheiner, Y. Bae (2015) Tethered Nanoassemblies for Enhanced Delivery and Transfection of siRNA. Drug Discovery and Development Symposium, Lexington, KY.

## POSTERS

- S. Rheiner, Y. Bae (2012) Cross-linked Nano Assemblies for siRNA Delivery. Pharmaceutics Graduate Student Research Meeting (PGSRM), Omaha, NB.
- S. Rheiner, Y. Bae (2012) Disulfide Cross-linked Nanoassemblies for siRNA Delivery. American Association of Pharmaceutical Scientists (AAPS), Chicago, IL.
- S. Rheiner, Y. Bae (2013) Crosslinked Nanoassemblies for In Vivo siRNA Delivery to Solid Tumors. 2nd International Conference of RNA Nanotechnology and Therapeutics, Lexington, KY.
- S. Rheiner, Y. Bae (2013) Crosslinked Nanoassemblies for siRNA Therapy. Markey Cancer Center Research Day, Lexington, KY.
- S. Rheiner, Y. Bae (2013) Crosslinked Nanoassemblies for Delivery of siRNA. Pharmaceutics Graduate Student Research Meeting (PGSRM), Iowa City, IA.
- S. Rheiner, Y. Bae (2014) Polymer Tethered Nano-assemblies for siRNA Delivery. Markey Center Research Day, Lexington, KY.

- S. Rheiner, Y. Bae (2014) Modified Polymer Tethered Nano-assemblies for siRNA DeliveryPharmaceutics Graduate Student Research Meeting (PGSRM), Chicago, IL.
- S. Rheiner, Y. Bae (2014) Polymer Tethered Nano-assemblies for siRNA Delivery. Drug Development and Discovery Symposium. Lexington, KY.
- S. Rheiner, Y. Bae (2014) Polymer Tethered Nano-assemblies for siRNA Delivery. Biomaterials Day. Lexington, KY.
- M. Takahashi, S. Rheiner, Y. Bae (2015) Chemosensitization of triple negative breast cancer by survivin protein reduction, Markey Cancer Center Research Day, Lexington, KY.
- S. Rheiner, P. Rychahou, Y. Bae (2015) Lipophilic Core Modification of Polymer Nanoassemblies for siRNA Delivery Markey Cancer Center Research Day, Lexington, KY.
- S. Rheiner, Y. Bae (2015) Nanoassemblies for Enhanced *In Vivo* siRNA Delivery and Transfection, 47$^{th}$ Pharmaceutics Graduate Student Research meeting, Lexington, KY.

## PROFESSIONAL SOCIETIES

**AAPS (2012-Current)**

American Association of Pharmaceutical Sciences

**AAPS, University of Kentucky Chapter (2013- 2016)**

Officer Position as Graduate Program Committee Representative. Helped in recruitment of new students. Participated in events, such as E-Day and others where AAPS had a presence, to represent AAPS. Attends Conferences for AAPS.

**AICHE (2007-2011)**

American Institute of Chemical Engineers

**AICHE University of Iowa Student Chapter (2007-2011)**

Officer Position (2009-2011) as Leader of the University of Iowa's ChemE Car team. Assisted in E Day. Helped AICHE Student Chapter at multiple events. Attended AICHE Regional and National Conferences as an Officer.

## ORGANIZATIONAL COMMITTEES

**Pharmaceutics Graduate Student Research Meeting (PGSRM) 2015 Planning Committee (2012-2015)**
Co-Head Chair with responsibility of planning the 47$^{th}$ annual conference hosted in Lexington, KY by The University of Kentucky. Responsible for choosing speakers, organizing activities, booking venues, and managing day of events.

## TEACHING EXPERIENCE

**University of Iowa (2010-2011)**

Teaching Assistantship Material Science Lab (057-171)

**University of Kentucky (2011-2012)**

Teaching Assistantship Introduction to Pharmaceutical Sciences (PHS-914/924)

**University of Kentucky (2012-2013)**

Teaching Assistantship Introduction to Pharmaceutical Sciences (PHS-914/924)

**University of Kentucky (2013-2014)**

Proctor for College of Pharmacy Classes

**University of Kentucky (2014-2015)**

Proctor for College of Pharmacy Classes

## AWARDS & FELLOWSHIPS

- University of Kentucky College of Pharmacy Travel Award
  - To Attend AAPS Conference (2012)
  - To Attend PGSRM Conference (2013)
  - To Attend PGSRM Conference (2014)
- Fellowship to attend 2nd International Conference of RNA Nanotechnology and Therapeutics (2014)